26232-6004-TU-01

NASA CR-152552

7.7-10221

CR-152552

EXPERIMENTAL STUDY OF DIGITAL IMAGE PROCESSING TECHNIQUES FOR LANDSAT DATA

S.S. Rifman
W.B. Allendoerfer
R.H. Caron
L.J. Pemberton
D.M. McKinnon
G. Polanski
K.W. Simon

TRW SYSTEMS GROUP
ONE SPACE PARK
REDONDO BEACH, CA. 90278

JANUARY 1976
FINAL REPORT

Prepared Under NASA Contract NAS5-20085 for

G O D D A R D   S P A C E   F L I G H T   C E N[TER]

Greenbelt, Maryland 20771

EXPERIMENTAL STUDY OF DIGITAL IMAGE PROCESSING TECHNIQUES FOR LANDSAT DATA

S.S. Rifman
W.B. Allendoerfer
R.H. Caron
L.J. Pemberton
D.M. McKinnon
G. Polanski
K.W. Simon

TRW SYSTEMS GROUP
ONE SPACE PARK
REDONDO BEACH, CA.   90278

JANUARY 1976
FINAL REPORT

1. Report No.. 26232-6004-TU-01	2. Government Accession No.	3. Recipient's Catalog No.
4. Title and Subtitle Experimental Study of Application of Digital Image Processing Techniques for LANDSAT Data		5. Report Date 31 January 1976
		6. Performing Organization Code
7. Author(s) S.S. Rifman, et al.		8. Performing Organization Report No.
9. Performing Organization Name and Address TRW Systems Group One Space Park Redondo Beach, Calif. 90278		10. Work Unit No.
		11. Contract or Grant No. NAS5-20085
12. Sponsoring Agency Name and Address NASA Goddard Space Flight Center Greenbelt, Maryland 20771 Technical Monitor: Bernard Peavey		13. Type of Report and Period Covered Final Report Apr. 1974-Jan. 1976
		14. Sponsoring Agency Code

15. Supplementary Notes

16. Abstract Results are reported for: (1) Subscene Registration; (2) Full Scene Rectification and Registration; (3) Resampling Techniques; (4) Ground Control Point (GCP) Extraction. Subscenes (354 pixels x 234 lines) were registered to ∿ 1/4 pixel accuracy and evaluated by change detection imagery for three cases: (1) bulk data registration; (2) precision correction of a reference subscene using GCP data; (3) independently precision processed subscenes. Full scene rectification and registration results were evaluated by the use of a correlation technique to measure registration errors of 0.3 pixel rms throughout the full scene. Resampling evaluations of nearest neighbor and TRW Cubic Convolution processed data included change detection imagery and feature classification. Resampled data were also evaluated for an MSS scene containing specular solar reflections. GCP extraction evaluations included measured accuracy and speed of existing automatic control point location techniques. MSS data at each of two sites, spanning a temporal separation as large as 954 days, were used to study the effects of season on automatic GCP location methods. Accuracy and implementation approach were evaluated for application to high volume daily operation (at least 30 scenes/day).

17. Key Words (Selected by Author(s)) Digital Image Processing Registration Change Detection Interpolation Ground Control Point Extraction	18. Distribution Statement		
19. Security Classif. (of this report) U	20. Security Classif. (of this page) U	21. No. of Pages 162	22. Price

*For sale by the Clearinghouse for Federal Scientific and Technical Information, Springfield, Virginia 22151.

TABLE OF CONTENTS

TABLE OF CONTENTS (Continued)

TABLE OF CONTENTS (Continued)

LIST OF FIGURES

LIST OF FIGURES (Continued)

Page

LIST OF FIGURES (Continued)

TABLE OF FIGURES (Continued)

LIST OF TABLES

1.0 INTRODUCTION AND SUMMARY

The objectives of Contract NAS5-20085 were registered to a fraction of a picture element (pixel) bulk LANDSAT subscene and full scene Multi-spectral Scanner (MSS) data, supplied by NASA in the form of bulk data recorded on Computer Compatible Tapes (CCT's), and to evaluate the results with respect to registration and change detection accuracy as well as implementation approach necessary to facilitate high volume daily operation. Existing digital image processing techniques developed prior to the start of this contract were employed for performance of all work described herein. Both image hardcopy and CCT data were generated in the course of this study.

The entire effort was divided into four parts: (1) Subscene Registration; (2) Full Scene Rectification and Registration; (3) Resampling Techniques; and (4) Ground Control Point (GCP) Extraction. For the Subscene Registration task, MSS subareas (354 pixels x 234 lines) derived from bulk LANDSAT MSS CCT data were registered to fractional pixel accuracy under three conditions: (1) No ancillary correction on the basis of GCP or attitude information to either subarea to be registered; (2) Precision processed reference data (one subscene) only; and (3) Independently precision processed subscenes. Change detection imagery indicated registration accuracy for bulk subarea registration was ~ 1/4 pixel. Precision corrected and registered subareas are derived from the full scene registration process for which rms errors can be ≤ 1/2 pixel globally, depending on the quality (correlation performance) of control points. Independently precision processed data did not exhibit as satisfactory registration performance as did data which were registered to each other and then warped to the precision coordinate frame (one interpolation).

Using manual feature extraction and registration methods the subarea registration process requires ~ 10-15 minutes, which includes generation of the registered image data, but does not include the bulk CCT reformatting. Automatic registration of subareas depends strongly upon feature characteristics. Assuming suitable feature characteristics, automatic registration of subareas can be performed at rates of 300 segments/day.

Full Scene Rectification and Registration comprised precision geo-
metric correction (rectification) of full scene LANDSAT MSS data and the
subsequent precision registration (and thus rectification) to a fraction
of a pixel of full scene data from a second spacecraft cycle. All-digital
techniques were employed to process bulk CCT data furnished by NASA,
making use of auxiliary Bulk Image Annotation Tape (BIAT) data for the
spacecraft attitude, ephemeris, altitude, etc. Use was also made of GCP's
to establish geodetic (absolute) control for the rectified scene, and
Registration Control Points (RCP's) for relative control between passes.
GCP data was furnished in the form of maps and tabular listings of geodetic
coordinates.

Registration accuracy was evaluated qualitatively by means of change
detection imagery. Quantitative measurements of full scene registration
errors were made by means of a correlation technique. An array of positions
lying on a regular grid of points were defined (identical positions were
utilized for each registered scene pair), and then a straightforward cross-
correlation between whatever features happened to be centered at these
grid positions was performed. The result was a series of relative dis-
placement measurements, which were plotted as a vector array to show
graphically the registration errors. It was found that if RCP's possess
suitable correlation properties that full scene rms errors approach
~ 20-30 meters.

Manual designation of GCP's or RCP's requires between 30 and 90
seconds per control point, depending upon the operator's familiarity with
the scene, the nature of features used as control points and scene con-
ditions (clouds, haze, flooding, etc.). Automatic techniques, applicable
for suitable control point properties, can reduce the search time to <10
sec per control point. Image resampling (interpolation) in software is
the slowest step in the entire full scene processing operation. Four
point interpolation using existing prototype software required about 16
minutes per band (10.5 MB), with nearest neighbor interpolation twice as
fast. In a production system (minimum 30 scenes/day) alternatives to the
use of all-software implementations with a single general purpose CPU are
required to effect as much parallelism as possible. Such configurations
are capable of processing several hundred full scenes in one day.

The Resampling Techniques activity involved geometric correction of full scene data by means of nearest neighbor (NN) interpolation and the Cubic Convolution (CC) Process, developed originally by TRW. Image details and corresponding change detection imagery were generated so as to demonstrate visually the artifacts created by the low order (nearest neighbor) interpolated data, which are absent from data processed by the high order (cubic convolution) techniques.

Processed data was delivered to the Jet Propulsion Laboratory for multispectral classification evaluation using their Image 100. Other processed data was evaluated by TRW using a Bayes classifier implemented in software. TRW evaluations indicate that on a single scene (4 band) basis the CC processed data gave superior results to NN processed data. Use of registered two scene (8 band) data results in 15-20% improvement in classification accuracy over single scene classification results.

Ground Control Point Extraction work included evaluation of accuracy and speed of existing automatic control point extraction software. The automatic extraction software evaluated was a combination of two techniques: sequential similarity detection algorithm (SSDA) for rapid location of the control point to within $\pm$ 4 pixels and $\pm$ 4 lines; high precision cross correlation throughout the residual search area, with location accuracy of ~ 1/10 pixel. Typical results for SSDA implemented in FORTRAN range from 2-4 seconds, for a 64x64 search area and 32x32 reference chip. Assembly language coding would reduce the running times <1 second per control point. The cross-correlation algorithm, coded in assembly language, requires ~ 1 second per control point.

Preprocessing the control points and search areas for gain and offset (mean and standard deviation) normalization appeared to provide some additional capability to find control points in scenes where the photometry changes significantly. Edge detection can be helpful for features suffering color inversion. Preprocessing of data results generally in faster running times.

Man made features (road intersections and airports) appear to give the best results, in terms of accuracy and speed. River bends and land/water boundaries (providing the water is deep and not subject to the

complications of turbidity and freezing) also appear to yield quite satisfactory performance. Intermittent features (lakes, the boundaries of which change; shallow water/land boundaries) are not susceptible to automatic extraction methods of the type explored in this study. Seasonal factors related to crop field color inversions (and vegetative effects in general) can be treated in three ways: (1) manual extraction; (2) preprocessing (solar elevation angle compensation, etc.) and (3) use of control point libraries which store seasonal representations of the chips for use at appropriate times of the year. Man-made features give best performance with either band 4 or band 5 data; non man-made features yield best results with either band 6 or band 7 data. More definitive results would require more extensive studies of a broad range of feature classes and seasonal factors, which is beyond the scope of this study.

2.0 SUBSCENE REGISTRATION

2.1 TASK DESCRIPTION

The objectives of this task were to register LANDSAT MSS subscenes (each 354 pixels x 234 lines) and to evaluate results from the point of view of change detection and implementation approach. This section contains hardcopy examples of the original subscenes, the registered subscenes, and change detection imagery for three different sites imaged at two different times. The LANDSAT scenes considered for this purpose were: 1267-17407 and 1304-17461 (adjacent orbits with coverage overlap) in Montana; 1339-17391 and 1411-17381 (same orbit, 72 days apart) in Canada; and 1062-15190 and 1080-15192 (same orbit, 18 days apart) in the Baltimore/ Washington area. Computer compatible tape (CCT) data corresponding to the aforementioned hardcopy examples has been delivered to NASA.

Registrations were performed under the following conditions:

a. No ancillary correction on the basis of GCP or attitude information to either reference or search (comparison) data;

b. Precision processed reference data only;

c. Precision processed both reference and search data ___

Inasmuch as bands 4 and 5 are highly correlated, and bands 6 and 7 are highly correlated, a sample of band 5 and band 7 was processed in each case. Change detection and enhanced imagery were produced by means of the Karhunen-Loeve transformation, applied to registered image pairs (separately for bands 5 and 7).

A functional description of the processing system employed for all work performed under this task is included in this report, along with engineering descriptions of all relevant algorithms. Evaluation of implementation approach is based on throughput of various processing modules; extrapolations of performance to high volume (300 subscenes) daily operation have also been made. All hardware and software techniques employed in the course of this contract were developed by TRW prior to the start of the contract under company sponsored programs. Therefore, only minor modifications to the extent software were required to accommodate the specific requirements of the contract.

2.2 BULK SUBSCENE REGISTRATION

2.2.1 Registration Technique

TRW's approach to the problem of registration of bulk LANDSAT MSS sub-
areas is outlined in Figure 2-1. First, NASA supplied LANDSAT MSS CCT's con-
taining bulk data for the subareas of interest are reformatted onto a mass
storage device. TRW employs for this purpose a moving head digital disk
system with a 58 Mbyte capacity.* Using TRW's Line Length Correction
Process, the desired subareas are stripped out and along-line corrected
before being stored on the CRT display system.

Feature extraction and length correction includes first the removal
of replicated pixels in each MSS scan line, resulting from nearest neighbor
interpolation of scan lines shorter than a predetermined length. NASA
currently makes this correction to bulk MSS image data to compensate for
small variations in the mirror scan dynamics (with a fixed detector sampl-
ing rate), which result in small variations in the number of pixels per
185 Km MSS scan swath width. TRW's Along Line Correction (TALC) employs
TRW's Cubic Convolution Process to stretch line length uniformly by means
of a high order interpolation technique (Reference (1)). Simultaneously,
detector commutation time effects** and the mirror scan nonlinearity are
also corrected, with the result that all three along-line corrections
(mirror scan, line length, commutation time) are achieved by means of a
single interpolation process. The mirror scan nonlinearity function used
in this study is shown in Figure 2 of Reference (3).

---

* Allowing for overhead, one system can hold well in excess of one full
ERTS scene, all four bands.

** From the Data User's Handbook (Reference (2)), this correction amounts
to 1/12 pixel successive offsets between scan lines in each group of
six (per band), generated during each mirror scan.
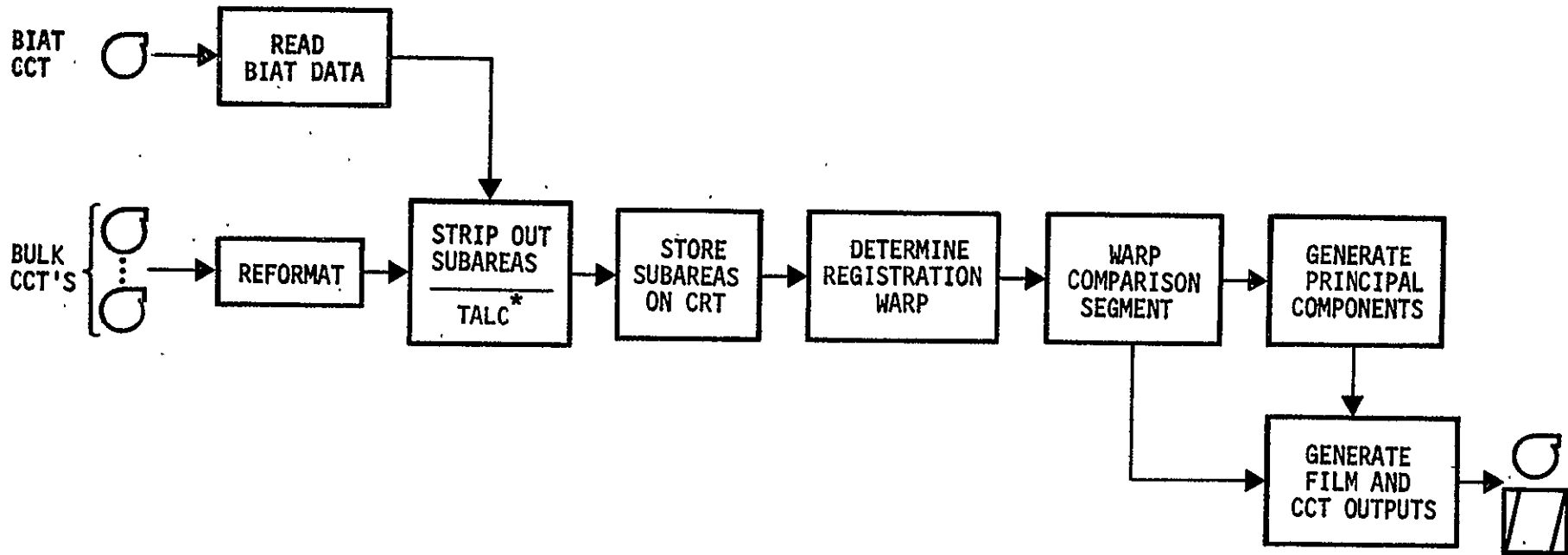
Figure 2-1. Bulk Subarea Registration Functional Flow

BIAT data is required for automatic subarea extraction. Alternatively, the subareas can be extracted manually, in conjunction with the CRT display system. Manual designation is required one time only for the reference image.

*TRW ALONG LINE CORRECTED

Once a pair of MSS along-scan corrected (TALC) image subscenes are
stored on the CRT display system, the warp necessary to bring about registra-
tion to a fraction of a pixel is determined. Determination of the warp is
accomplished first by manually identifying features (Registration Control
Points, or RCP's) on the reference image which appear also on the other
(comparison or test) image. Each RCP is designated manually by means of
the trackball feature of the display system, and its coordinates are auto-
matically stored in the computer. A 32 pixel x 32 line neighborhood
centered around each RCP is then automatically stripped out and separately
stored on the CRT system. After all pairs of RCP's (corresponding to the
reference and test images) have been designated and their neighborhoods
stripped out and stored, each pair in turn is magnified (or "zoomed") by
means of TRW's Cubic Convolution Process, a desired factor (4:1 was em-
ployed throughout this task). No more than four pairs of RCP's are re-
quired to bring about registration of subareas of the size considered in
this task (Reference (1)).

In the manual mode of operation each pair of zoomed RCP's is com-
pared by flickering back and forth on the CRT display. Misalignments are
estimated by eye and appropriate corrective displacements of the com-
parison zoomed feature are then entered into the computer from the keyboard,
and the comparison zoomed feature is then shifted accordingly. When rela-
tive displacements are thereby reduced to a minimum*, the coordinates
of the RCP in the comparison image are updated (those for the reference
image remain unaltered); and the process is repeated until all pairs of
RCP's have been processed, and the final comparison RCP coordinates stored.

For successive scenes containing a given subarea, manual processing
is not always necessary. TRW's Feature Extraction and Location Process
automatically strips out the RCP features (TALC), avoiding the time con-
suming manual process. Also registration need not be performed in the

---

* Note that 1 pixel misregistration errors using images zoomed 4:1 cor-
responds to only 1/4 pixel error in the unzoomed images. Typically,
the error is less. Limiting precision is determined by aliasing in
the sensor scan process, and is dependent upon the RCP in question.

manual fashion outlined above, TRW's Feature Extraction and Location Process automatically performs the correlation operation. Thus, in a production environment, operators need only mount magnetic tapes containing bulk CCT data and BIAT data (utilized for automatic feature extraction). The necessary RCP properties for automatic processing are the subject of Section 5 of this study.

Using the stored pairs of RCP coordinates in the reference and comparison images, a bilinear distortion model is automatically fit to the measured relative distortions (the differences of RCP coordinates in the comparison and reference images). For example, the four x-distortions are given by:

$$\delta x_1 = u_1 - x_1 = a_0 + a_1 x_1 + a_2 y_1 + a_3 x_1 y_1$$

$$\vdots$$

$$\delta x_4 = u_4 - x_4 = a_0 + a_1 x_4 + a_2 y_4 + a_3 x_4 y_4 \,,$$

where

$\delta x_i = u_i - x_i = $ measured displacement in x direction of RCP i

u_i = x-coordinate of RCP i measured in the comparison image

x_i = x-coordinate of RCP i measured in the reference image

y_i = y-coordinate of RCP i measured in the reference image

i = 1,2,3,4.

The corresponding y displacements satisfy a similar set of equations:

$$\delta y_i = v_i - y_i$$

$$= b_0 + b_1 x_i + b_2 y_i + b_3 x_i y_i \quad (i = 1,2,3,4),$$

where

v_i = y-coordinate of RCP i measured in the reference image.

There are thus two independent systems, each consisting of four linear equations in four unknowns (the a's or the b's), the solutions for which are readily obtained.

For each pixel x and line y desired in the warped image, the corresponding pixel u and line v in the unwarped (comparison image) is given by:

$$u = x + \delta x = a_0 + (a_1 + 1)x + a_2 y + a_3 xy \qquad (2\text{-}1)$$

$$v = y + \delta y = b_0 + b_1 x + (b_2 + 1)y + b_3 xy.$$

As in general no pixel value is defined at each such (u,v) coordinate in the unwarped comparison image, this pixel value must be computed from the available image data corresponding to coordinates (u_K, v_K). In one dimension this computation is of the form:

$$I(x) = I(u) = \sum_{u_K} I(u_K) \, f(u - u_K), \qquad (2\text{-}2)$$

where $f(\cdot)$ is an interpolation kernel, and $I(x)$ is the sought for intensity, computed for pixel location x in the warped image (or position u in the unwarped image). $I(u_k)$ represents the available bulk data, to be interpolated.

The process described in Equation (2-2) is an interpolation process. Extended to two dimensions, and applied to image data, this process is also known as image resampling.[*] TRW has developed an implementation of image resampling, known as the TRW Cubic Convolution Process, which is greatly superior to other standard interpolation methods, such as nearest neighbor or bilinear interpolation (Reference (4)). The TRW Cubic Convolution Process uses for the interpolation kernel f in (2-2) a cubic spline approximation to sinx/x, and a grid of 16 pixel values (four u_k by four v_k) in the unwarped image to compute each pixel (x,y) in the warped image.

2.2.2 Registration Results

Figures 2-2 and 2-3 are reproductions of NASA system corrected products for an area in Montana imaged on two different orbits, 37 days apart in time, and correspond to scenes 1304-17461-7 and 1267-17400-7 (because of haze in 1267-17404, the infrared band 7 shows generally more detail than the visible bands). Figure 2-4 shows a subarea 354 pixels x 234 lines designated by NASA, obtained from NASA bulk CCT data for band 5, following TRW's along line correction (TALC). This area was chosen as

---

[*]Resampling assumes the pixel locations u have been computed per Eq. (2-1).
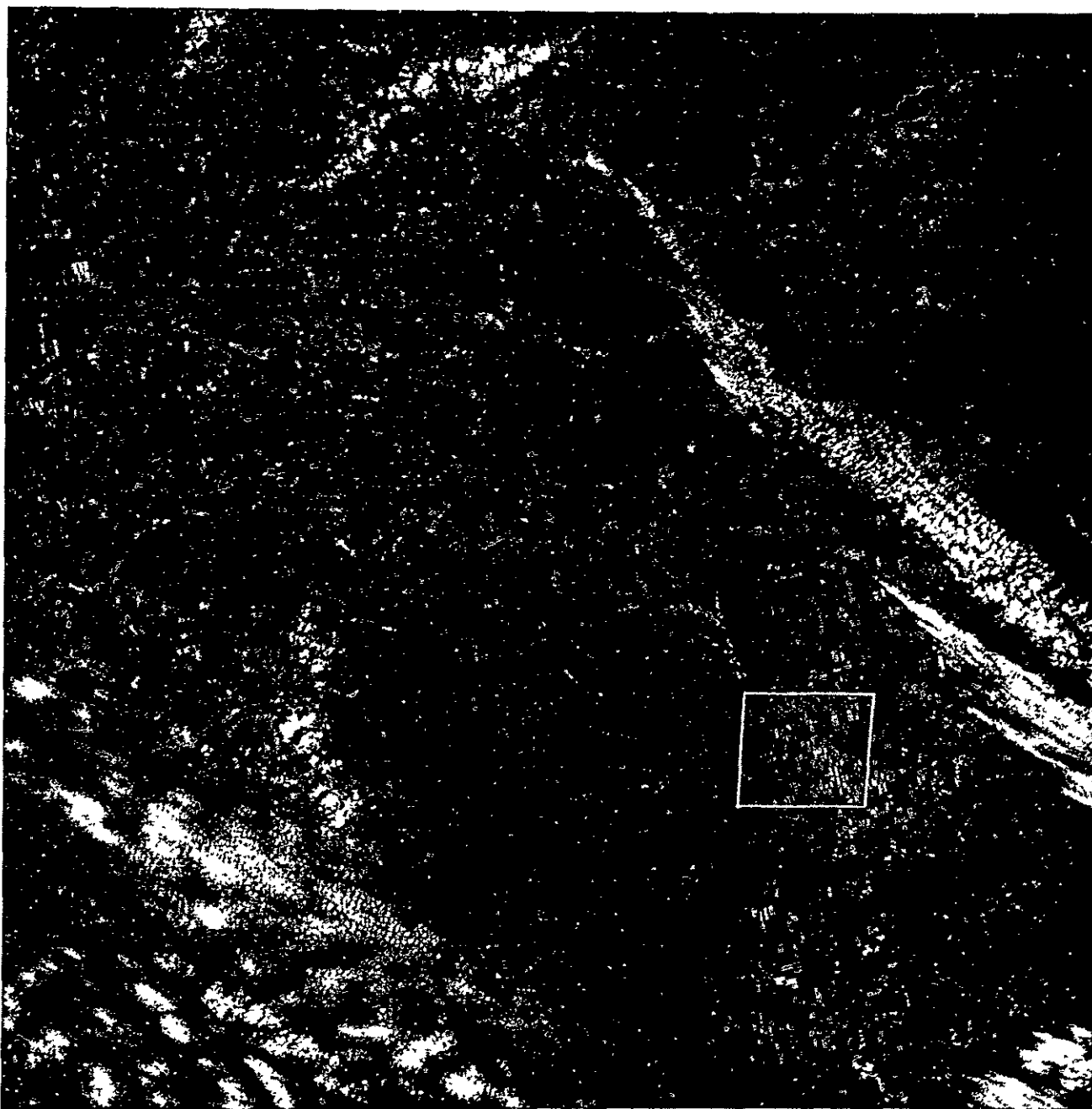
Figure 2-2. NASA System Corrected Scene 1304-17461-7.
The subarea outlined in the figure was chosen as the reference image.
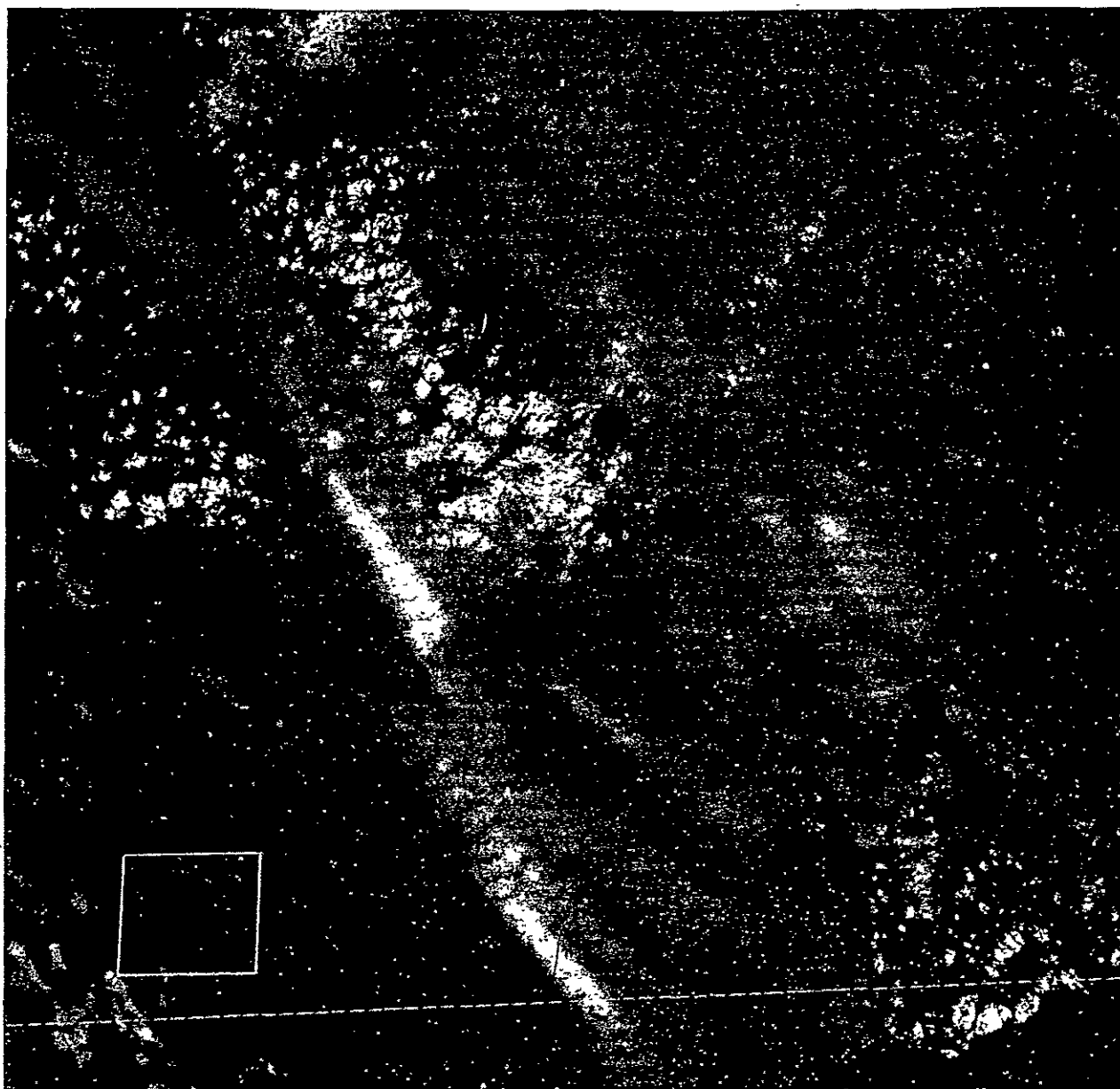
Figure 2-3. NASA System Corrected Scene 1267-17404-7,
The subarea in the figure was chosen as the comparison image.

Figure 2-4. TALC Reference Subarea from Scene 1304-17461-5.

Figure 2-5. TALC Comparison Subarea from Scene 1267-17404-5.

the reference subarea. Figure 2-5 shows the corresponding comparison sub-
area obtained from scene 1267-17404-5. Figure 2-6 shows the warped version
of Figure 2-5, following the registration procedure outlined in the pre-
vious section. Table 2-1 lists the subarea coordinates for the Montana
subareas used in this study.

Figure 2-7 shows the first principal component (enhanced) image and
Figure 2-8 shows the second principal component (change detection) image
obtained from the images of Figures 2-4 and 2-6. The last two images
were obtained by means of the Karhunen-Loève transformation described
in Reference (5).

It can be seen at once from Figure 2-8 that the perimeter of the lake
and the agricultural areas are subject to significant change over the space
of 37 days. Notice also the indication of a cloud and its shadow in the
lower left. Certain other areas, particularly the interior of the lake
and the area in the upper middle, extending from the left of the lake,
are little changed and appear as a neutral gray in the figure (no images
have been contrast enhanced in this study). No misregistration effects,
such as smeared or replicated feature boundaries, are in evidence in
Figures 2-7 and 2-8, confirming the high registration accuracy.

Figures 2-9 and 2-10 are the infrared (band 7) counterparts of
Figures 2-4 and 2-5. Figures 2-11 and 2-12 similarly correspond to
Figures 2-7 and 2-8. The change detection image in this case (Figure 2-12)
indicates substantially the same changes in features described with re-
spect to Figure 2-8, though the changes visible in the upper part of the
lake (band 5) are not apparent in the infrared (Figure 2-12).

Figure 2-13 shows a NASA system corrected image for scene 1339-
17391-5, an area in Canada which is also rural in nature, and characterized
by a number of agricultural fields. Figure 2-14 shows an arbitrarily
selected* TALC subarea 354 pixels x 234 lines in size obtained from NASA
bulk CCT data for band 5. Figure 2-15 shows the corresponding subarea
obtained from scene 1411-17381-5, imaged 72 days later than the preceding

---

* Consistent with visibility in the comparison image.

Figure 2-6. Warped TALC Comparison Subarea from Scene 1267-17404-5.

This image, generated as a result of TRW's digital processing of bulk
LANDSAT CCT data, is registered to the corresponding TALC subarea of
Figure 2-3.

Table 2-1. Subarea Location Coordinates

All lines are measured in the bulk image (same
as the TALC image). All pixels are measured in
the TALC image, i.e., one corrected for line
length, scan nonlinearity and detector commuta-
tion time. Subarea dimensions are 354 pixels x
234 lines.

	SCENE	SUBAREA UPPER LEFT CORNER	
		LINES	PIXELS
Montana	1267-17404	1718	428
	1304-17461	1438	2183
Canada	1339-17391	1015	1810
	1411-17381	929	1715

Figure 2-7. Enhanced TALC Subarea for Scenes 1304-17461-5 and
1267-17404-5
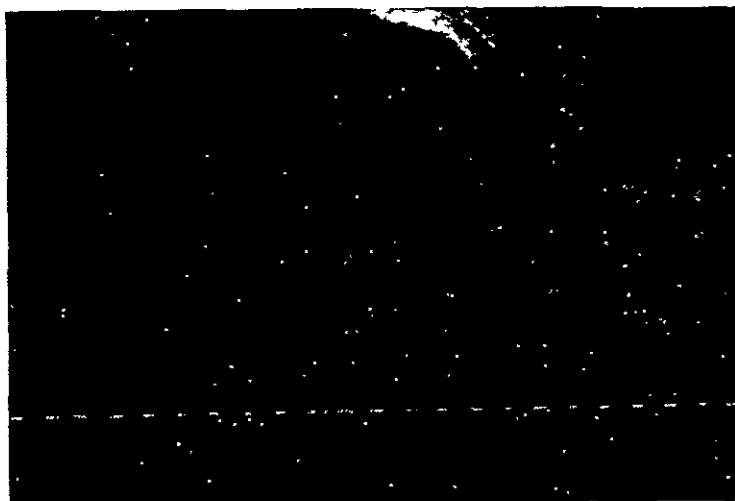
Figure 2-8. Change Detection TALC Subarea for Scenes 1304-17461-5
and 1267-17404-5.

No change appears as neutral gray; black and white correspond
to either additive or subtractive changes (compare with Fig-
ures 2-3 and 2-4).

Figure 2-9. TALC Reference Subarea from Scene 1304-17461-7.
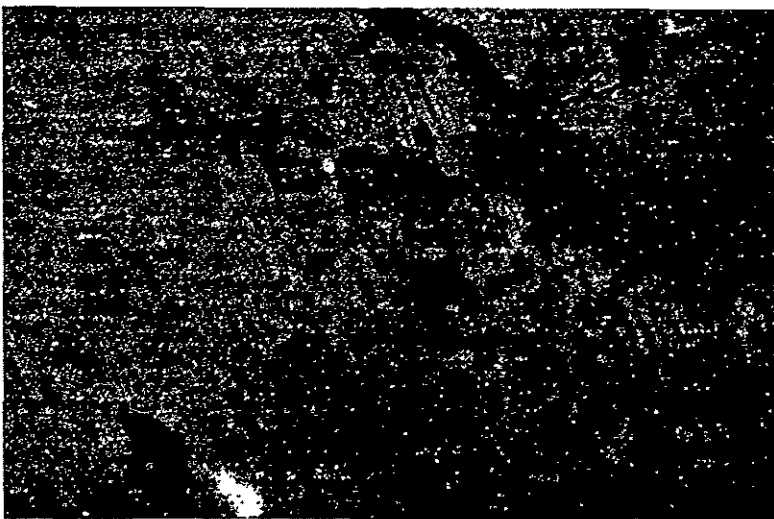
Figure 2-10. TALC Comparison Subarea from Scene 1267-17404-7.
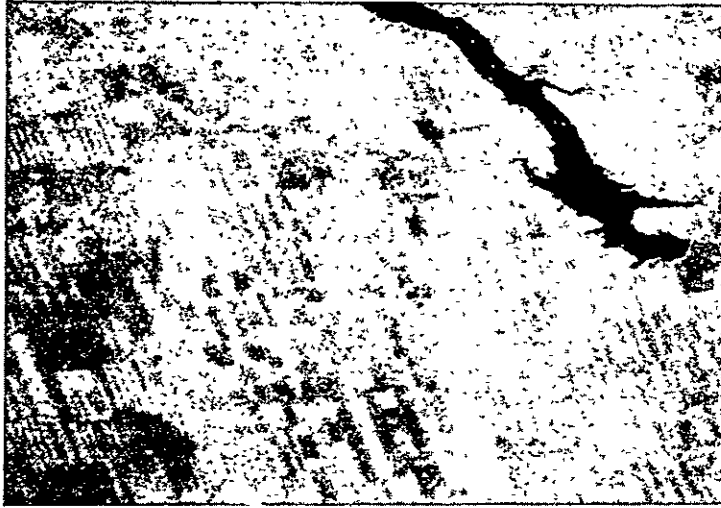
ORIGINAL PAGE IS
OF POOR QUALITY

Figure 2-11. Enhanced TALC Subarea for Scenes 1304-17461-7
and 1267-17404-7.
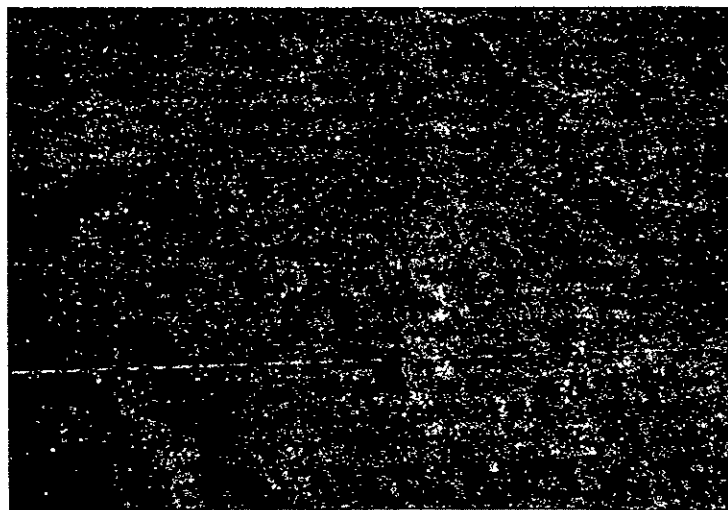
Figure 2-12. Change Detection TALC Subarea for Scenes 1304-17461-7
and 1267-17404-7.
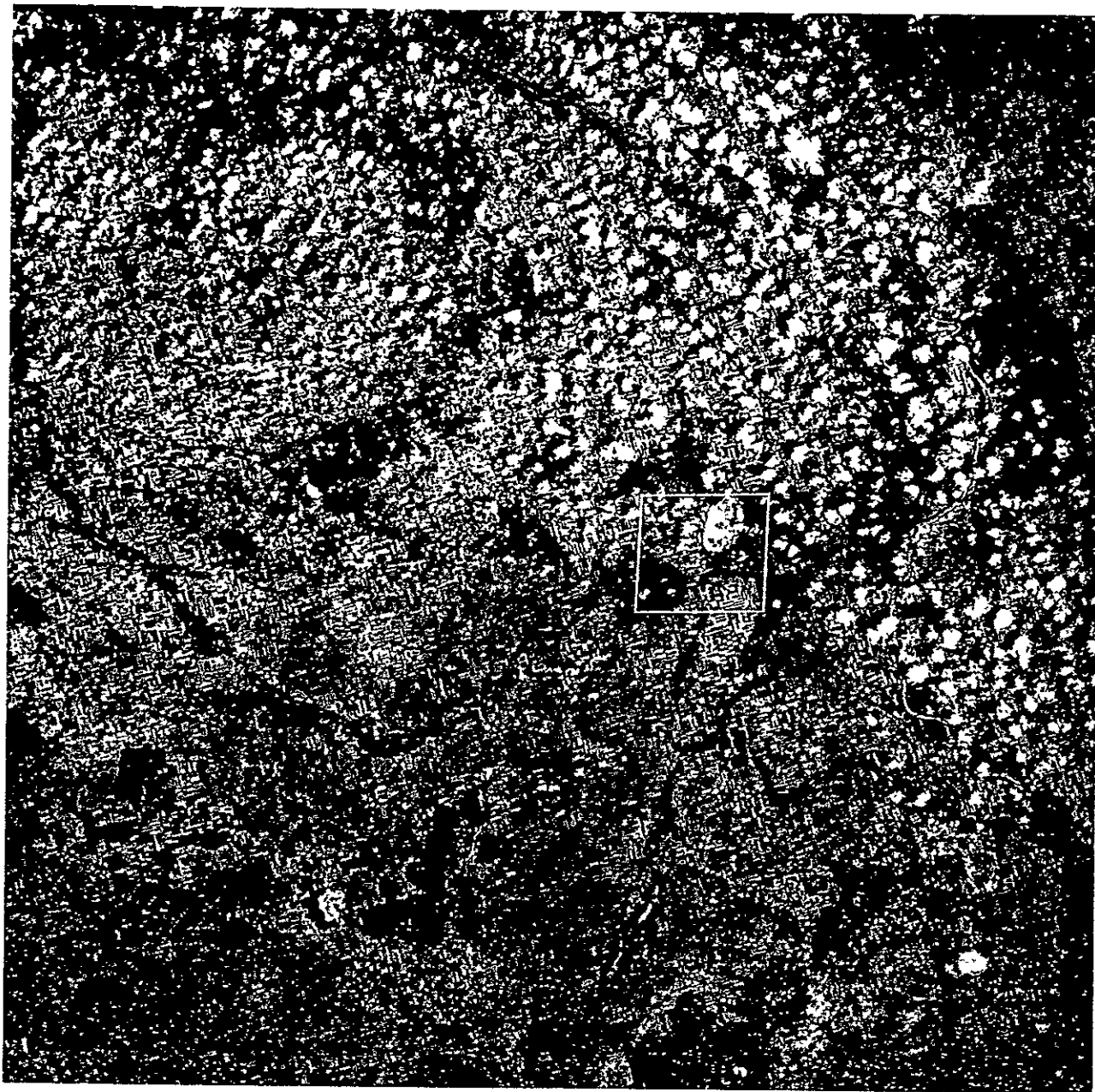
Figure 2-13. NASA System Corrected Scene 1339-17391-5.

Figure 2-14. TALC Subarea from Scene 1339-17391-5,
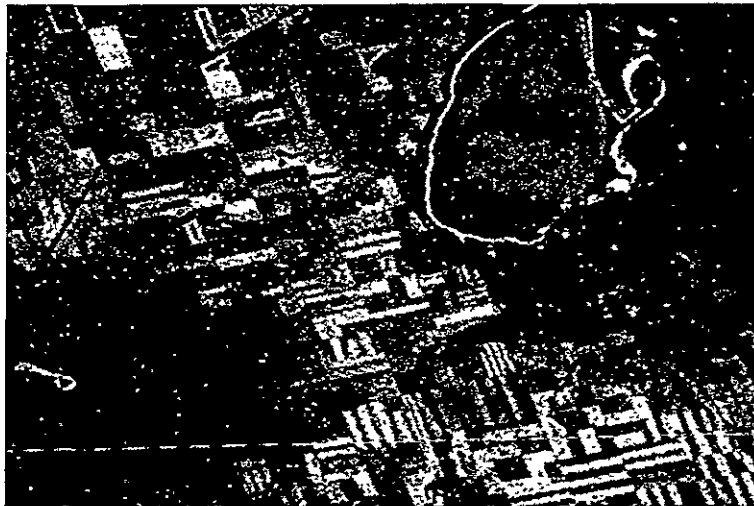
Figure 2-15. TALC Subarea from Scene 1411-17381-5,

scene. Table 2-1 lists the subarea coordinates for the Canadian scenes.

Figure 2-16 is the enhanced image obtained following registration of the two preceeding image subareas. Figure 2-17 is the change detection image. As in the case for the Montana scenes, Figure 2-17 indicates registration accuracy to a fraction of a pixel. It can be seen at once that the boundary of the lake and the agricultural areas are subject to considerable change over a period of 72 days. Nonetheless, certain other areas, particularly the area in the lower left and the area to the right of the lake, are little changed and appear as neutral gray in the change detection image. The infrared data show similar behavior, as in the case of the Montana subareas.

For comparison purposes, the image of Figure 2-4 was shifted 1/2 pixel and 1/2 line using TRW's Cubic Convolution Process. The change detection image resulting from this shifted image and that of Figure 2-4 is shown in Figure 2-18. It can be compared to the change detection imagery of Figures 2-8, 2-12 and 2-17 so as to indicate the relative precision of the registration process.

Figure 2-16. Enhanced TALC Subarea for 5 Scenes 1339-17391-5 and 1411-17381-5
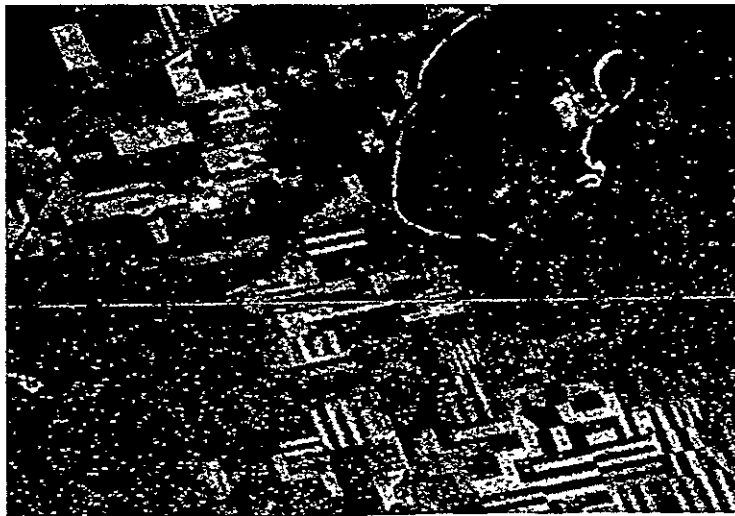
Figure 2-17. Change Detection TALC Subarea for Scenes 1339-17391-5
and 1411-17381-5,

(a) The Image of Figure 2-4 Shifted

(b) Result for the Image of Figure 2-4 Shifted and Compared Against Itself

Figure 2-18. 1/2 Pixel and 1/2 Line Misregistration Error Effect Using
1304-17461-5 Bulk Segment

2.3 PRECISION SUBSCENE REGISTRATION

2.3.1 Registration Technique

TRW's approach to the registration of a bulk comparison subimage to a precision reference subimage is outlined in Figure 2-19. First, the reference image must be processed so as to determine the warp from the bulk image coordinate system to the precision image coordinate system (full image). The subarea resampling then proceeds as a subset of the full scene resampling, utilizing the specific warp parameters for an arbitrarily selected subarea defined in the precision corrected image. Thus, only the subarea is resampled, while its warp coefficients are determined on the basis of processing control points for the full scene. In this way, results obtained are in every way identical to the accuracy of the full scene, while processing time is optimized for the volume of data to be processed. Furthermore, the size of the segments processed can be made arbitrarily large (or small), without compromising accuracy.

The full image warp is computed for the reference scene by designating Ground Control Points (GCP's) in the bulk scene corresponding to available U.S. Geological Survey Maps or tabulations, and estimating spacecraft attitude and altitude errors using a linear sequential estimator. The estimator is driven by the errors between known geodetic coordinates (ground truth) and estimates of geodetic coordinates of the control points based upon the current estimates of spacecraft attitude, mirror scan, ephemeris, altitude, etc. (Reference 6)[*]. Additional features, called Registration Control Points (RCP's), are also designated on the basis of their location in the image and their ease of extraction (a subject for Section 5 of the present contract). The designated GCP's and RCP's are TRW Along Line Corrected (TALC) for mirror scan nonlinearity, line length and commutation skew by means of TRW's Cubic Convolution Process, before being stored in a digital random access file (on disk). The corresponding earth centered coordinates for the GCP's and RCP's are stored along with the image data.

---

[*] Initial values for the spacecraft altitude, ephemeris and attitude are derived from BIAT data for each scene.
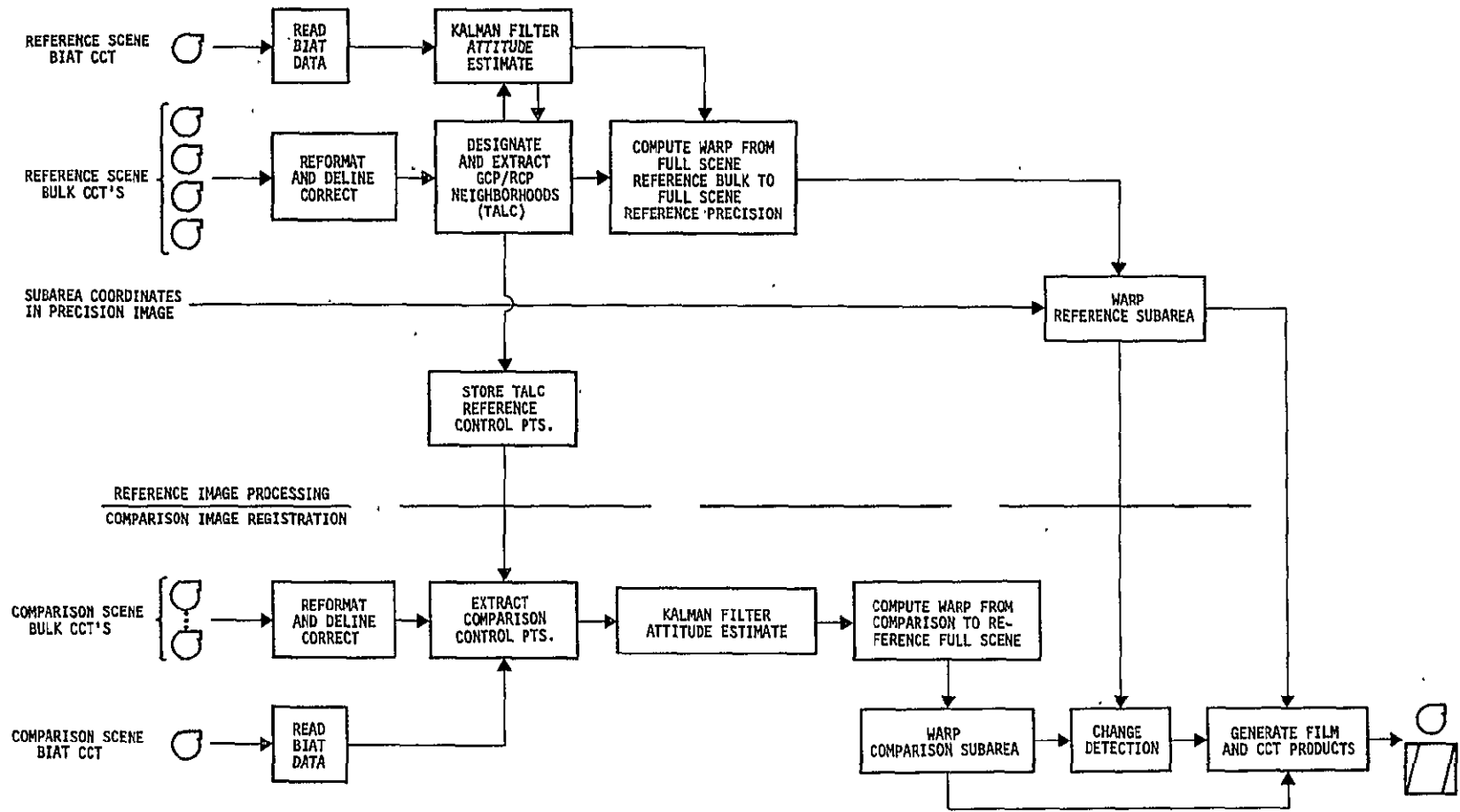
Figure 2-19. Precision Subarea Registration Functional Flow

The comparison image BIAT data is used for automatic feature extractions; manual operation is also possible and does not require BIAT data. Manual designation of GCP's and RCP's is required one time only for each, in the reference image.

The full scene registration warp for a comparison image is computed by utilizing the BIAT data for the scene to initialize the (same) Kalman filter, and repeating the error refinement process described above, utilizing extracted bulk image control point positions to estimate corresponding earth centered coordinates which are compared to the previously stored control point earth centered coordinates. The control points used for registration correspond to the RCP's and GCP's designated and extracted previously when processing the reference scene. The filter's refined estimate of the attitude time series and altitude bias permits speeding up the control point location process. Note that the correlation process need be done only once per scene, resulting in considerable processing efficiencies in the event of multiple subareas per scene. Further, if several passes for a subarea are registered together, the control point storage file need be generated only once and can be utilized for all of the comparison subareas.

Were it desired to process a comparison subimage alone, that is, making use of no BIAT comparison scene data and using no control points in parts of the scene external to the subimage, a result would be achieved with less than the accuracy of the method just described. The TALC subimage from the comparison scene would have to be registered to the corresponding TALC subarea for the reference scene by the techniques described in Section 2.2. The precision warp coefficients for the reference scene could then be utilized to generate a net warp for the comparison subimage by simple addition of the reference-precision warp to the reference-comparison warp (the technique is discussed in Appendix A of this report). The precision limiting factor is the need to resample the already along scan resampled TALC sub-areas. Furthermore, the technique entails a different procedure than for the full scene registration. The full scene reference precision processing of GCP's is required in any event. Thus, the preferred method, from the point of view of simplicity, accuracy, and quality is the method outlined herein.

2.3.2 Registration Results

Scenes 1062-15190 and 1080-15192 for the Baltimore/Washington area were utilized for precision subarea registration. Figures 2-20 and 2-21 show, respectively, the TALC reference and comparison subareas considered in this study. Table 2-2 lists the coordinates for these subareas.

Figure 2-22 shows the warped reference subarea after precision processing. Figure 2-23 shows the warped comparison subarea, following registration processing. The image has been warped only one time. The enhanced subarea is shown in Figure 2-24; and the change detection image is shown in Figure 2-25. The latter two images show clearly the precision of the registration process.

TABLE 2-2. SUBAREA LOCATION COORDINATES FOR THE BALTIMORE/WASHINGTON AREA[*]

SCENE	SUBAREA UPPER LEFT CORNER	
	LINES	PIXELS
1062-15190	626	493——
1080-15192	665	560

---

[*] Lines are measured in the precision corrected image. Scene 1062-15190 was shosen as the reference image.
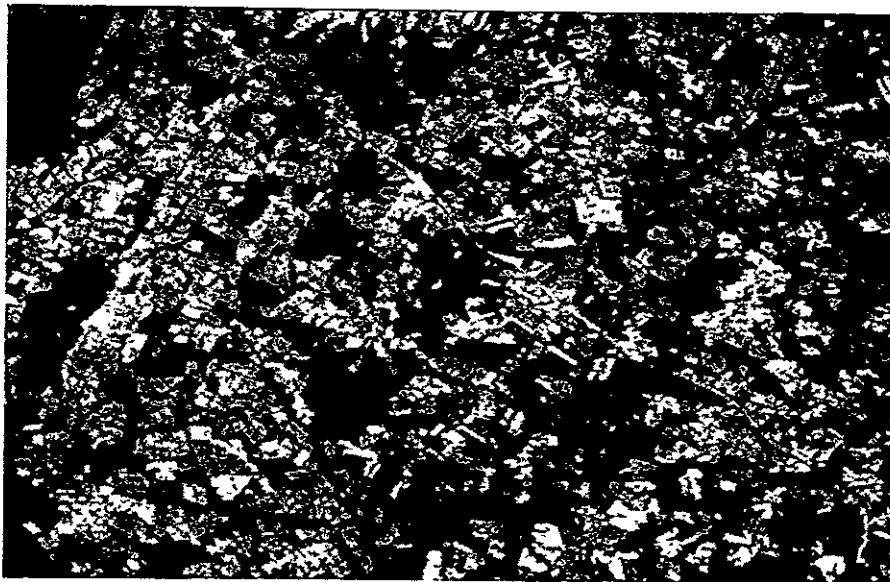
Figure 2-20. Bulk Reference Subarea from Scene 1062-15190-5.
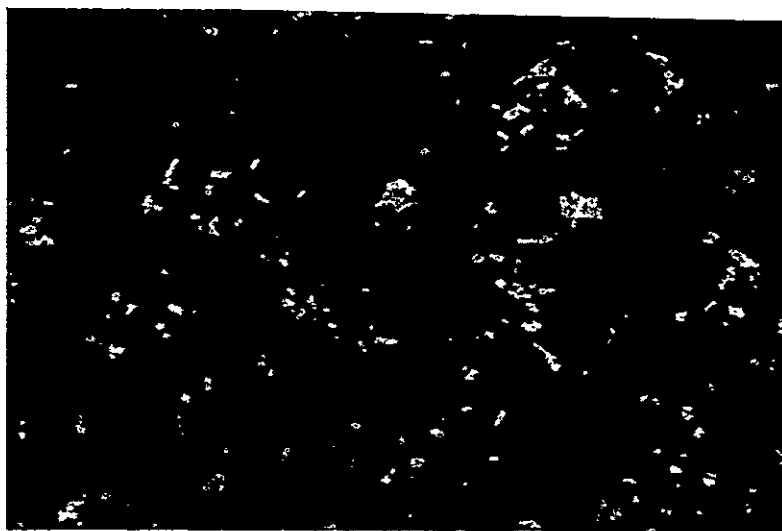
Figure 2-21. Bulk Comparison Subarea from Scene 1080-15192-5.
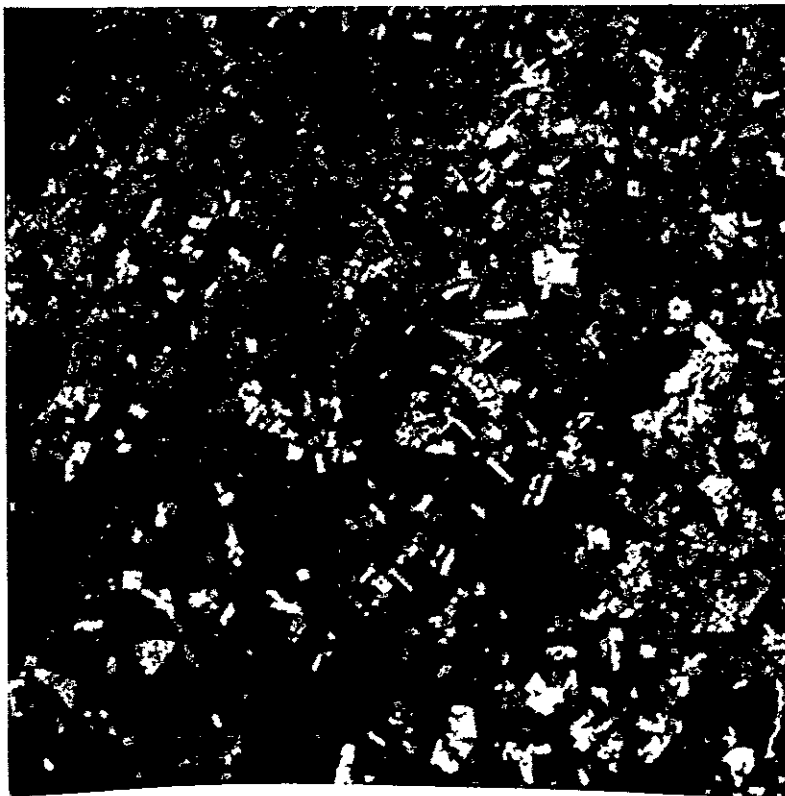
Figure 2-22. Precision Corrected Subarea from Scene 1062-15190-5
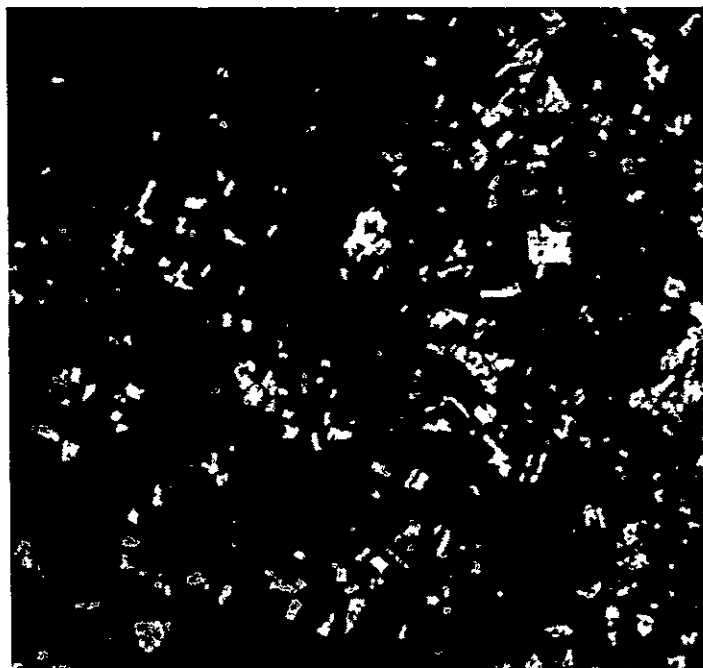
Figure 2-23. Precision Registered and Corrected Subarea from
Scene 1080-15192-5
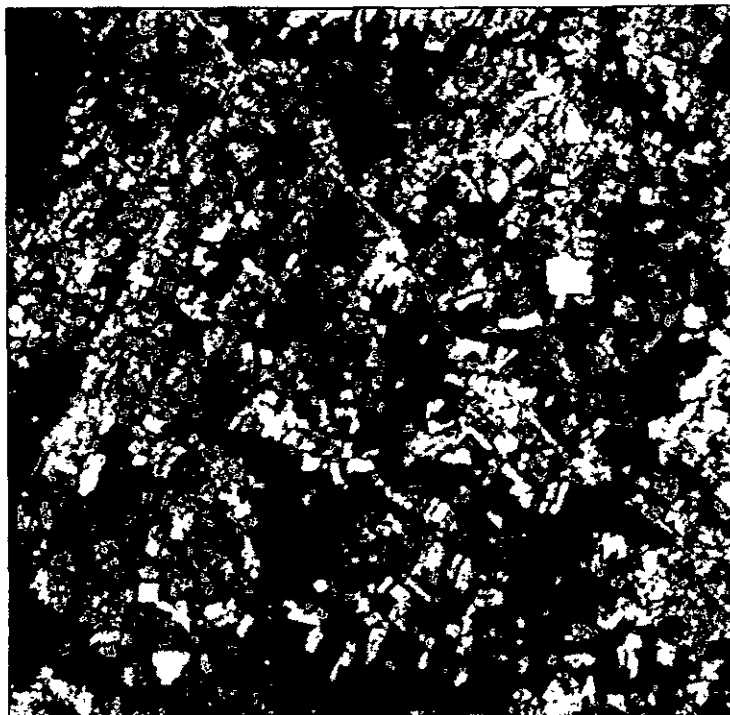
Figure 2-24.   Enhanced Image for Precision Corrected and Registered
Subareas from Scenes 1062-15190-5 and 1080-15192-5
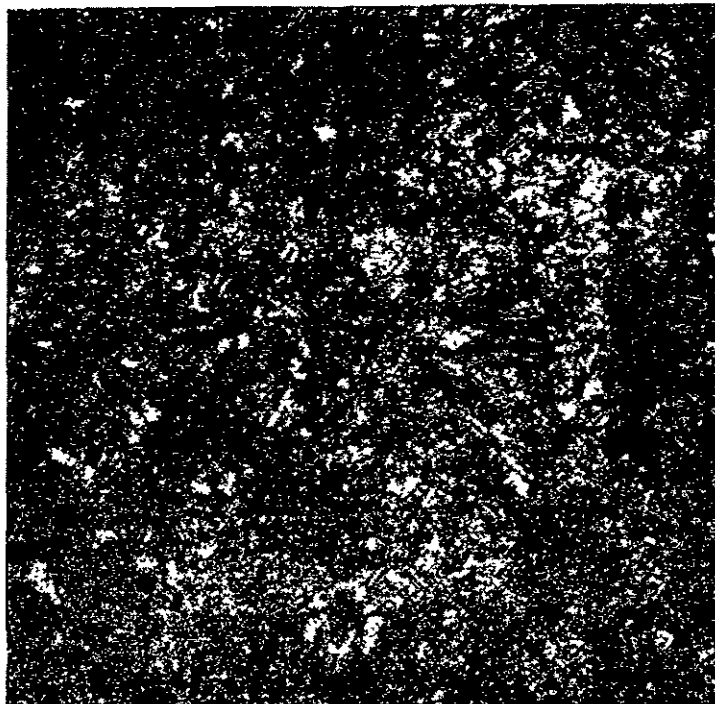
Figure 2-25.   Change Detection Image for Precision Corrected and
Registered Subareas from Scenes 1062-15190-5 and 1080-15192-5

2.4 INDEPENDENT PRECISION PROCESSING OF SUBSCENES

2.4.1 Technique

The objective of this subtask was to precision process independently corresponding subscenes from reference and comparison images, and to compare registerability of the resultant processed subscenes. The technique is identical to the reference subarea processing described in Section 2.3, as outlined in Figure 2-19. In this case, however, it is not necessary to refer to either image as the "reference" or "comparison." In order to eliminate rotational and displacement discrepancies, both precision processed images are oriented in the same direction and centered at the same UTM coordinate, taken as that for one of the two scenes considered.

2.4.2 Results

Subscenes used in this analysis were drawn from non-urban areas of scenes 1062-15190 and 1080-15192. The change detected image for the independently rectified scenes is shown in Figure 2-26 for the subareas. For comparison the corresponding change detection detail derived from full scene registered data is also shown in Figure 2-26. The increase in structure in the change detection imagery for independently processed data is due to the inaccuracy of manually designated geodetic control point locations ($\pm$ 1/4 pixel) relative to the accuracy of feature correlation between successive scenes (1/10 pixel). That is, the GCP designation accuracy is degraded by manual interaction and by limited knowledge of the exact locations of the features. The conclusion to be drawn is that fractional-pixel registration requires correlation of features between the scenes to be registered.

It is important to recognize that the processing procedures for scene-scene registration and for independent precision geometric correction are identical with the exception of the way in which control points are handled. For independent correction, GCP's are input manually and are used for their geodetic locations. For scene-scene registration, the scene from the first pass of the spacecraft over an area is geometrically corrected using GCP's as in independent correction. However, subareas 32 pixels on a side are extracted from this reference scene and stored with their precision locations in the control point library. Later comparison scenes of the same area are processed in the same way, except that control points

TOP RIGHT:
  Segment from 1062-15190-5
  Upper left corner is 500 lines,
    500 pixels

BOTTOM LEFT:
  Independent Precision Correction
  Change Detection Image Segment

BOTTOM RIGHT:
  Standard Precision Registration
  Change Detection Image Segment
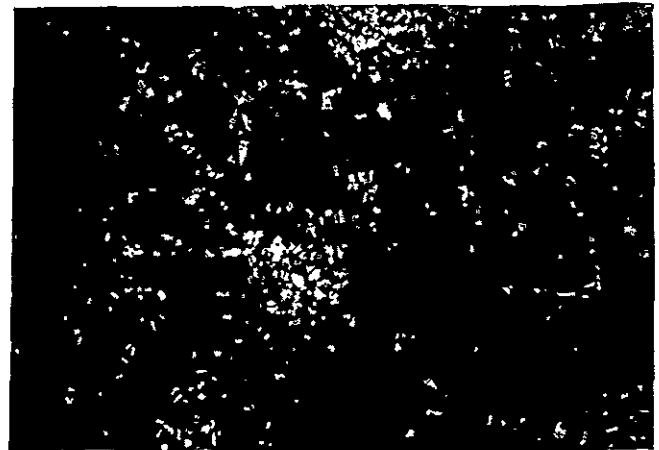
Figure 2-26. Independent Precision Processing Results

  Scene 1080-15192-5 was precision corrected (rectified). Scene
  1062-15190-5 was independently rectified, centered and rotated
  to the coordinate system defined by 1080-15192-5. The resulting
  change detection image segment derived from the full scene data
  is in the lower left. The change detection segment resulting
  from standard full scene precision registration is shown in
  the lower right.

(now called Registration Control Points - RCP's) are located by automatic correlation with the 32 x 32 subareas stored in the control point library and are used for their desired locations in the precision registered coordinate system. The RCP location process is several times more accurate than the GCP location process, and the resulting registration accuracy is thus many times more accurate than the geodetic correction process, i.e., geodetic accuracy is 1-2 pixels-throughout the scene, but registration accuracy is < 1 pixel.

2.5 CONCLUSIONS

2.5.1 Precision

It has been conclusively demonstrated during the course of this task that registration of subareas (354 pixels x 234 lines) extracted from bulk LANDSAT CCT data can be accomplished with high precision (1/4 pixel). Both change detection and enhancement imagery have been included in this report and verify the quoted accuracy for three different sites, typified by features such as farm lands, rivers, and lakes.

2.5.2 Procedure

Registrations performed during this task were accomplished using manual methods for designation and correlation of RCP's. TRW has developed automated procedures to establish the RCP correlation which can considerably speed up the process. Critical to the automatic processing operation is the need to establish the class of RCP's which are best suited for automatic correlation. This problem is discussed in Section 5 of this report. Note that in general, automatic procedures are not as flexible or adaptable to as wide a class of image content as are the manual methods.

2.5.3 Throughput

The system configuration utilized for the work performed for this task utilized a single CPU with one 9-track, 800 bpi, 120 ips tape drive, two 58-megabyte disks, and a CRT display with integral refresh disk. Timings were compiled for each subtask in the process. Since the processing configuration used here has not been optimized for high-throughput subscene registration, extrapolations to throughput of a somewhat augmented hardware system are included.

The input tape reformatting process at 800 bpi requires 6.5 min. per scene at 120 ips, assuming dual tape drives for overlap of rewind and tape mounting time. Use of 1600 bpi tapes would reduce this time to half without exceeding the disk transfer rate capability. Output tape formatting to 800 bpi tapes takes the same amount of time for full scenes and 4.7 sec per 354 x 234 pixel reference subarea and 1.6 sec per 193 x 117 pixel

comparison subarea, or approximately 15 minutes for 300 subareas (half reference, half comparison). The output tape process can be overlapped with the input tape process, given two separate tape drives and controllers.

The bulk-to-bulk registration process described in Section 2.2.1 requires display of the desired subareas on the CRT with NASA line-length-correction removed and TRW Cubic Convolution along-line correction (TALC) performed, a process which takes approximately 15 seconds per pair of subareas, limited by the CRT transfer rate and operator response time. Designation of correlation features (Registration Control Points) in the subareas is a manual and thus time-variable process. The operator flickers back and forth between the reference and comparison subareas to select four suitable features, then designates one of the features in both the reference and comparison areas and the other three in the reference subarea only. A well-trained operator with imagery with good correlation features (see Section 5) can achieve this within approximately 30 seconds per subarea pair. The RCP's are then precisely correlated automatically and the warp function derived within 5 seconds per subarea pair. Warping of the comparison subarea takes place from disk to disk and requires 11 sec per comparison subarea (4 bands) of 193 x 117 pixels (or 40 sec for 354 x 234) in software using TRW Cubic Convolution. Using the special purpose hardware TRW Cubic Convolution Interpolation (CCI) reduces the warp time to approximately 1 sec for 193 x 117 pixels, limited by disk transfer rates. Total time estimate for a production facility is thus 1 minute per subarea pair (4 bands) with resampling in software plus 6.5 minutes for each scene loaded from which subareas are extracted. Difficult subareas (marginal correlation feature content) will raise the time required to 2 minutes per subarea pair due to increased operator designation time.

The prototype process actually used for this subtask performed the comparison subarea warp from one channel of the CRT to another rather than from disk to disk, thus requiring loading all four bands onto the CRT, one at a time, warping them and then transferring them back to disk. This increased processing time by 4 minutes per subarea pair. This procedure would not be used in a production process. The developmental operator-

computer interface further includes unnecessarily time-consuming prompters and diagnostics which account for additional processing time in the proto-type.

Processing a reference subarea to determine the warp function for absolute geodetic accuracy is required for both precision registration and independent precision subarea correction, Sections 2.3 and 2.4. The warp function determination process is identical to that for full scene proces-sing, the subject of Section 3. The actual warping of the subareas is sub-stantially faster than for full-scene processing, due to the substantially reduced number of pixels and to some software efficiencies possible with the smaller subareas.

To achieve 300 subarea throughput in 8 hours, a single computer with two input tape drives at 120 ips and one output tape drive, three 58-megabyte disks, and TRW Cubic Convolution resampling in software will suf-fice. (Again, because the architecture of the TRW prototype processing system is not optimized for high-throughput subarea processing, it will not achieve these rates as it stands.) Significant events in precision proces-sing include: input tape reformatting and NASA line-length correction re-moval; Geodetic and/or Registration Control Point processing; distortion function calculation; image resampling on the desired coordinate grid; and output tape formatting. Processing time for independently geodetically rectified scenes is the same as for a comparison scene registered to a reference scene with the exception of control point processing. Registra-tion Control Points in a comparison scene can be located automatically by correlating with features from the reference scene which have been previous-ly stored in the Control Point Library. This eliminates time-consuming manual operations and is consequently substantially faster.

Using three disks allows overlap of input and output tape reformat-ting with distortion calculation and resampling. For reference scene pro-cessing for independent geodetic correction, GCP's are designated manually using the CRT display. This process takes 40-60 seconds/GCP, limited by transfer time to the display, operator recognition time, and zooming of the control point to allow more precise designation. Although only 6-10 GCP's are required (if properly placed), typically 15 control points are designated as RCP's to allow for the possibility of partial cloud cover in

later comparison scenes. The GCP process thus requires approximately 16 minutes/reference scene. Calculating the distortion coefficients for the desired warp function requires another 1/2 minute.

For comparison scene processing, a semi-automatic RCP designation process is used whereby the approximate location of the RCP is designated manually and the precise location is computed by automatic digital correlation with the 32 x 32 pixel digital RCP cnip stored in the CPL. For well-defined RCP's, this process takes less than 20 seconds per point plus one minute of overhead per scene. For partial cloud cover of the RCP, the automatic correlation may fail, which causes the control point to be zoomed to the CRT for possible manual correlation with a zoomed version of the RCP from the CPL. The manual operation can take up to a minute per RCP. Fully automatic RCP processing can be performed using the Sequential Similarity Detection Algorithm (SSDA) for approximate location of the RCP, replacing the manual approximate designation process, with the exception of the first control point, whose location uncertainty is too large to ensure adequate performance of the SSDA within a reasonable time. For the second and following control points, the sequential distortion estimator predicts their locations with sufficient (and increasing) accuracy to result in a speed improvement for SSDA over manual designation. For scenes. with a high degree of cloud cover or haze, the SSDA performance is inferior to the manual process. Distortion coefficient calculation again requires approximately 1/2 minute. Thus, if 10 RCP's were used, the comparison scene distortion calculation would take about 11 1/2 minutes for the semi-automatic processing.

The warping or resampling process takes place in two passes, along- and across-scan. Cross-scan skew buffering for the subareas takes place in core. Total processing time in software for TRW Cubic Convolution is 60 seconds per reference subarea (4 bands) and 20 seconds per comparison subarea, limited by processing overhead and pixel processing. A microprocessor implementation of the resampler would reduce this time to approximately 12 seconds per reference subarea (4 bands). A special-purpose-hardware implementation using the TRW CCI reduces this to approximately 4 seconds per subarea. Assuming 10 reference and 10 comparison scenes

with 15 subareas for each, the image registration requires 8 hours for processing of the 300 subareas. If several spacecraft passes, or comparison subareas, are registered to each reference subarea, the processing time is correspondingly reduced due to the faster RCP processing. If fewer subareas than 15 are utilized from each scene, the hardware resampler or a second computer is required to achieve 300 subareas (4 bands each) per 8 hours.

For independent precision correction, the added time required for manual designation of GCP's on both comparison and reference scenes necessitates hardware resampling to achieve 300 subareas per day. If GCP's are saved from one scene to use with automatic GCP correlation in another scene, the process of Section 2.4 becomes that of Section 2.3.

3.0 FULL SCENE RECTIFICATION AND REGISTRATION

3.1 TASK DESCRIPTION

The objective of this contract task is to precision correct (rectify) full scene LANDSAT MSS data and to precision register to a fraction of a pixel (and thereby rectify) data from a different spacecraft cycle. All-digital techniques were utilized to process bulk CCT data furnished by NASA, making use of auxiliary Bulk Image Annotation Tape (BIAT) data for the spacecraft attitude, ephemeris, altitude, etc. Use was also made of Ground Control Points (GCP's) to rectify a scene (i.e., establish geodetic control) and Registration Control Points (RCP's) for relative control between passes. Processed full scene data recorded on CCT (see Appendix B) was delivered to NASA.

BIAT, GCP, and scene data were supplied for two pairs of scenes: 1062-15190 and 1080-15192, of the Baltimore-Washington area; and 1411-17391 and 1339-17381 of Saskatchewan, Canada. TRW's Cubic Convolution Process and nearest neighbor interpolation were utilized to resample the scene data, using the same geometric warp in both cases. Change detection imagery were generated to illustrate the effect of the interpolation process on the quality of the result. Details of the full scene data are also generated to illustrate more clearly these effects.

Registration accuracy was evaluated numerically by designating positions at regular intervals in the corrected full scene data (identical positions were utilized for the registered image pair), and then performing a precision crosscorrelation between corresponding features from the two scenes centered at the respective positions. The result was a series of relative displacement measurements, the statistics for which are included herein.

Timing analyses of the various processing functions were also conducted. Implementation approach was evaluated for the throughputs of at least 30 scenes per day.

3.2 TECHNIQUE

Existing techniques for image registration were developed prior to this contract by TRW. A detailed discussion of the algorithms used in the rectification process was included in a previous contract report (Reference 4), and so will not be repeated; only a brief summary of the technique will be included here. Figure 3-1 shows a functional flow diagram for the process. First, bulk NASA scene data on CCT's are reformatted onto a digital disk storage system to permit separating and ordering the individual bands and scan lines of data. The disk storage system must be capable of storing at least one full scene of corrected data. Because NASA uses nearest neighbor line length correction, a preprocessing operation is then employed to strip out the replicated pixels in each scan line of data. De-line-length corrected data can be written back out onto the same disk used to store the reformatted data.

BIAT data for spacecraft ephemeris, heading, altitude and attitude are also input to the rectification processing operation. These parameters are utilized to initialize a 13 state linear sequential estimator (Kalman filter) for the spacecraft attitude time series and altitude bias errors. Each GCP filter update diminishes the size of the uncertainty interval containing each successive GCP sought, and thereby speeds up the GCP location process. (The geodetic coordinates supplied by the USGS are converted to line, pixel coordinates for the GCP location search.)

It is necessary to manually identify a control point (RCP or GCP) the first time it is processed. A CRT equipped with an interactive cursor (track ball) is employed for this purpose. The TRW Cubic Convolution Process is employed to digitally enlarge (zoom) 4:1 a 32 x 32 chip centered at each tentative control point location. Designation of the zoomed chip ensures $\leq$ 1/4 pixel designation accuracy. Prior to display, each chip is TRW Along Line Corrected (TALC) by employing the TRW Cubic Convolution Process in the bulk data scan line direction to correct for line length, detector commutation time, and mirror scan nonlinearity.

Figure 3-1. Functional Flow Diagram for Rectification

Both TRW's Cubic Convolution Process and nearest neighbor inter-
polation were used to resample the scene data. Samples of full scene
imagery resampled by TRW's Cubic Convolution Process are included herein.
Change detection imagery resulting from both resampling processes are
included herein as well. Subimages are also included to bring out de-
tails more clearly. A more extensive treatment of interpolation algorithms
is contained in Section 4 of this report.

Registration accuracy was evaluated by accurate cross correlation
of image subareas centered at precisely the same locations (lines,
pixels) in the registered scene data. The cross correlation process in
two dimensions results in a matrix of the following form:

$$C(n,m) = \sum_{\delta y, \delta x = -14}^{+14} f(x_i + \delta x + n, y_j + \delta y + m) \; g(x_i + \delta x, y_j + \delta y)$$

where   f,g   =   respective data values from corresponding
                        registered scenes

x_i, y_j =   selected pixel positions (pixels, lines) at
                        which correlation features are located

C   =   cross correlation matrix

A biquadratic polynomial fit to the results for integer values of n,m
permits accurate determination of a correlation peak and the correspond-
ing non-integer n,m location of this maximum. Tabulation of statistics
from features which exhibited a satisfactory correlation matrix permitted
determination of rms error, average absolute error and worst case
registration error.

The TALC chip centered at the designated position is stored in the Control Point Library (CPL) on disk for subsequent use in the registration process. The same disk which stores bulk sensor data can also be used to store the Control Point Library.

Registration Control Points (RCP's) that have been previously stored in the Control Point Library (CPL) from an earlier scene can be located in the current scene by automatic digital correlation between the RCP in the CPL and a search area in the current scene. This process takes place in two steps: search and precision location. The search step finds the correct alignment within a few pixels via either the Sequential Similarity Detection Algorithm (SSDA) or by approximate manual designation. The search is initialized by the best estimate of the RCP location on the basis of all control points processed up to that time point in the scene, greatly reducing processing time after the first control point. Manual designation is always faster for the first point due to relatively large bias errors in apriori spacecraft data on the BIAT's. The precision location process utilized is a straightforward crosscorrelation algorithm with normalization to determine the correlation on integer sample-spacings, with polynomial interpolation to find the precise location to 1<10 of a pixel. In the event that automatic crosscorrelation fails (due to partial cloud cover or poor choice of RCP), the reference and comparison RCP's are zoomed to the CRT for manual crosscorrelation.

The estimated earth-centered coordinates for each GCP, calculated on the basis of the current estimates from the 13 parameter Kalman filter, are compared to known earth centered coordinates computed from USGS supplied data to form an error. This error drives the filter and produces a refined estimate of the 13 state error vector. The process repeats until errors are reduced to about 1 pixel average absolute error. No more than 6-9 GCP's are required for this accuracy, in general. Further error reduction is limited only by the accuracy of available GCP's.

With precision models for the mirror scan nonlinearity, refined attitude time series and altitude bias errors, spacecraft ephemeris and the earth shape, it is then possible to calculate with very high accuracy

the distortion anywhere throughout the scene. Rather than do so for every pixel (picture element, or sample of data) the distortion is approximated by fitting a piecewise low-order model to the distortion calculated precisely on a regular grid of points in the corrected image coordinate system. If the grid of points is sufficiently dense (in fact, fewer than 100), the residual modeling errors can be made < 1/4 pixel, worst case. This approach will thereby obviate the modeling errors of global models of arbitrarily high degree, and is quite fast in terms of processing time (a matter of seconds/full scene).

Once the image distortion is computed, it is necessary to correct (or resample) the bulk data, so as to produce corrected image data defined on a regular grid of pixels. Thus, if the image distortion is approximated by a piecewise bilinear model of the following form:

$$\delta x = u-x = a_0 + a_1 x + a_2 y + a_3 xy$$

$$\delta y = v-y = b_0 + b_1 x + b_2 y + b_3 xy$$

where

u,x = input, output pixel coordinates

v,y = input, output line coordinates

δx = pixel distortion

δy = line distortion

$a_0, \ldots, b_3$ = bilinear distortion model coefficients

then the corrected image data is in general computed from

$$f(x,y) = \sum_{u,v} g(u,v) \, h(x-u, \, y-v)$$

where

g = bulk data values

h = interpolation kernel.

Note that for integer values of x,y the corresponding bulk image coordinates

$$u = x + \delta x$$

$$v = y + \delta y$$

are non-integer values – hence, the need for interpolation.

For spatial frequency band-limited data, the ideal interpolation kernel is of the form:

$$\frac{\sin\pi(x-u)\ \sin\pi(y-v)}{\pi^2(x-u)(y-v)}.$$

However, this function has significant magnitude until very high $|x-u|$, $|y-v|$; thus, the interpolation convolution includes an extremely large number of summation terms for each interpolated value (> 1000), rendering high throughput implementation impractical if not impossible. Thus, in light of this and the fact that LANDSAT MSS data is not band-limited, but fact contains aliasing errors (which are not removable after sampling without severe resolution degradation), a limited-extent approximation is made to this function. We are concerned here with only two approximations: nearest neighbor and the TRW Cubic Convolution Process.

The TRW Cubic Convolution Process employs a cubic spline function approximation to sinx/x. The cubic spline in one dimension is defined on a grid of four points. Equivalently, in two dimensions a grid of bulk data values 4 pixels x 4 pixels is required to resample one corrected image pixel. This approach (Reference 4) was shown to yield very superior results, even in comparison with sinx/x truncated at $\pm$ 5 pixels (or 10 x 10 points in two dimensions).

For nearest neighbor resampling the bulk data value closest to the position of the corrected image pixel (at u = x + δx) is chosen for the result of the interpolation operation. Clearly this is equivalent to a position error throughout the nearest neighbor resampled image as large as $\pm$ .5 pixel, or $\pm$ 1 pixel registration error between scenes. Compared to sinx/x resampling, nearest neighbor resampled data is characterized by one pixel discontinuities.

In practice, the resampling process is implemented as two one-dimensional interpolations: First in the direction of bulk data scan lines, and then in the orthogonal direction. In this manner, scan related distortions (line length, mirror scan nonlinearity, and detector commutation time) can be accurately corrected. Also, there is a small improvement in processing time over a single pass interpolation method (for example, along output lines).

There is no real difference between the registration processing operations and those required for rectification. No control points need be designated during registration processing (though more could be designated if features were obscured previously). The computed earth centered coordinates of RCP's, using the last Kalman filter attitude/ altitude refinement obtained during rectification processing, are used as ground truth against which current estimates based upon filter updates during the registration processing are compared. With the exception of locating the first control point, which may require a minute or more depending upon actual BIAT data and image distortion, all succeeding control points in the registration mode are located very quickly (<< 1 minute) and automatically.* In all other respects registration processing operations are identical to rectification processing operations.

---

* The extent to which control points lend themselves to automatic processing is treated in Section 5 of this report.

3.3 PERFORMANCE RESULTS

Two sets of full scenes were processed by both TRW Cubic Convolution and nearest neighbor resampling for precision registration. The first set consists of precision-corrected LANDSAT 1062-15190 and registered 1080-15192 (Washington/Baltimore area). The second set consists of two passes over an area in Canada, Scenes 1411-17381 precision-rectified and 1339-17391 registered. The precision coordinate system is a rotated UTM projection in all cases. The rectification passes utilized 10 GCP's randomly spaced within the image with an additional 5 RCP's to allow for obscuration or poor choice of control point features. The registration passes utilized 10 of the RCP's, not necessarily the same as the GCP's. The distortion correction process was repeated twice, once with the TRW Cubic Convolution process and once with nearest neighbor resampling, both using the same distortion coefficients generated by the distortion calculation process.

Change detected images were generated for each set by a process called principal component decomposition (Ref. 5). This involves treating each pixel in the corrected scene (one band at a time) as a two-vector, one component from the rectified scene at a given pixel location and the other component from the registered scene at the same pixel location. A linear two-dimensional vector rotation is determined for the scene as a whole and applied to the two-vector at each pixel, resulting in a new set of two-vectors. The image corresponding to one component of the new two-vectors is a linear combination of the original two scenes which contains the joint information in the scene, whereas the image corresponding to the other components represents the orthogonal information between the scenes, or the "change-detected" image. This process of generating change-detected scenes is linear (and reversible) and has the advantage over straight differencing of the two registered scenes of accounting for differences in average intensity and contrast range. Misregistration shows in these change-detected images as apparent lineal structure at the boundaries of scene features. No change between the scenes appears as neutral gray, while additive or subtractive differences appear black or white, with intensity proportional to the error magnitude.

A second process for evaluating registration error was utilized. A grid of points in the precision-corrected coordinate system was defined. Centered at each of these points, a 32 x 32 pixel subarea was extracted from both the reference and comparison images and submitted to the same automatic correlation process utilized for RCP location. A plot of registration error as a function of location was then generated for those points which could be correlated (the Canadian scenes had a high degree of cloud cover and haze) and a RMS error magnitude calculated.

Figure 3-2 shows band 5 of precision-rectified 1062-15190 and Figure 3-3 shows the same band of registered 1080-15192, both processed via TRW Cubic Convolution. Figures 3-4 and 3-5 show corresponding images for band 7. No contrast enhancement or MTF compensation has been performed on the scenes. (Since uncalibrated MSS bulk tapes were not available, the radiometric calibration of the detectors is as supplied by NASA.) The corresponding full scenes using nearest neighbor are indistinguishable from the above full scenes in a half tone reproduction with the exception of the presence of uncorrected commutation skew in the nearest neighbor products. Figure 3-6 shows the TRW Cubic Convolution change detected image and Figure 3-7 the nearest neighbor change-detected image for band 5. Figure 3-8 shows corresponding data for band 7. Figure 3-9 shows a plot of the misregistration on a grid of points in the scene.

For comparison purposes, the two Washington/Baltimore scenes were independently processed for geodetic correction to the same map projection using only GCP's (no RCP's). The resulting change-detected image for band 5, Figure 3-10., shows noticably greater misregistration than that resulting from the use of RCP's, due to the much lesser precision of the GCP locations than RCP locations.

Subscenes were selected from the registered full scenes and change-detected images and printed at a much larger scale (Figures 3-11 and 3-12). Table 3-1 shows the image coordinates for each of the subareas and the corresponding subscene areas. A comparison of the nearest neighbor and TRW Cubic Convolution change-detected images shows the registration errors due to line- and pixel-replication and uncorrected commutation skew aspects of nearest neighbor resampling.

Figure 3-2. Precision-Rectified 1062-15190-5 Using TRW Cubic Convolution
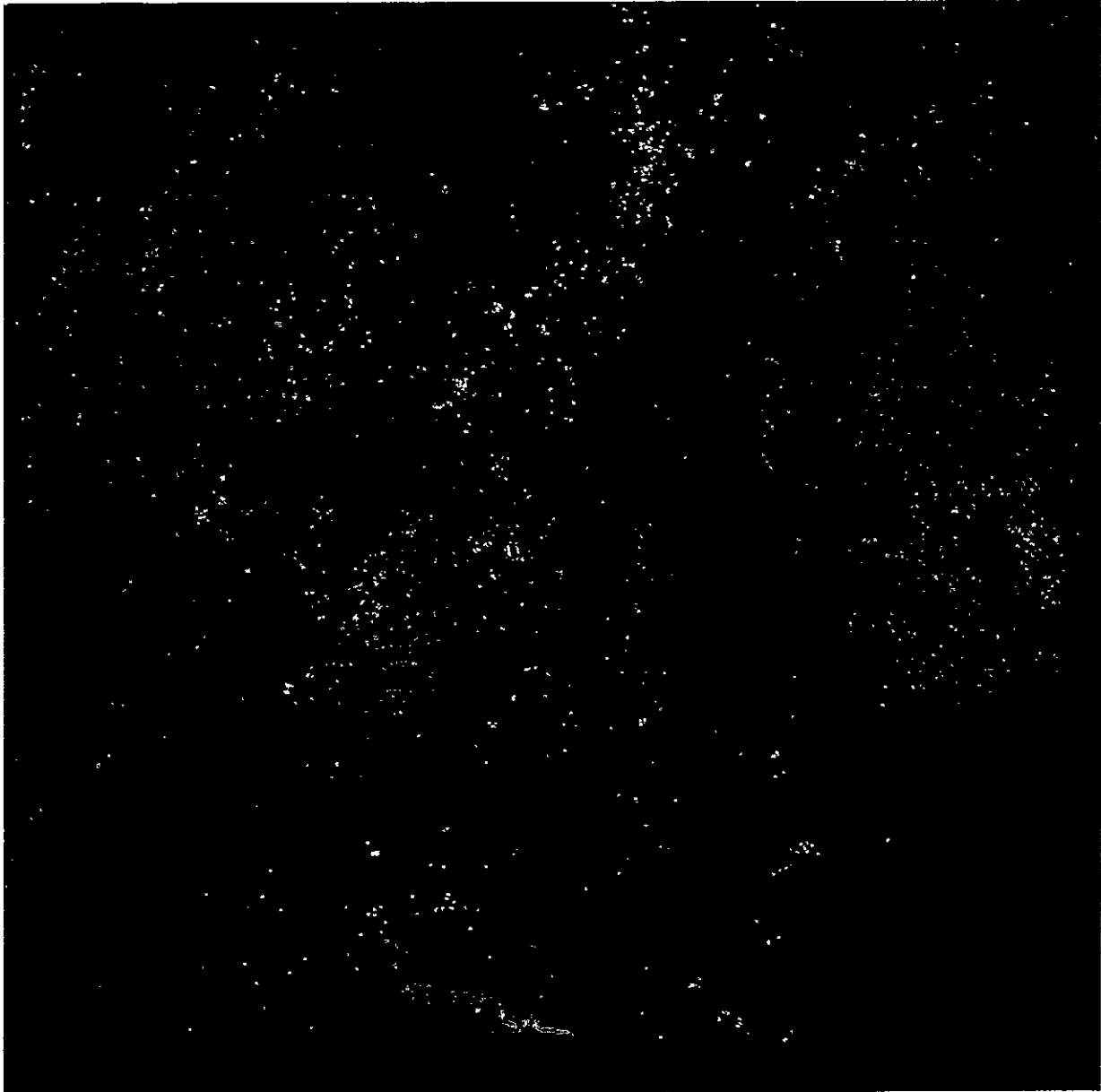
Figure 3-3. 1080-15192-5 Registered to 1062-15190-5 - The image was
rectified using the TRW Cubic Convolution Process
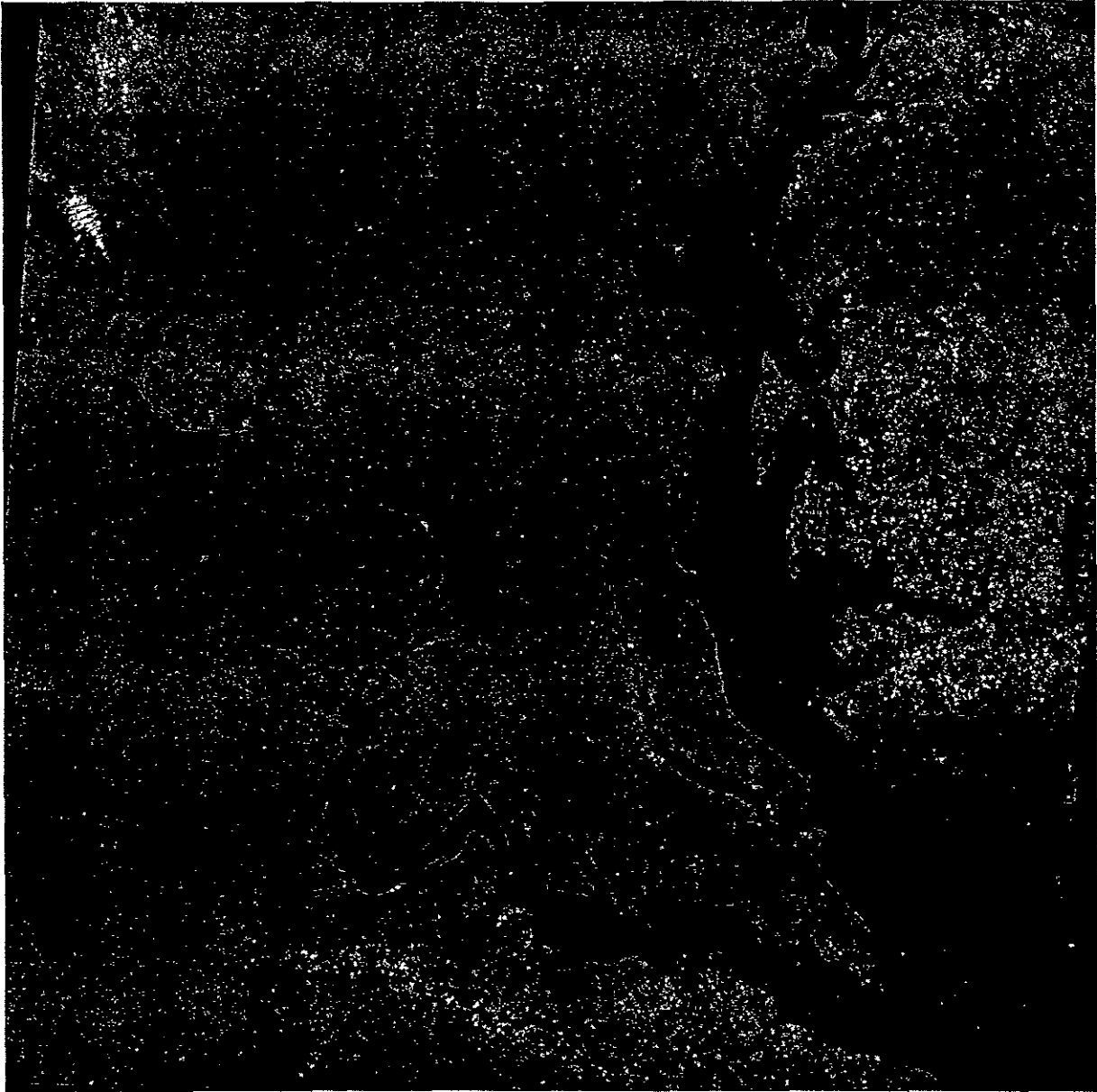
Figure 3-4. Precision-Rectified 1062-15190-7 - Using TRW Cubic Convolution
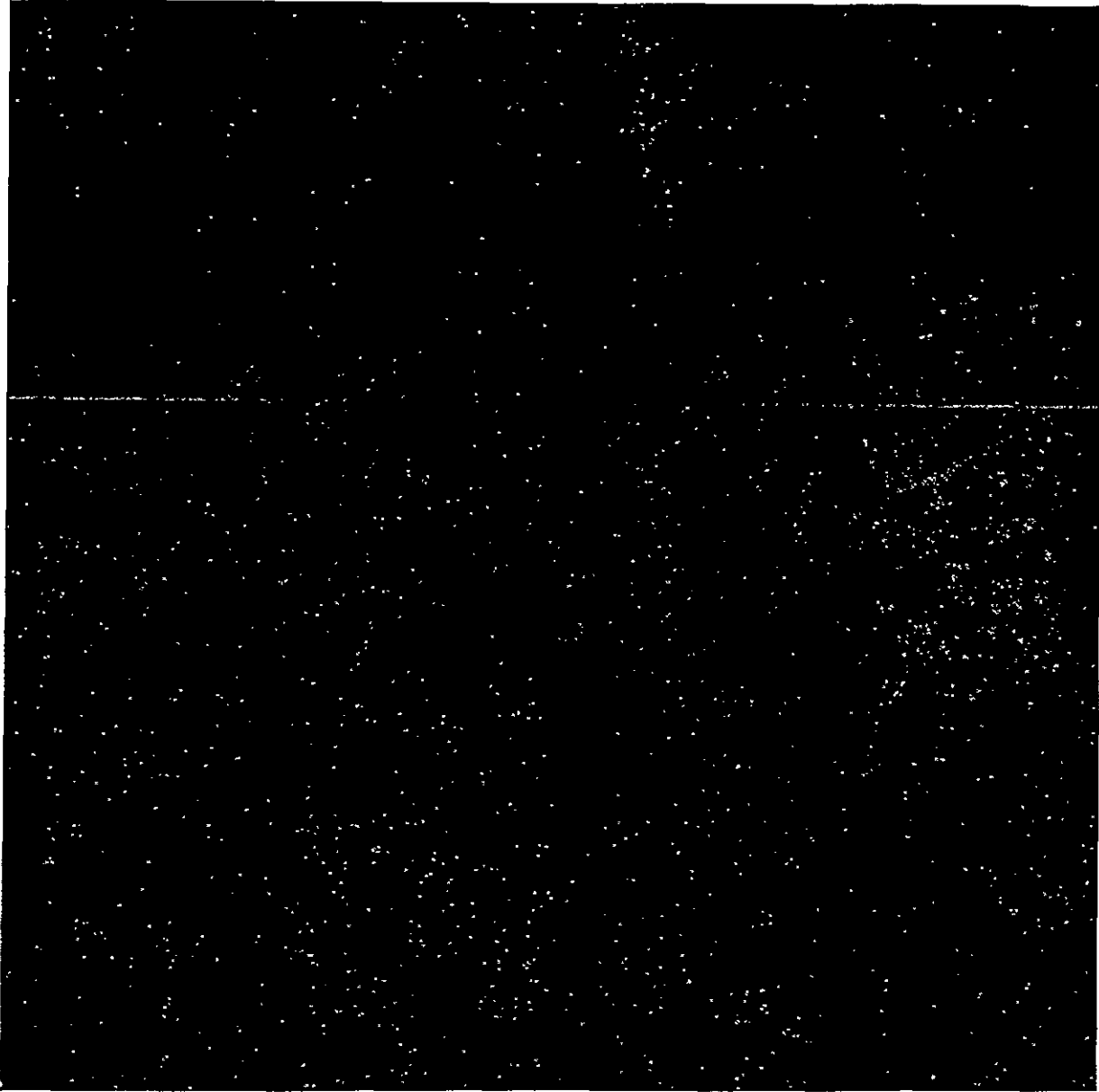
Figure 3-5. 1080-15192-7 Registered to 1062-15190-7 - The image was
processed using the TRW Cubic Convolution Process
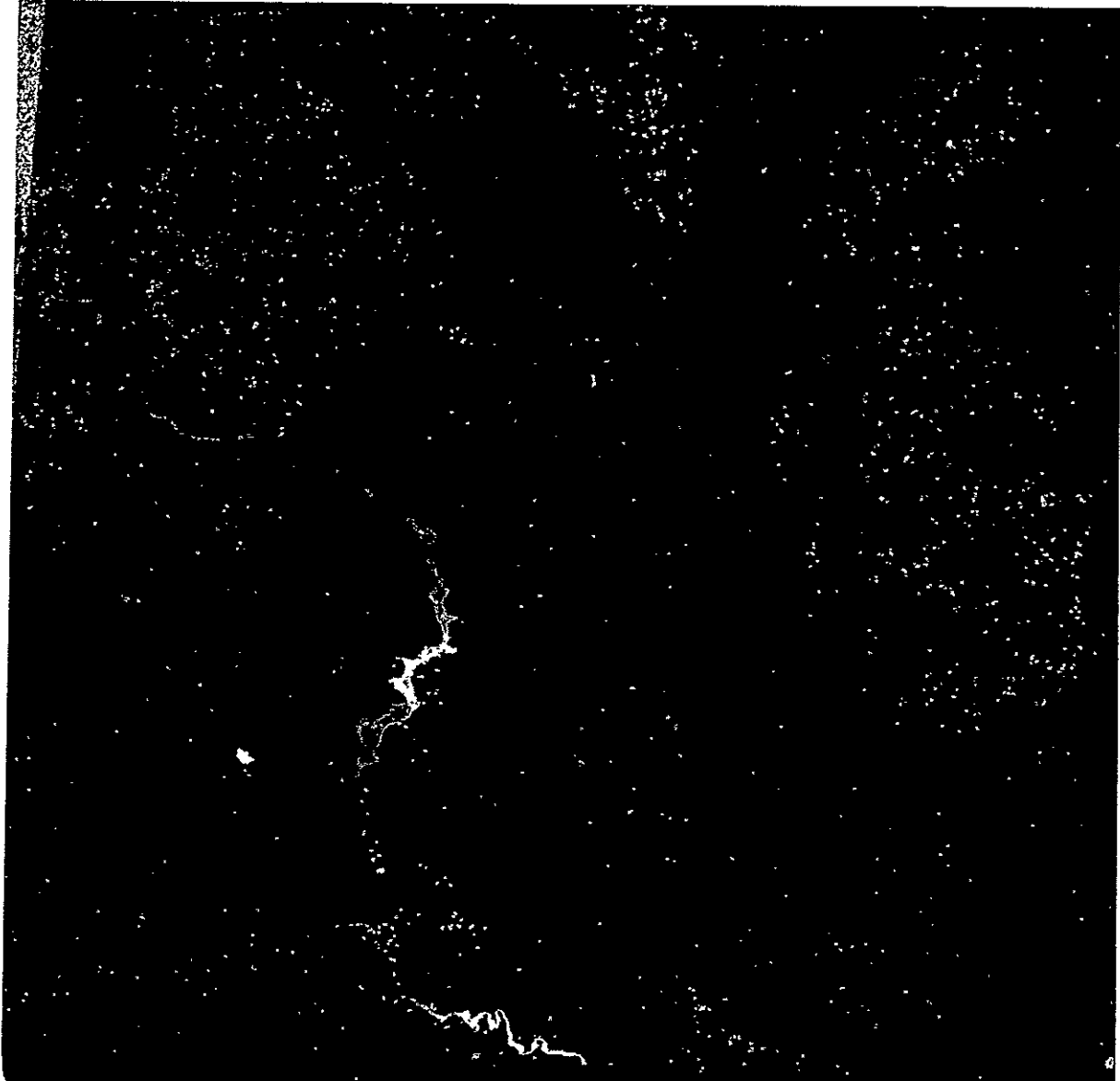
Figure 3-6.   Change Detection Image of 1062/1080, Band 5, Processed by
TRW Cubic Convolution

Figure 3-7. Change Detection Image of 1062/1080, Band 5, Processed by
Nearest Neighbor Interpolation
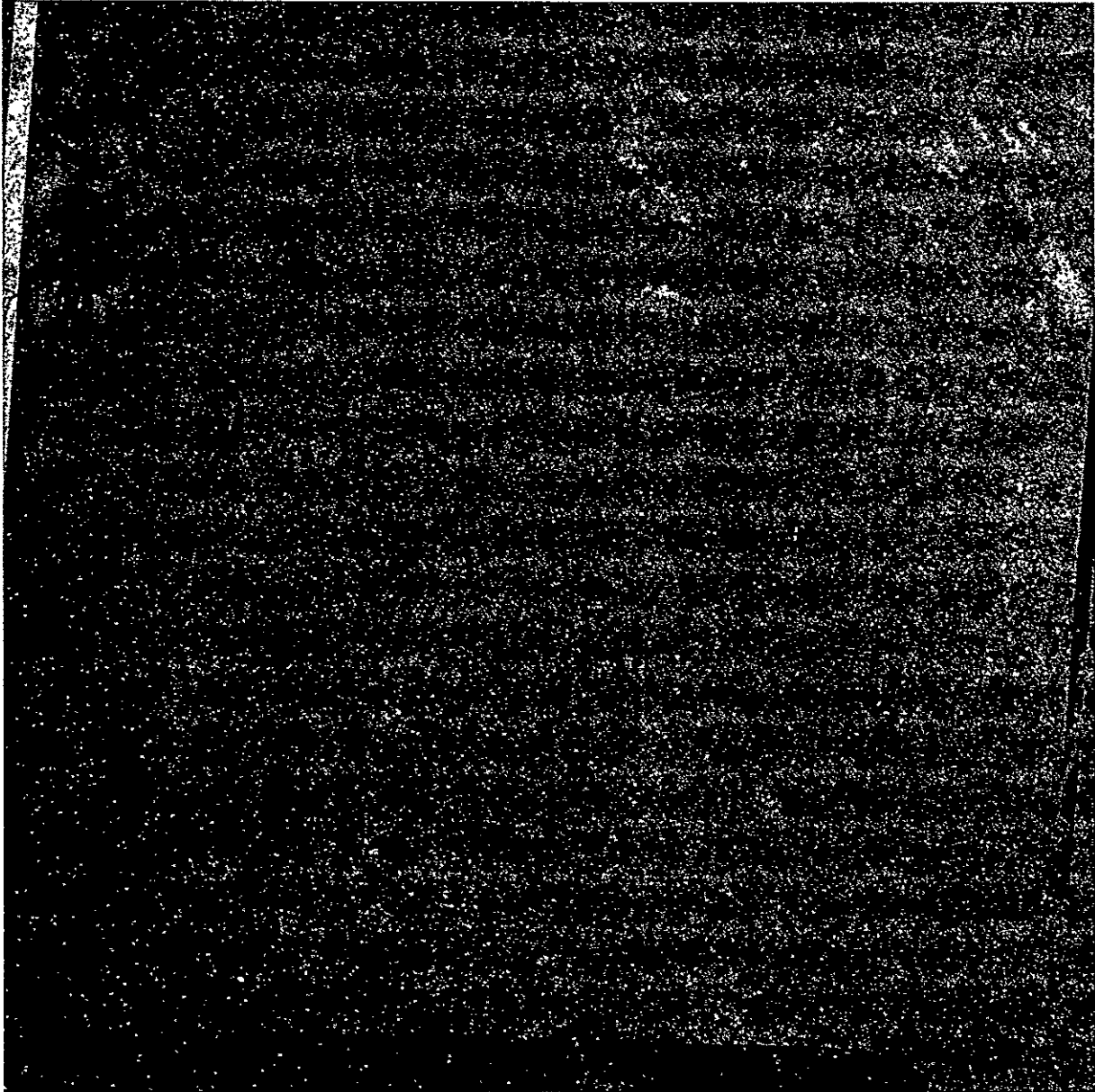
Figure 3-8. Change Detection Image of 1062/1080, Band 7, Rectified by
TRW Cubic Convolution
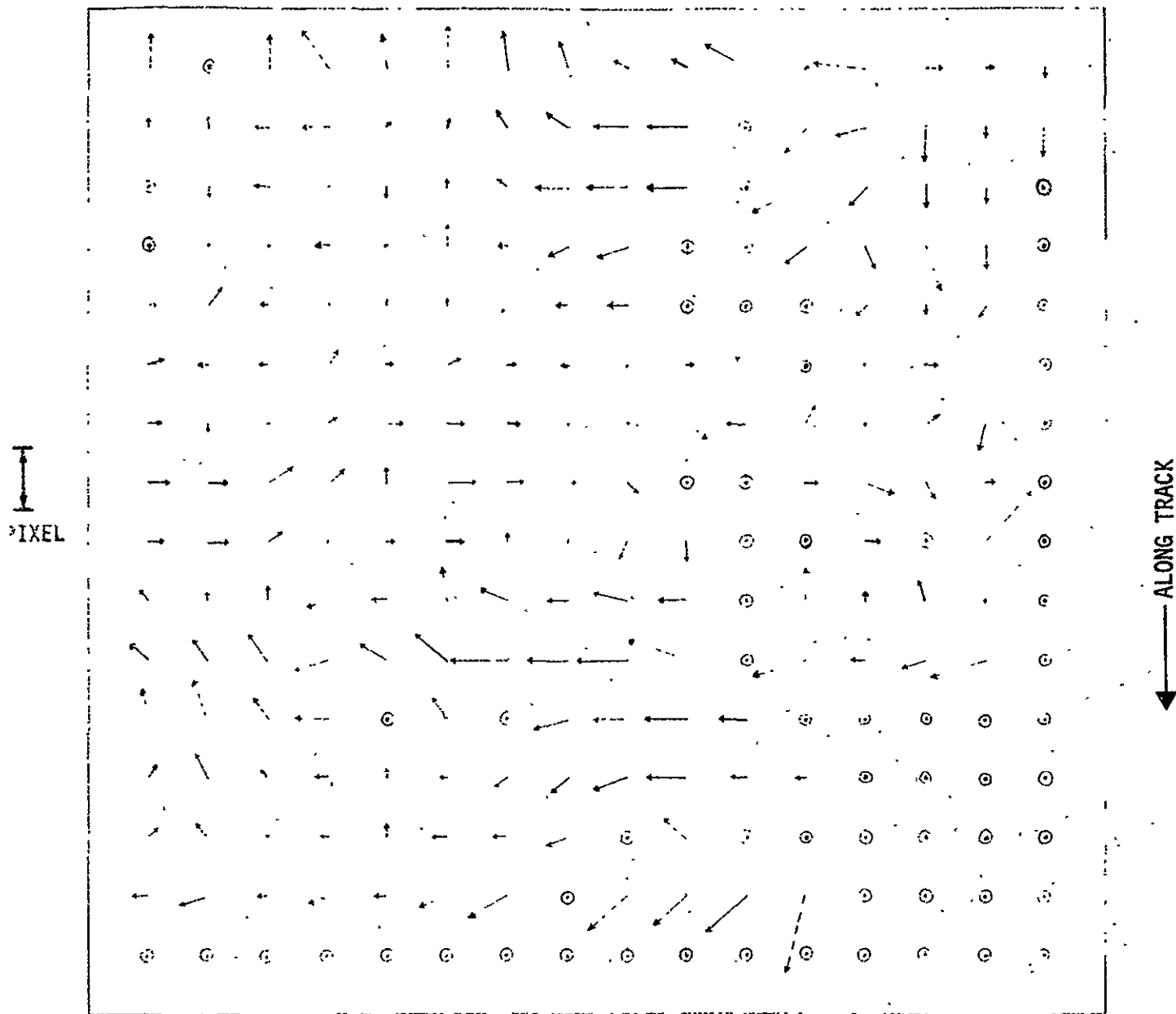
⊙ - NO CORRELATION

1080 - 1062   REGISTRATION

Figure 3-9.   Plot of 1062/1080 Misregistration at Points on a
Superimposed Regular Grid
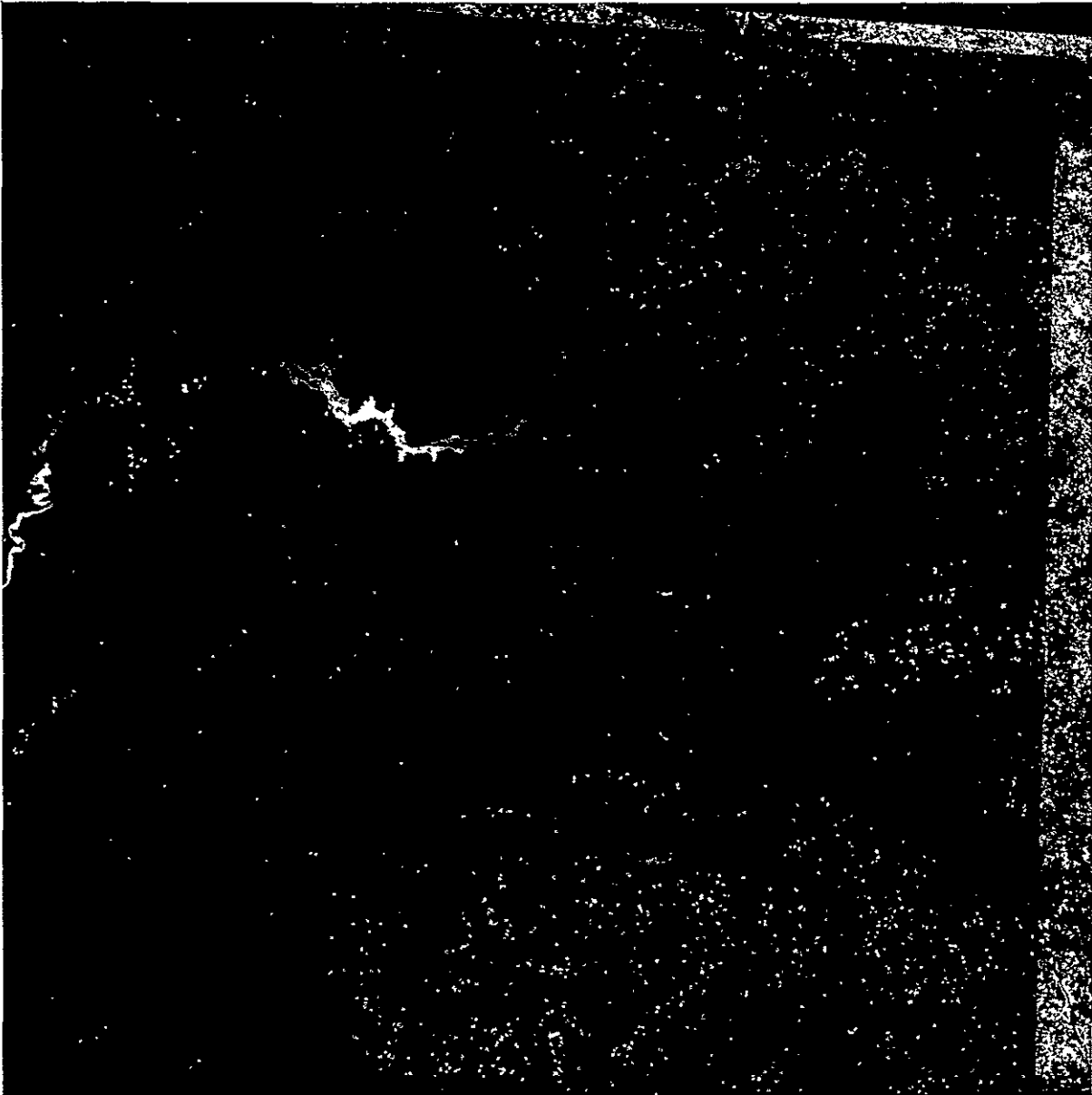
Figure 3-10.   Change Detection Image of Independently Processed 1062 and
1080, Band 5

CUBIC CONVOLUTION

NEAREST NEIGHBOR

1062
BAND FIVE
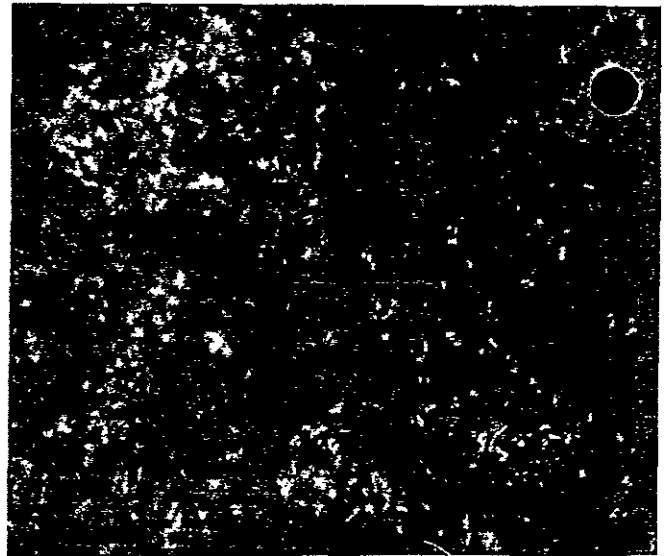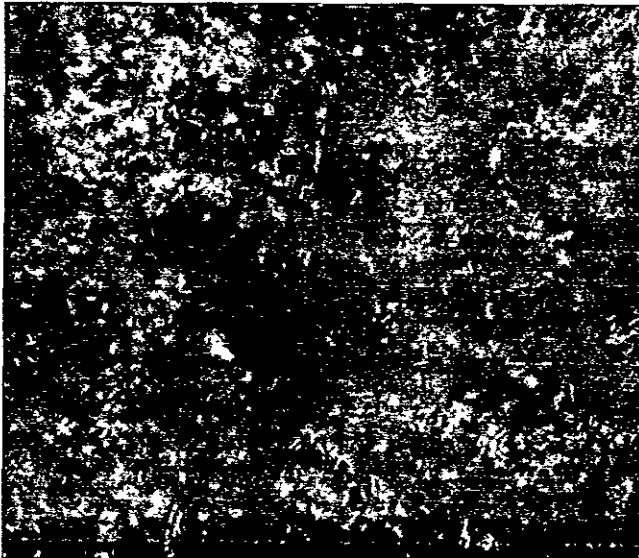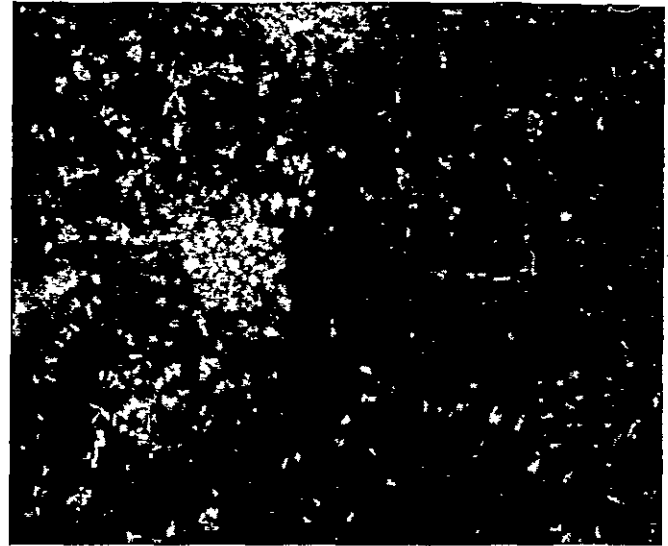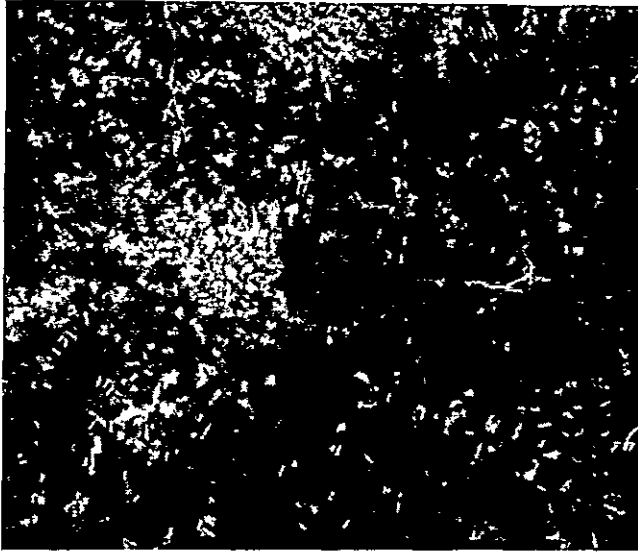
CHANGE
DETECTION

Figure 3-11. Subscene Details from Upper Left Portion of 1062, Band 5, from Figures 3-2, 3-6, Nearest Neighbor Resampled Image, and Figure 3-7. This area was selected specifically because of its rural character. Structured areas show differences more clearly.

NEAREST NEIGHBOR

CUBIC CONVOLUTION

1062
BAND 5
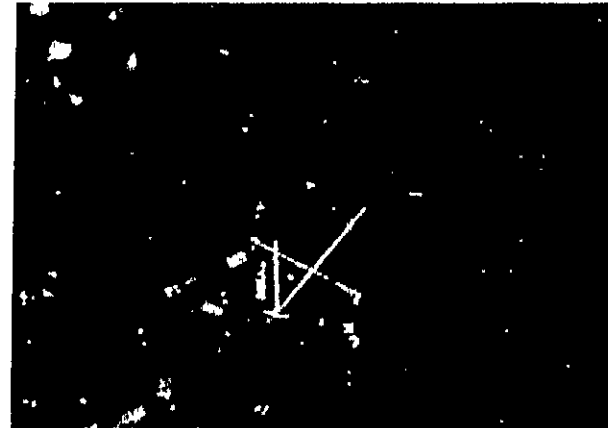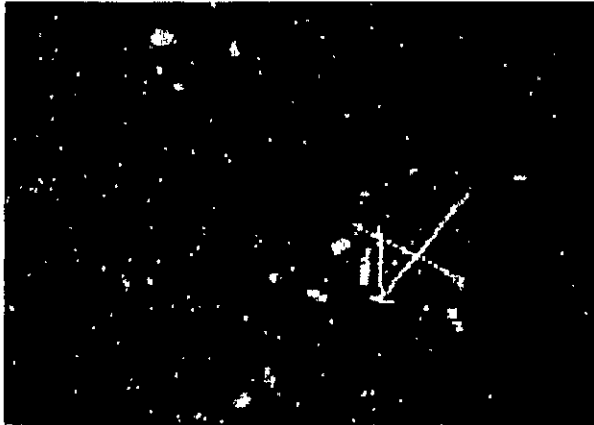
CHANGE
DETECTION
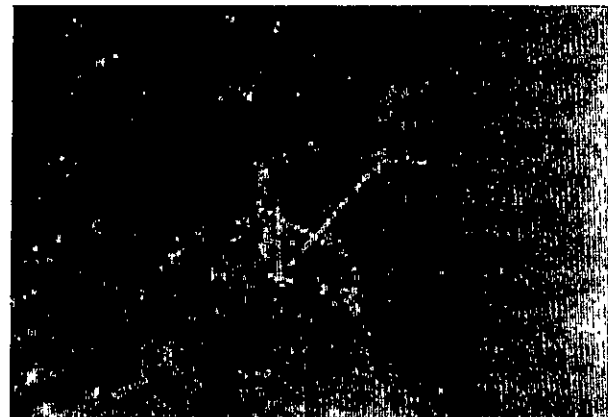
Figure 3-12.   Subscene Details from Lower Right Portion of 1062, Band 5,
from Figures 3-4, 3-8, Nearest Neighbor Resampled Image,
and Figure 3-9.

Table 3-1. Subscene Locations

DETAIL FIGURE NUMBER	UPPER LEFT CORNER	
	Lines	Pixels
Figure 3-11	500	500
Figure 3-12	2106	1956

The Canadian scenes contained a significant percentage of cloud cover in all scenes, resulting in somewhat less registration accuracy. The full scenes as processed by TRW Cubic Convolution for band 6 are shown in Figures 3-13 (precision-rectified 1411-17391) and 3-14 (registered 1339-17381) with the change-detected image in Figure 3-15.

3.4 THROUGHPUT AND IMPLEMENTATION APPROACH

Processing for this task was performed using a single mini-computer CPU with 28K 16-bit words, two 58-MB disks, a 1600 bpi, 120 ips tape drive, a CRT display and image resampling via TRW Cubic Convolution in software. Processing times were compiled for each of the process subfunctions by -actual wall clock timing and are used in this section to extrapolate throughput capability and hardware requirements of a 30-scene-per-day precision registration system. Significant events in the process for timing consideration are: input tape reformatting and NASA line-length correction removal; control point processing; distortion calculation; along-scan resampling; across-scan resampling; and output tape formatting. (It is noted that 30 scenes of 4 bands per 8 hours leaves only 16 minutes per scene.)

Input-tape reformatting and de-line-length correction is limited by tape speed to 6.5 minutes per full scene, using 800 bpi, 120 ips dual drives for overlapped rewind/mount with transfers. Use of 1600 bpi tapes with full-line records would allow storage of a full scene on one tape and transfer of the scene to disk in 3.3 minutes. Output tape formatting takes longer due to generation of a square aspect ratio (3240 x 3240 pixels) from the input non-square aspect ratio (3240 x 2340 pixels) and requires 8.5 minutes/scene for 800 bpi tapes and 4.5 minutes for 1600 bpi.

Control point processing requires about 40 seconds per GCP if the control points are manually designated, or approximately 11 minutes for a rectification pass with 15 control points. If the control points are already in the control point library and if the semi-automatic correlation process is successful, control point processing takes only 20 seconds, or 4.5 minutes total for 10 RCP's per scene. Once the control points have been located, distortion coefficient calculation requires only 0.5
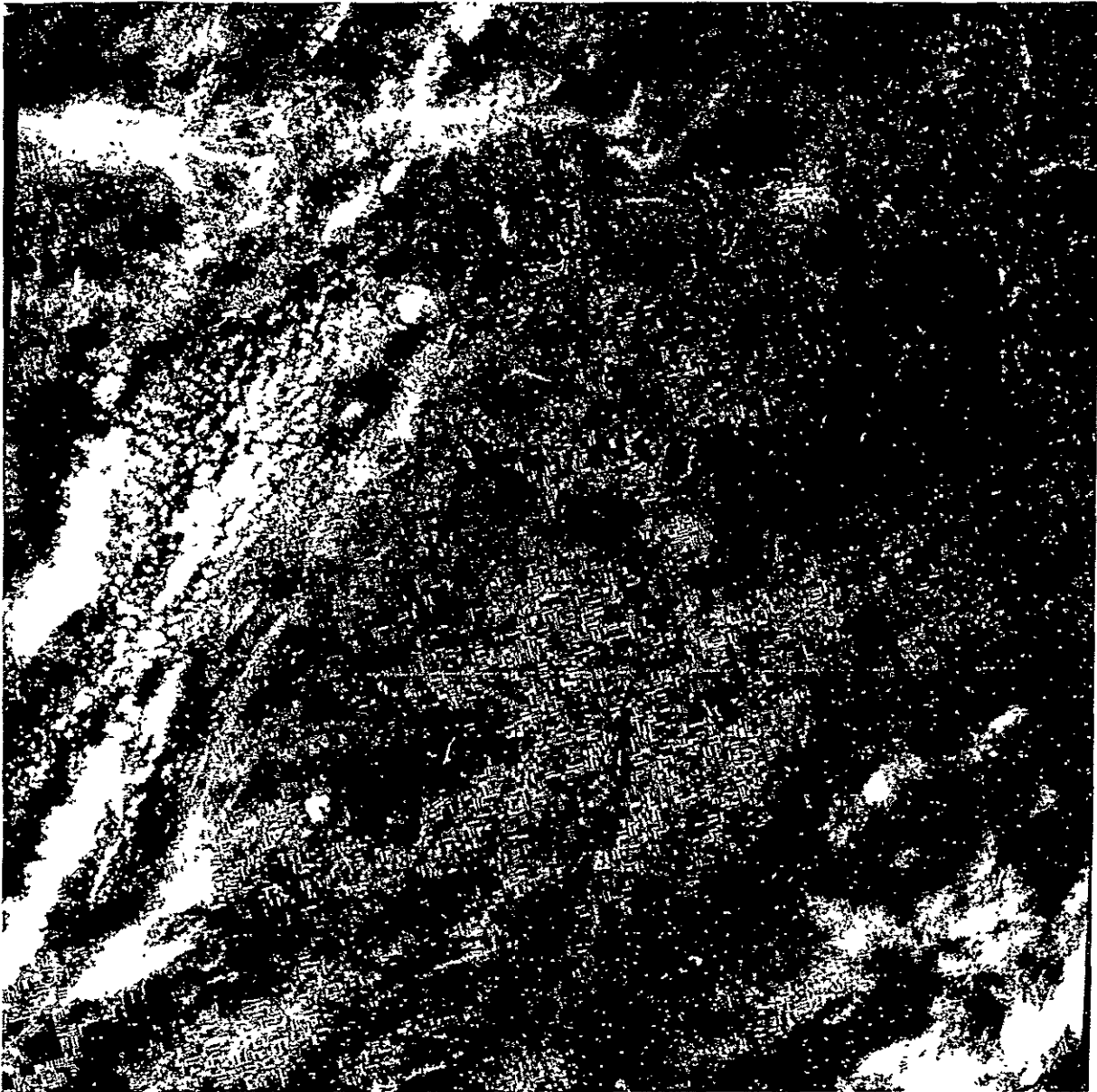
Figure 3-13. Precision Rectified 1411-17391-6 Using TRW Cubic Convolution
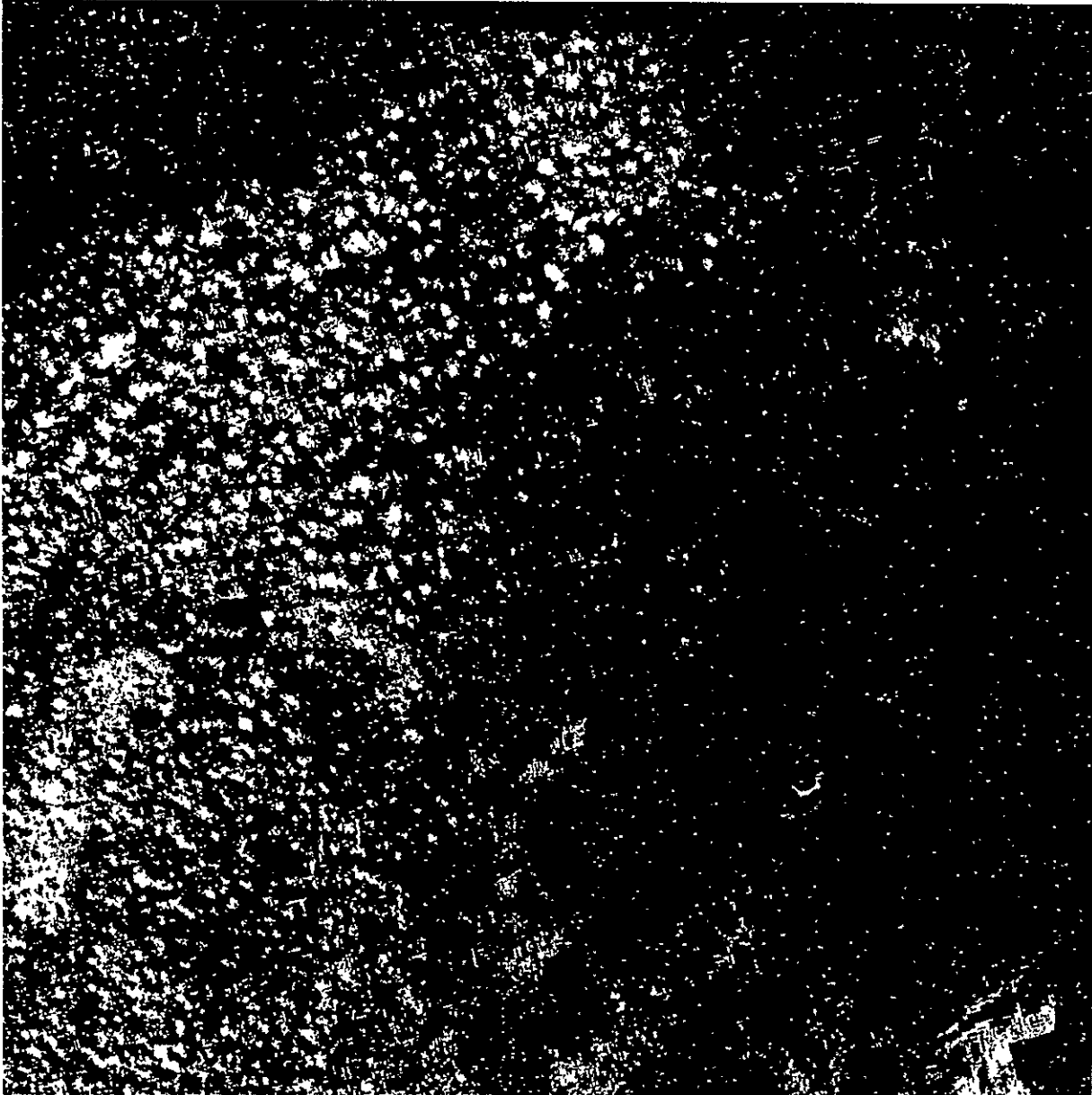
Figure 3-14. 1339-17381-6 Registered to 1411-17391-6 - The image was
rectified using the TRW Cubic Convolution Process
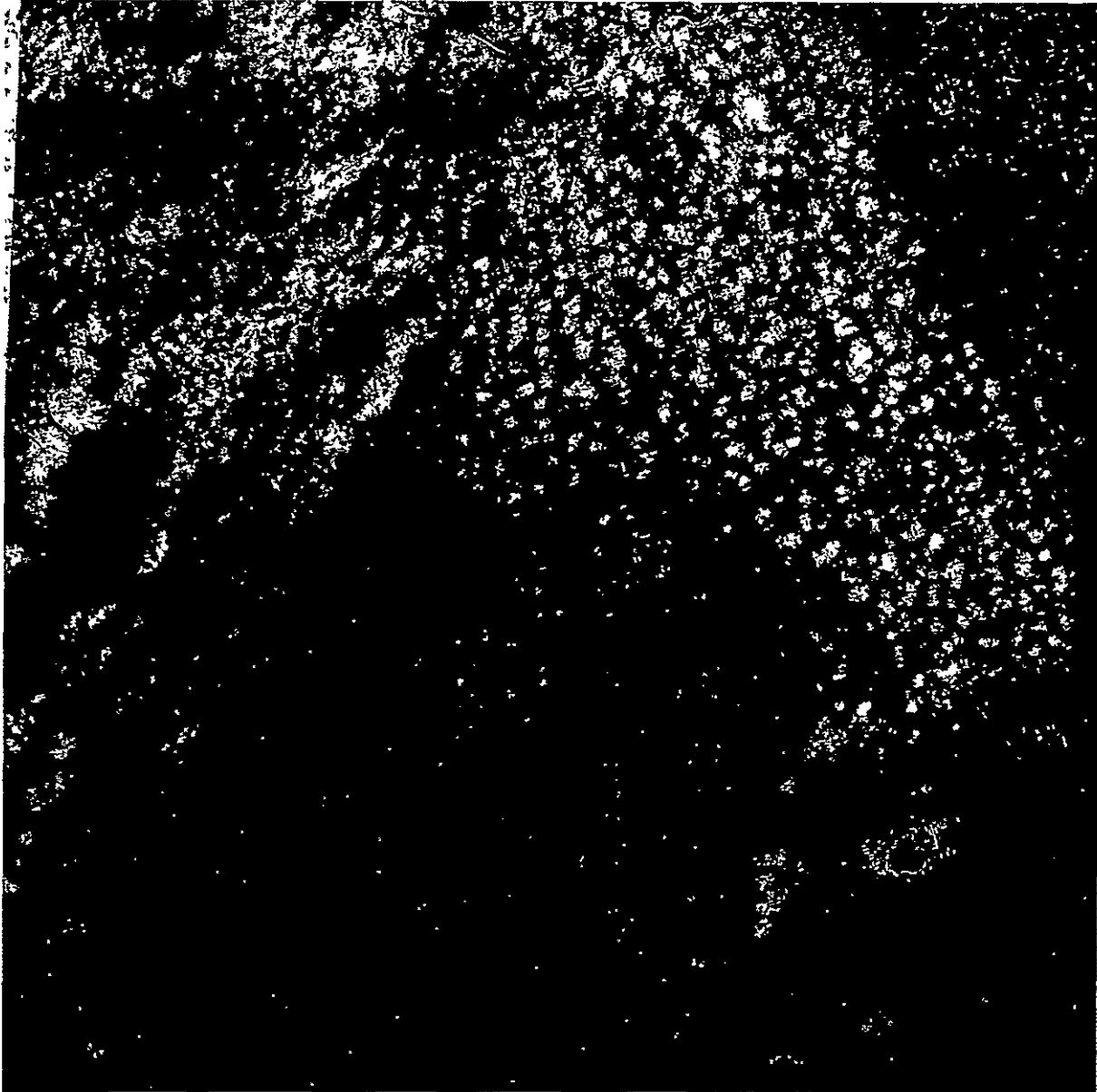
Figure 3-15. Change Detection Image of 1411/1339, Band 6, Rectified by TRW Cubic Convolution

minutes. Initial setup adds approximately one minute to the distortion calculation time in a production environment.

Image resampling via TRW Cubic Convolution in software requires 62 minutes for four bands. Software optimized for nearest neighbor re-sampling would require approximately 20 minutes per scene. Utilization of a microprocessor (20 µs/pixel) would reduce resampling time to 14 minutes/scene for both TRW Cubic Convolution and nearest neighbor due to I/O limits in the microprocessor. The special-purpose hardwired TRW Cubic Convolution Interpolator (CCI), using highly parallel operation would allow resampling in only 7.5 minutes/scene for both TRW Cubic Convolution and nearest neighbor, limited by disk transfer rates. Use of 3330-class disks would cut the CCI resampling in half to 3.5 minutes/scene.

Processing a minimum of 30 scenes/8 hours necessitates special processor approaches to resampling and parallel operation of distortion calculation and correction. A microprocessor implementation would require overlap of resampling and output formatting. Input and output tape density of 1600 bpi is assumed. The microprocessor input/output, initialization, and control would be handled by a low-cost minicomputer, while a separate processor would handle input and output tape reformatting, control point processing, and distortion calculation. Three large (60 MB) dual-ported disks are utilized in a triple buffer arrangement to provide necessary overlap. If a substantial portion of the control points require manual entry, a fourth disk is needed for additional overlap.

If the TRW CCI is utilized together with 1600 bpi tapes, three 2314-class disks will provide the necessary overlap to achieve 30 scenes per 8-hour day. In fact, if two 3330-class disks are used with the CCI, and 30 scenes per day is required only for those scenes with control points established in the Control Point Library (CPL), it is feasible to process the 30 scenes with a single CPU. In reality, partial cloud cover and less-than-optimal RCP's may limit the feasibility of this configuration, especially in light of the low cost of the second CPU. Control point requirements are addressed in more detail in Section 5 of this report.

·3.5 CONCLUSIONS

It has been demonstrated that operational full scene registration two within a fraction of a pixel is both desirable and feasible, with as few as 10 Registration Control Points per scene. The registration takes place at the same time as geodetic correction, with the first scene of an area establishing geodetic control and subsequent scenes being registered to it with the same process. TRW Cubic Convolution resampling is superior to nearest neighbor with respect to registration accuracy (and thus change detection performance) image quality: nearest neighbor results in image discontinuities and is unable to correct detector commutation skew.

Processing time requirements are compatible with 30 scene/8-hour-day throughput utilizing a modest complement of existing off-the-shelf mini-computers and peripherals. Special purpose hardware resampling, either by high-speed microprocessor or by hard-wired parallel processing algorithm, is required to achieve these rates. Use of 1600 bpi line-interleaved CCT's would facilitate processing and reduce the hardware required. Higher throughput systems (several hundred scenes/day) require alternatives to CCT input/output and more hardware to effect parallelism.

Manual designation of GCP's or RCP's requires between 30-90 seconds per control point, depending upon the operator's familiarity with the scene and the nature of the features used as control points. Automatic techniques for GCP/RCP location in subsequent scene data achieve superior location performance over sequential similarity detection alone, at some cost to through-put. Such techniques reduce search time to ~1 second per control point, with location accuracies of ~0.1 pixel.

4.0 RESAMPLING TECHNIQUE

4.1 TASK DESCRIPTION

The objective of this task of the contract was to precision-correct (rectify) LANDSAT MSS data using nearest neighbor interpolation and TRW's Cubic Convolution Process, and to evaluate the results in terms of radiometric, geometric and resolution performance, as well as overall implementation approach. Processed data was also subjected to feature classification at TRW to determine the impact of resampling methods on classification results. Processed data was delivered to the Jet Propulsion Laboratory (JPL) for similar analysis.

All-digital techniques were utilized to process bulk CCT data furnished by NASA, making use of auxiliary Bulk Image Annotation Tape (BIAT) data for the spacecraft attitude, ephemeris, altitude, etc. Use was also made of Ground Control Points (GCP's), when available, to rectify scene data.

BIAT, GCP and scene data for scene 1080-15192 of the Baltimore-Washington area was chosen for analysis. Precision correction of bulk CCT data was realized by both nearest neighbor interpolation and TRW's Cubic Convolution Process, using the same geometric warp in both cases. Details of the full scene data are included in this report, and illustrate clearly the difference in appearance of image data resampled by the two methods: nearest neighbor resampled data is characterized by 1 pixel discontinuities; whereas Cubic Convolution Processed data is free of this artifact, with no significant loss of information. Data for scene 1072-18001 (Goldfield, Nevada) was system corrected using nearest neighbor interpolation and Cubic Convolution, and delivered to JPL for multispectral classification analysis.

In order to objectively compare scene data processed by the two methods, a high resolution (2.4m) aerial image was blurred to 22.4m resolution, with 87.5% overlap of successive samples. Every eighth such blurred sample was used as a basis for interpolation at the seven interstitial positions (in each direction). Interpolated results were compared to the blurred image, and error histograms were generated.

Additional resampling evaluations with LANDSAT data were performed in a previous study (Reference 4). These evaluations included spatial frequency analyses and comparisons of resampled data with sinx/x resampled data for the same warp. For convenience, the highlights of these studies are reproduced herein as well.

Classification of resampled data was performed at TRW by means of a supervised Bayes classifier (Reference 7). This method consists of first identifying training areas, and then testing every pixel in turn. Both single scene (4 band) data and registered, two scene (8 band) data were so evaluated, for data processed by both nearest neighbor interpolation and the TRW Cubic Convolution Process.

4.2 TECHNIQUE

The problem of correcting bulk LANDSAT CCT data can be divided into two tasks: 1) It is necessary to determine the geometric distortion present in the bulk data, which it is desired to correct[*]; and 2) It is necessary to process (resample) all the bulk data values so as to produce corrected data. Determination of the desired geometric transformation is a straightforward calculation. TRW (Reference 4) employs a piecewise bilinear distortion model approximation to the distortions calculated with high accuracy at fewer than 100 image points. The accuracy of this geometric transformation calculation is the result of: 1) Using precision models for spacecraft attitude uncertainty, spacecraft motion, MSS mirror scan nonlinearity, earth curvature and rotation; and 2) Using a piecewise low order approximation to the accurately computed distortion values, thereby eliminating modeling errors.

Once the image distortion is computed, it is necessary to correct (or resample) the bulk data, so as to produce corrected image data defined on a regular grid of pixels. Thus, if the image distortion is approximated by a piecewise bilinear model of the following form:

$$\delta x = u-x = a_0+a_1x+a_2y+a_3xy$$

$$\delta y = v-y = b_0+b_1x+b_2y+b_3xy$$

where

u,x = input, output pixel coordinates

v,y = input, output line coordinates

δx = pixel distortion

δy = line distortion

$a_0, \ldots, b_3$ = bilinear distortion model coefficients

---

[*] In general there may also be radiometric (sensor calibration) errors in the bulk data. These errors can be treated very simply by the straightforward table look-up method, prior to geometric correction.

then the corrected image data is in general computed from

$$f(x,y) = \sum_{u,v} g(u,v) \; h(x-u, \; y-v)$$

where

g = bulk data values

h = interpolation kernel.

Note that for integer values of x,y the corresponding bulk image coordinates

$$u = x + \delta x$$
$$v = y + \delta y$$

are non-integer values - hence, the need for interpolation.

For spatial frequency band-limited data, the ideal interpolation kernel is of the form

$$\frac{\sin \pi (x-u) \; \sin \pi (y-v)}{\pi^2 (x-u)(y-v)}$$

However, this function has significant magnitude until very high $|x-u|$, $|y-v|$; thus, the interpolation convolution includes an extremely large number of summation terms for each interpolated value (> 1000), rendering high throughput implementation impractical if not impossible. Thus, in light of this and the fact that LANDSAT MSS data is not band-limited, but in fact contains aliasing errors (which are not removable after sampling without severe resolution degradation), a limited-extent approximation is made to this function. We are concerned here with only two approximations: nearest neighbor and the TRW Cubic Convolution Process.

The TRW Cubic Convolution Process employs a cubic spline function approximation to sinx/x. The cubic spline in one dimension is defined on a grid of four points as shown in Figure 4-1. Equivalently, in two dimensions a grid of bulk data values 4 pixels x 4 pixels is required to resample one corrected image pixel.

The kernel for nearest neighbor interpolation is also shown in Figure 4-1. For nearest neighbor resampling, the bulk data value closest to the position of the correct image pixel (at $u = x + \delta x$) is chosen for the result of the interpolation operation. Clearly this is equivalent
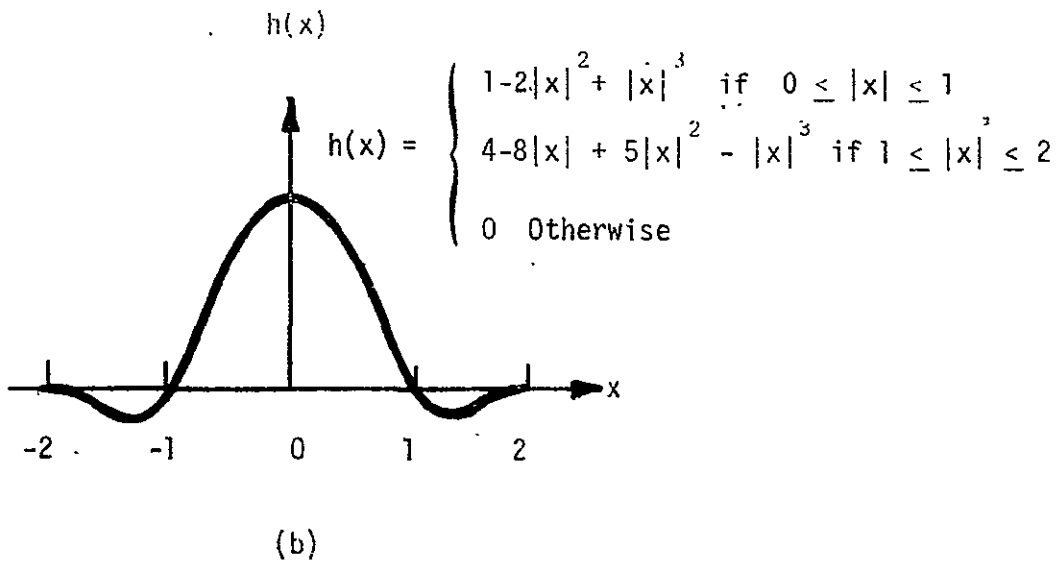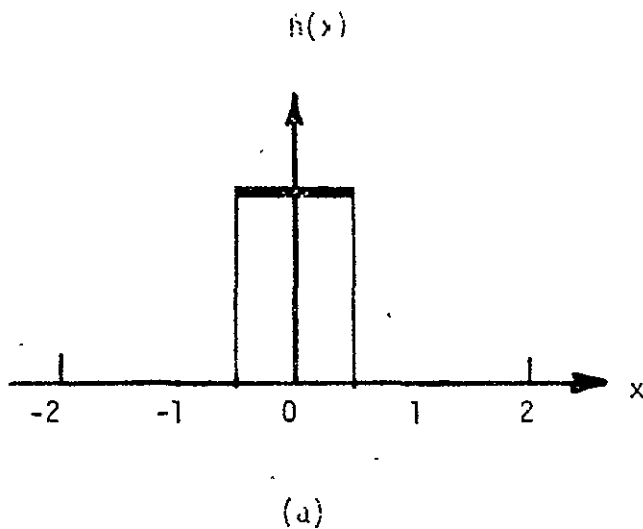
$$h(x) = \begin{cases} 1-2|x|^2 + |x|^3 & \text{if } 0 \le |x| \le 1 \\ 4-8|x| + 5|x|^2 - |x|^3 & \text{if } 1 \le |x| \le 2 \\ 0 & \text{Otherwise} \end{cases}$$

Figure 4-1. Two Interpolation Kernels

The two kernels correspond to (a) nearest-neighbor interpolation and (b) TRW's Cubic Convolution Process.

to a position error throughout the nearest neighbor resampled image as
large as $\pm$ .5 pixel, or $\pm$ 1 pixel registration error between scenes, as
shown in Figure 4-2. Compared to sinx/x resampling, nearest neighbor re-
sampled data is characterized by one pixel discontinuities.

In practice, the resampling process is implemented as two one-
dimensional interpolations: First in the direction of bulk data scan
lines, and then in the orthogonal direction. In this manner, scan re-
lated distortions (line length, mirror scan nonlinearity, and detector
commutation time) can be accurately corrected as shown in Figure 4-3.
Also, there is a small improvement in processing time over a single pass
interpolation method (for example, along output lines).

A numerical example of the interpolation calculation is contained
in Appendix C.

□ - BULK DATA VALUES

O - NEAREST NEIGHBOR SAMPLES
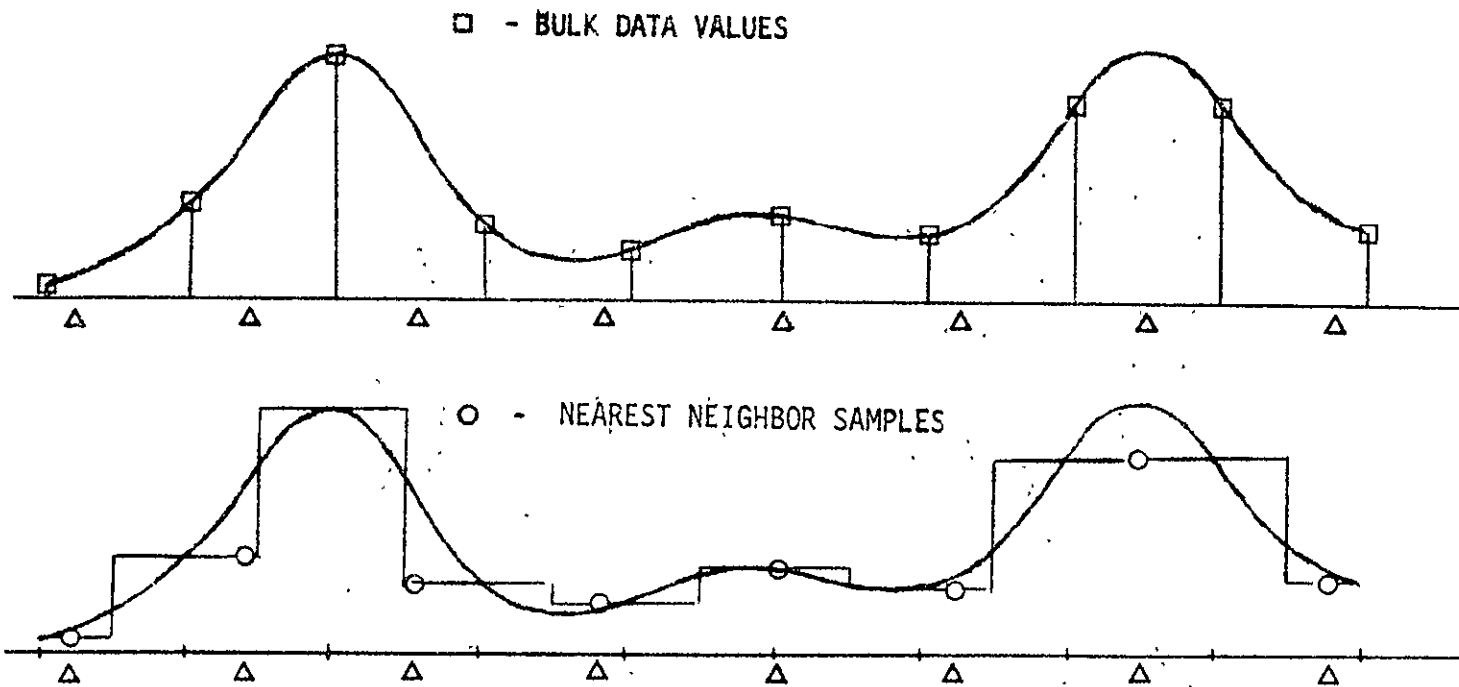
Note: Input (bulk) data values to be interpolated are defined by the solid vertical lines. The symbol "Δ" denotes output positions (or equivalently times) for which interpolated values are desired. The result for TRW Cubic Convolution would be indistinguishable from the original data (smooth curve).

Figure 4-2. Nearest-Neighbor Interpolation in One Dimension
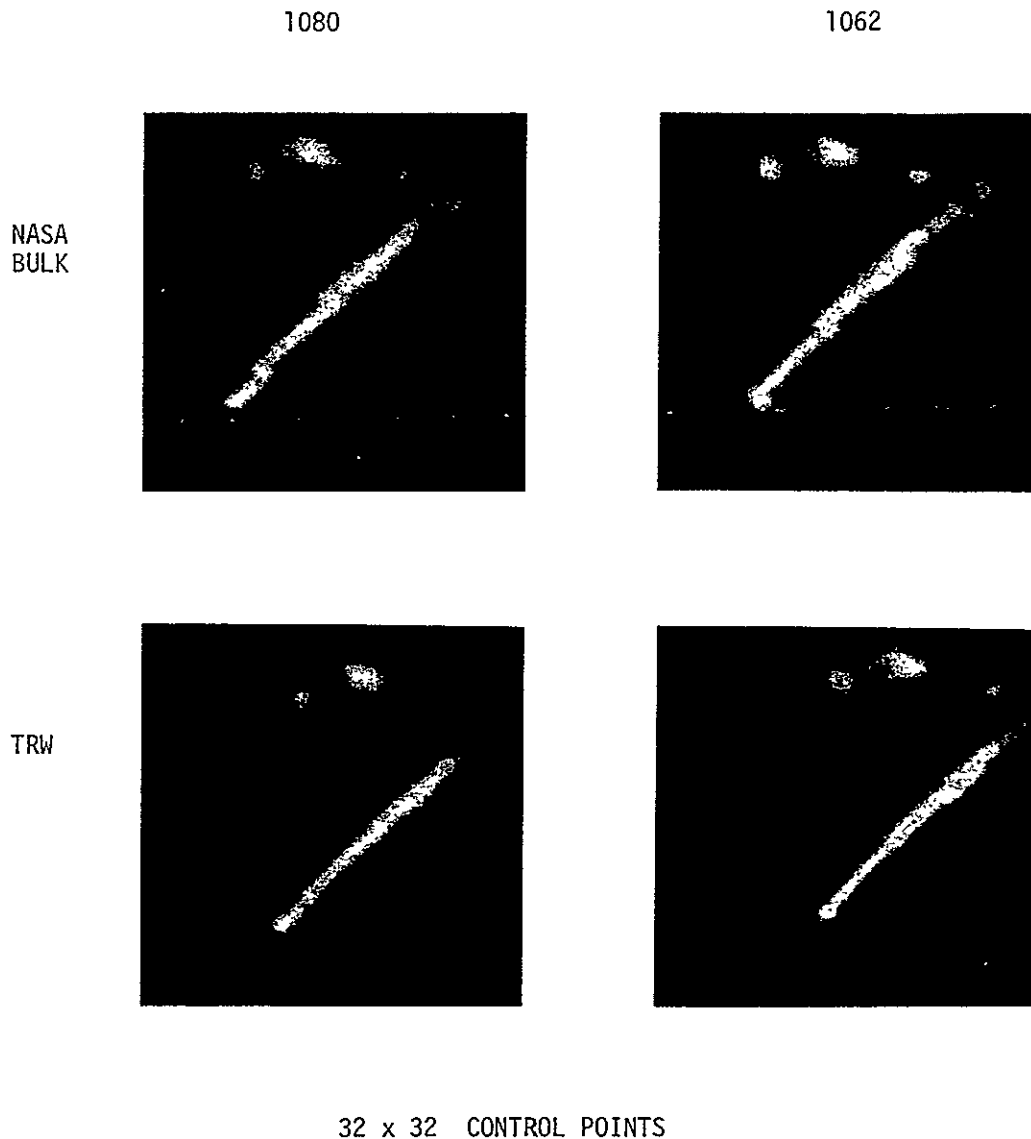
FIGURE 4-3. CORRECTION OF ALONG SCAN RELATED DISTORTIONS

The 32x32 pixel images on the upper row were obtained from nearest neighbor length corrected bulk CCT data for 2 scenes 18 days apart in time (1062-15190 and 1080-15192). The images on the lower row were along scan corrected by TRW's Cubic Convolution Process.

4.3 RESAMPLING RESULTS

Figure 3-2 shows the full scene 1062-15190-5, precision rectified and resampled using TRW's Cubic Convolution Process. Figure 3-12 shows a detail from the full image data of Figure 3-2, as well as the corresponding detail from the full scene data resampled using nearest neighbor interpolation (with the identical geometric transformation). Note the one pixel discontinuities in nearest neighbor resampled data, in contrast to data processed by TRW's Cubic Convolution Process. Figure 3-12 also shows change detection results for precision registered full scene data, using TRW's Cubic Convolution Process and nearest neighbor interpolation. Note the presence of a larger number of interpolation artifacts in the change detection imagery resulting from nearest neighbor interpolated data, in contrast to data processed by TRW's Cubic Convolution Process.

In a previous study (Reference 4), certain other tests comparing performance of various interpolation algorithms were performed. In view of their pertinence, key results are reproduced here as well. Thus, Figure 4-4 shows change detection (error) imagery obtained by resampling an image detail at pixel positions midway between the values in bulk LANDSAT data. The reference image was obtained using $\pm$ 15 point sinx/x interpolation (i.e., a grid of 30 x 30 points was used to resample each reference pixel value); and comparison imagery was resampled in turn with: nearest neighbor (one point), bilinear (2x2 point), TRW Cubic Convolution (4x4 point), and sinx/x (10x10 point) interpolation. The change detection or error imagery was obtained by computing pixel by pixel the absolute value of the difference of corresponding pixel values in the reference and comparison image data. Figure 4-5 shows the histograms of these error (change detection) images. Note that with the exception of 1 pixel (out of nearly 50,000) Cubic Convolution resampled image data yielded the best results, in terms of both the change detection (error) images and the error histograms.

SINC(X±5)   TRW CUBIC CONVOLUTION

|—— 240 PIX ——|

240 LINES

ERTS MSS - BALTIMORE
1062-15190-4
INTENSITY RANGE: 0-63

NEAR-NEIGHBOR   BILINEAR INTERP

REGISTERED IMAGE ERROR
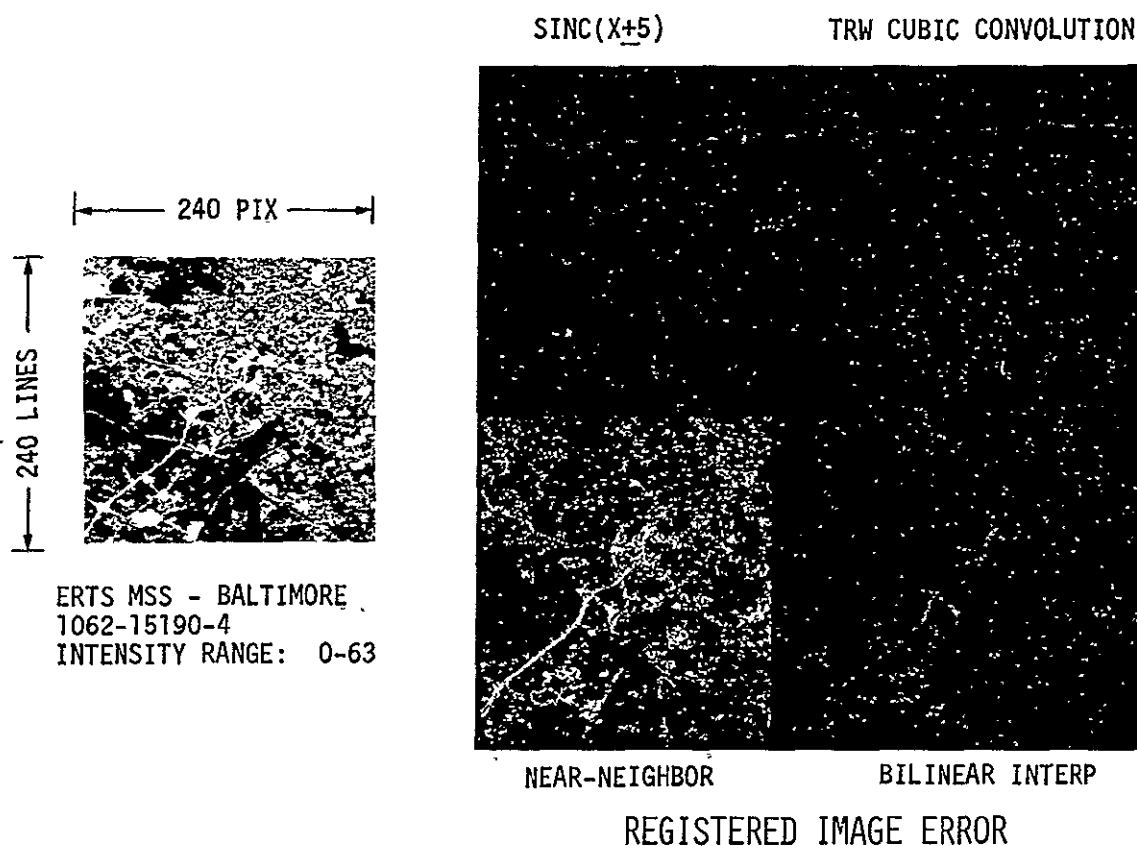
FIGURE 4-4. ERROR IMAGERY - RELATIVE PERFORMANCE

A reference image was generated by 30x30 point sinx/x. The other
imagery was generated by 10x10 point sinx/x, 4x4 point TRW Cubic
Convolution, 2x2 point bilinear and 1 point nearest neighbor
interpolation.
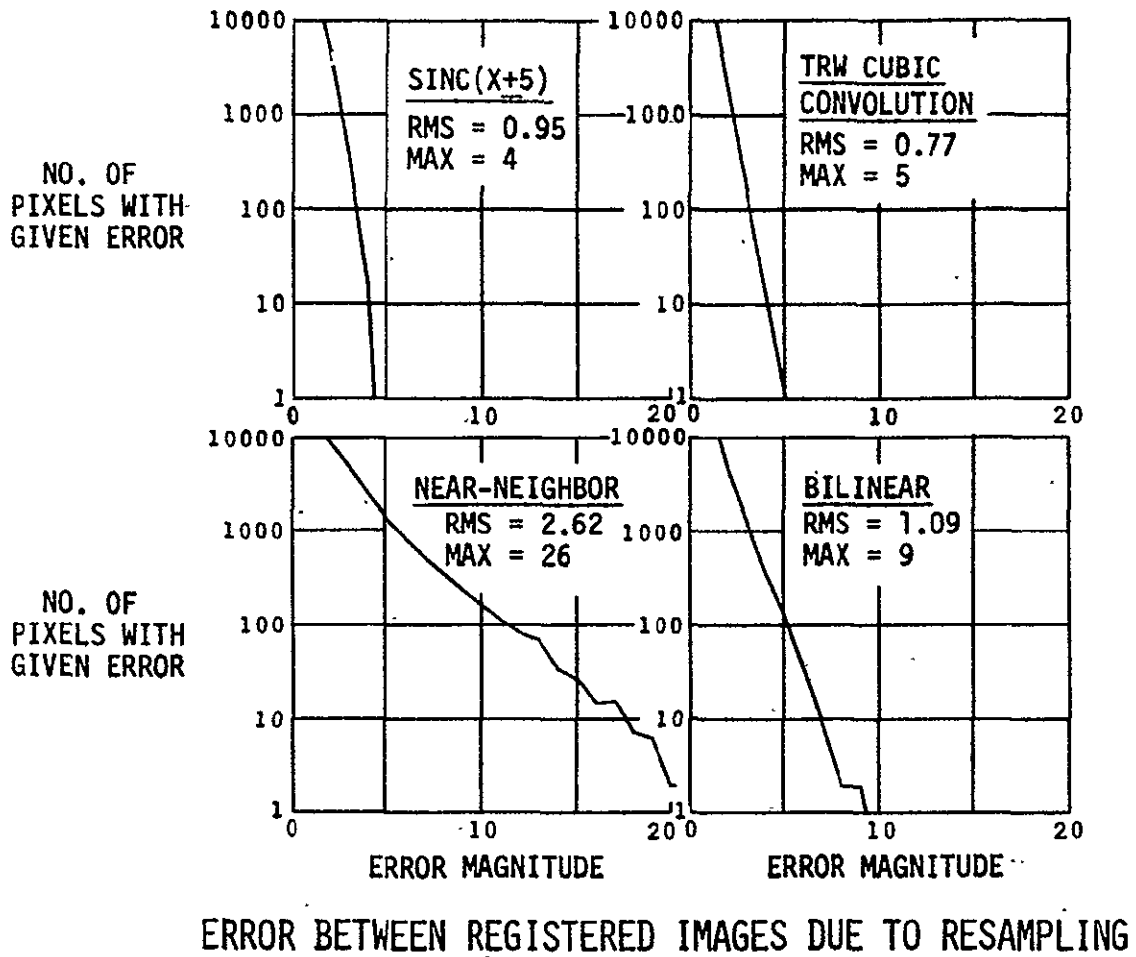
FIGURE 4-5. ERROR HISTOGRAMS - RELATIVE PERFORMANCE

These error histograms correspond to the absolute value difference imagery of Figure 4-7.

The difficulty with this interpolation evaluation is that all errors are relative to interpolated data (i.e., 30x30 point sinx/x data) derived from the LANDSAT sensor. An absolute evaluation of interpolation error requires use of comparison data undegraded by the ERTS sensor. This evaluation has been made by TRW, and results are included later in this section.

In the same previous study, spatial frequency comparisons were also made. For the same image subarea, an FFT (fast frequency transform) algorithm was utilized to compile the frequency transform for each of 100 lines, which were then averaged (frequency by frequency). It was noted that the spectrum for bilinear interpolated data fell faster at the higher frequencies than did the spectra of Cubic Convolution or nearest neighbor resampled data. The spectra for the latter two interpolations were not significantly different; i.e., both processed similar high frequency content.

In an effort to determine the absolute error attributable to sampled imagery data, TRW had a high resolution aerial photograph digitized with an equivalent 2.8m square aperture, equal to the sample and line spacing. This image was then blurred by averaging a cell 8x8 pixels on a side, and stepping the cell by one pixel. The result is imagery equivalent to 8x2.8 = 22.4m resolution. Every eighth line and sample value of this blurred image was used as a basis for interpolating 7 interstitial values (in both directions), i.e., reconstruct the blurred reference image. Both TRW's Cubic Convolution Process and nearest neighbor interpolation were employed, and the reconstructed image data was compared pixel by pixel with the original blurred data.

Figure 4-6 shows the blurred 22.4m image data. Figure 4-7 shows the 22.4m nearest neighbor reconstructed image; the Cubic Convolution resampled image is shown in lFigure 4-8. The error histograms for the two resampled images are shown in Figure 4-9. Note that TRW Cubic Convolution statistics (mean absolute, root mean square, and standard deviation) are all superior to results obtained by nearest neighbor interpolation.
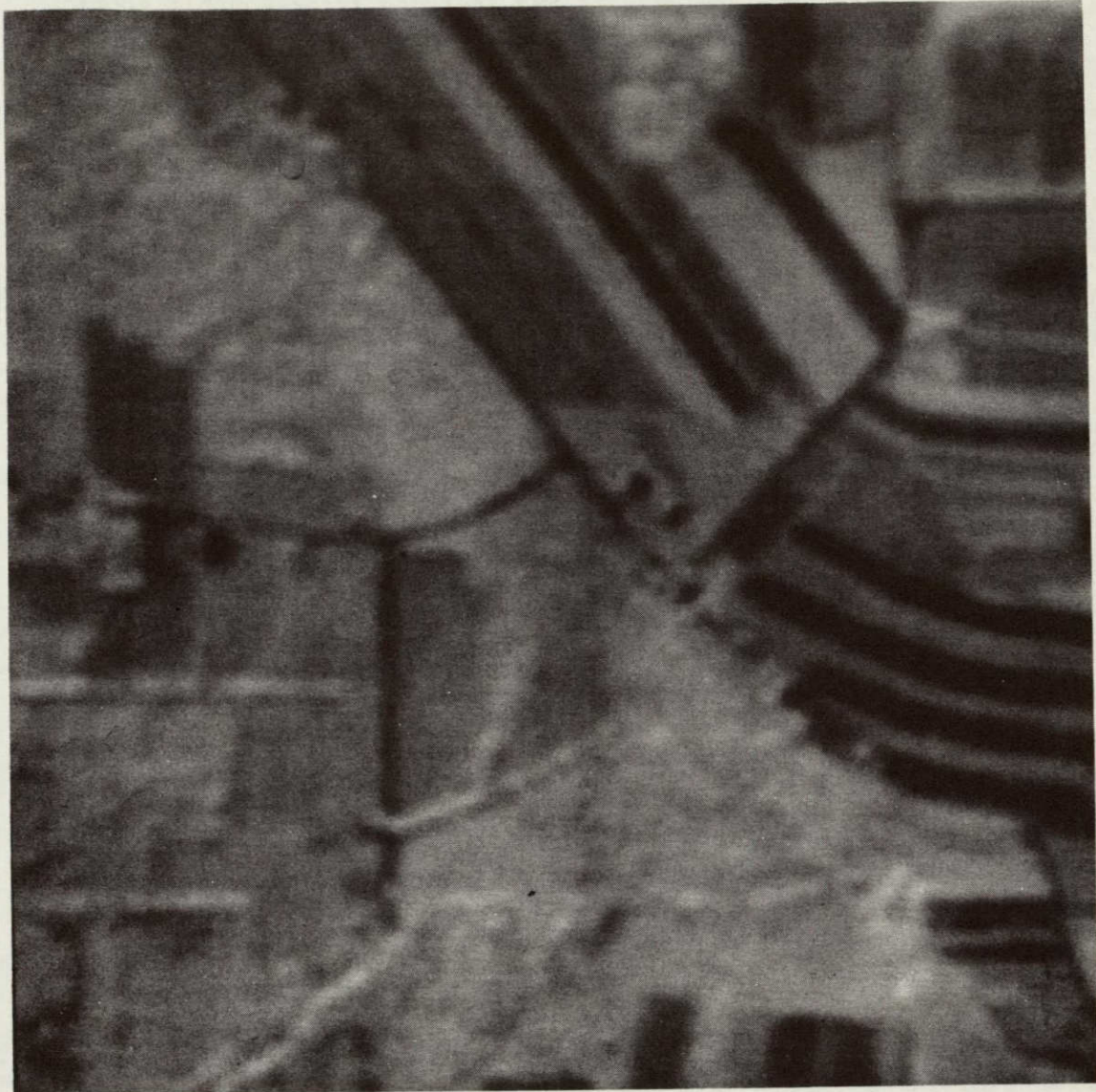
FIGURE 4-6. BLURRED REFERENCE IMAGE

This image was derived from 2.8m resolution digitized
aerial imagery and blurred to 22.4m resolution (87.5%
overlap of adjacent samples).
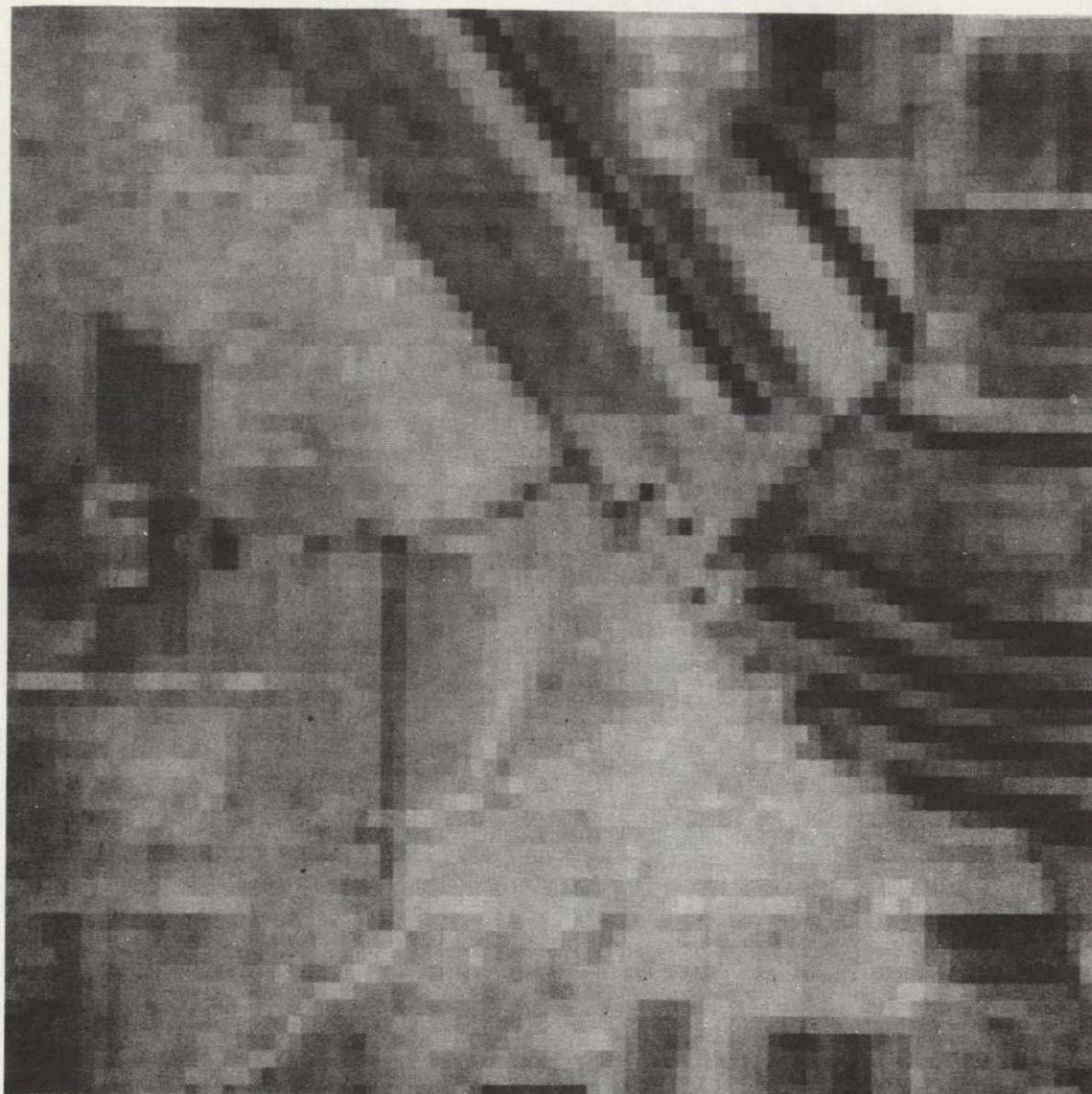
FIGURE 4-7. NEAREST NEIGHBOR RECONSTRUCTED IMAGE

The blurred image of Figure 4-9 was sampled every eighth
line and pixel and reconstructed by nearest neighbor resampling.
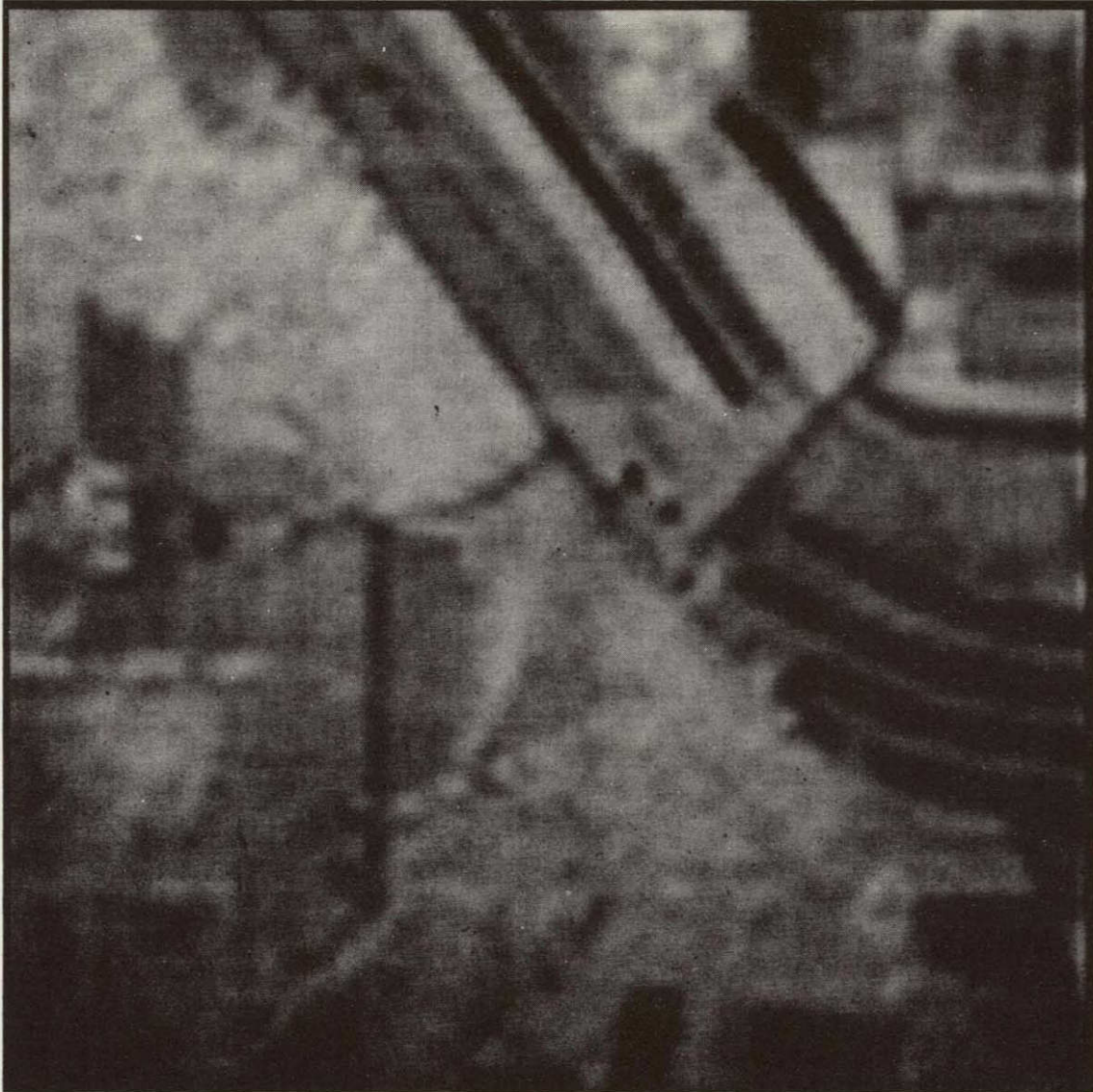
FIGURE 4-8. CUBIC CONVOLUTION RECONSTRUCTED IMAGE

The blurred image of Figure 4-9 was sampled every eighth
line, sample and reconstructed by TRW's Cubic Convolution
Process.
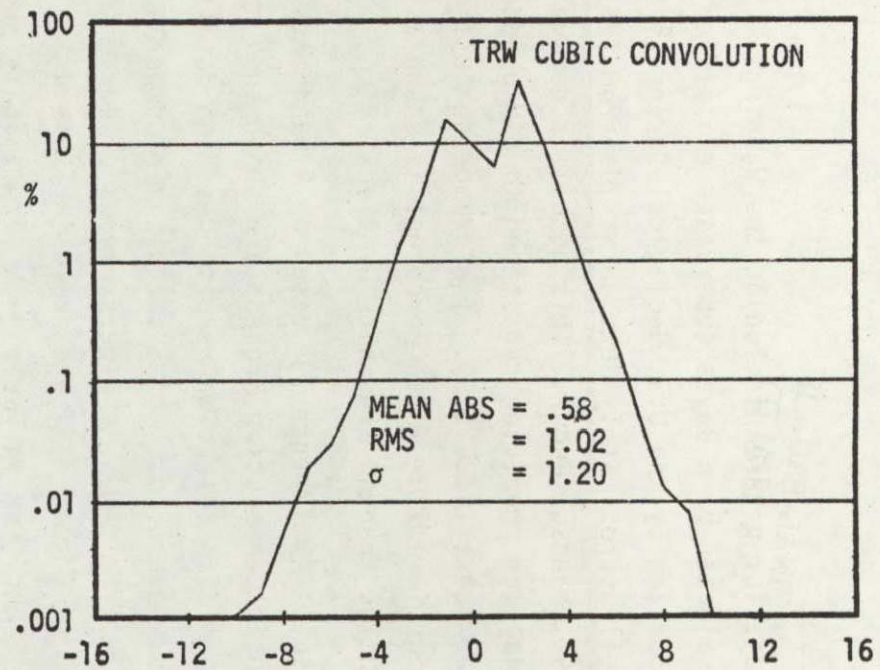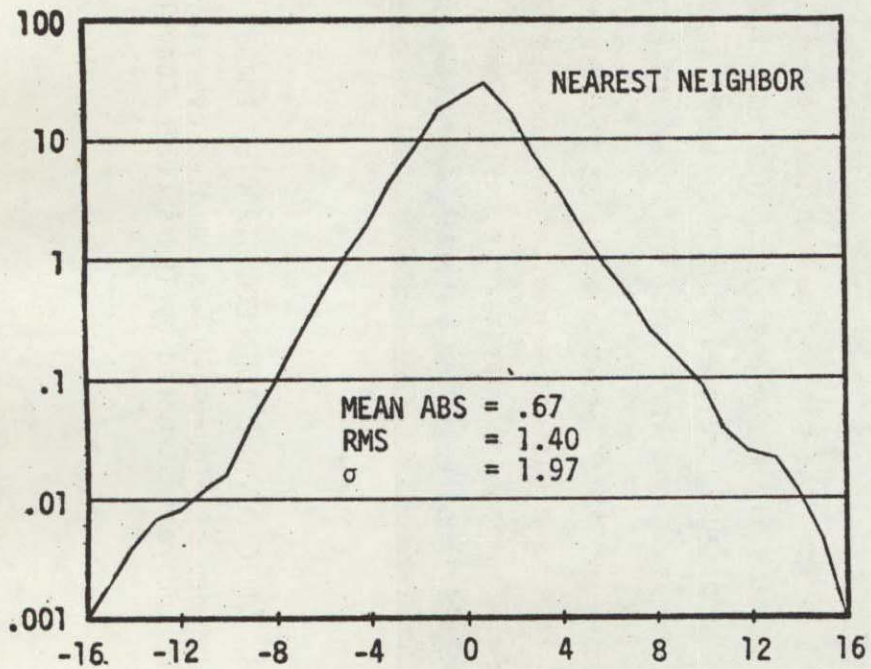
FIGURE 4-9. Reconstruction Difference Histograms

4.4 RESAMPLING EVALUATIONS

Resampled image data for an area including the Washington, D.C.
metropolitan area was evaluated by a Bayes supervised classifier, and compared to ground truth supplied by the U.S. Geological Survey (Reference 8)
Figure 4-10 shows a detail approximately 30km on a side from full scene
data for scene 1080-15192, bands 5 and 7. This detail is derived from
full scene data which has been precision registered to UTM gridded, precision rectified data for scene 1062-15190. The change detection imagery
for the two bands is shown in Figure 4-11 (no change is shown as neutral
gray; positive and negative changes are white or black).

Classification results (Reference 7) based on 4 band data resampled using the TRW Cubic Convolution Process are shown in Figure 4-12.
The same figure also shows classification results based on data from the
two precision registered scenes (total of 8 bands). In comparison with a
USGS ground truth map (Reference 8) , the percentages of correct classification corresponding to Figure 4-12 are shown in Table 4-1. The land
use signature types are identified in Table 4-2. Preliminary results for
data processed by nearest neighbor interpolation indicate < 2% deviation
from the data listed in Table 4-1. It is clear that for areas significantly larger than a few pixels that the classification results will be insensitive to the interpolation algorithm employed. The importance of the
interpolation algorithm is directly related to the classification of a
particular pixel, i.e., areas of one acre or so in size, and edge detail.

Further evaluations of TRW's Cubic Convolution Process are contained in Appendix D. These evaluations are based on the use of bulk
CCT data furnished by NASA having specular mirror reflections (small
features, one or two pixels in size, which saturate or nearly saturate
the MSS detectors).
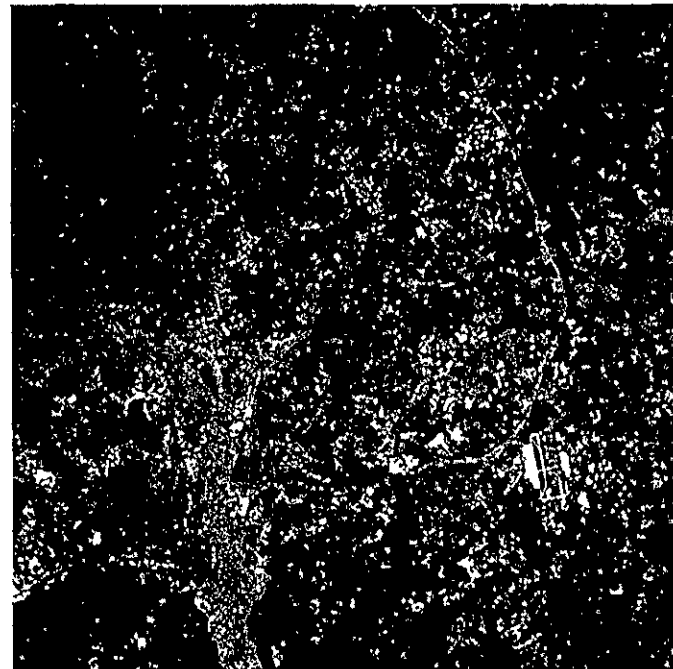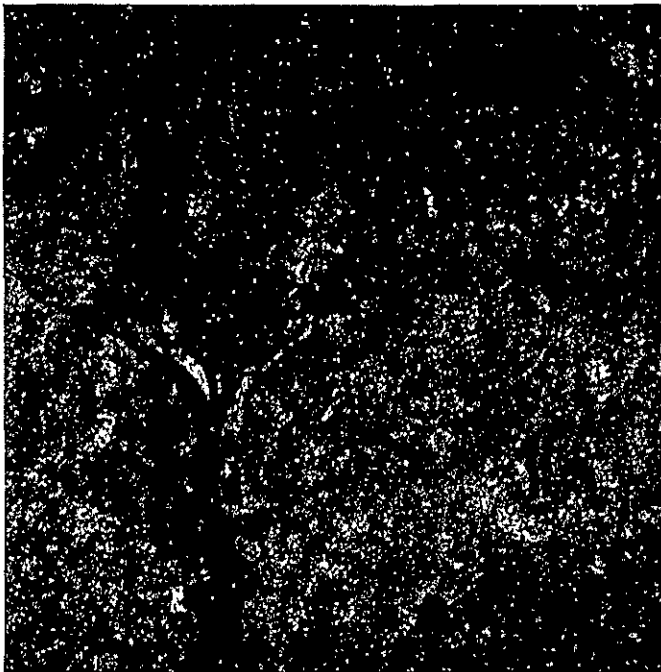
FIGURE 4-10. DETAIL OF SCENE 1080-15192 Bands 5 and 7

This ERTS subimage is about 30Km on a side, and is located
in the Washington, D.C. urban area.
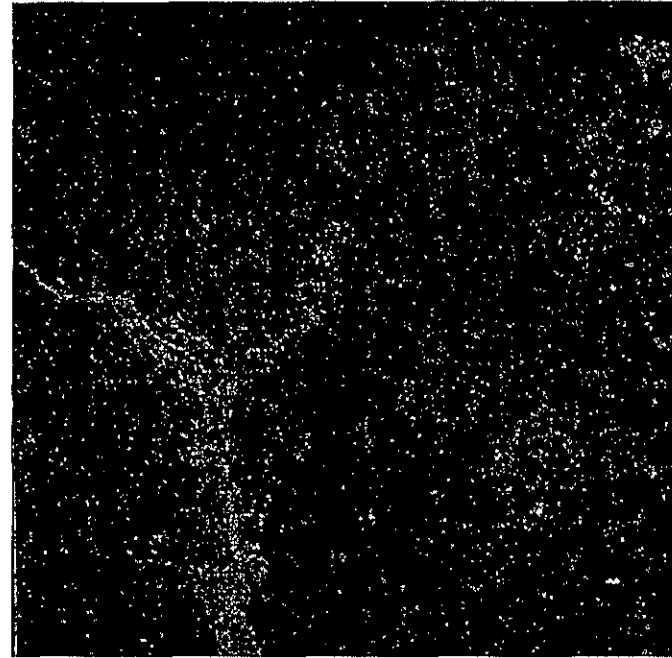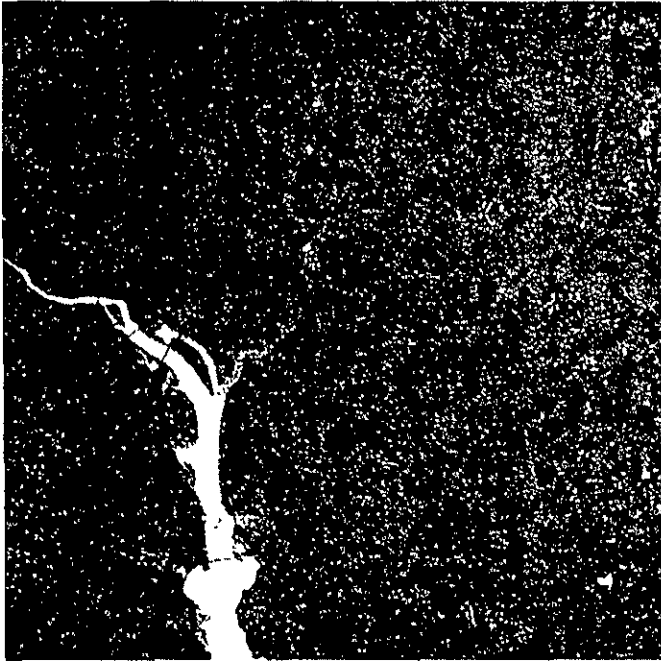
FIGURE 4-11. CHANGE DETECTION IMAGE DETAIL

Scene 1080-15192 was registered to 1062-15190 on a full scene basis, and this change detection area corresponds to Figure 4-13. TRW's Cubic Convolution Process was used throughout.
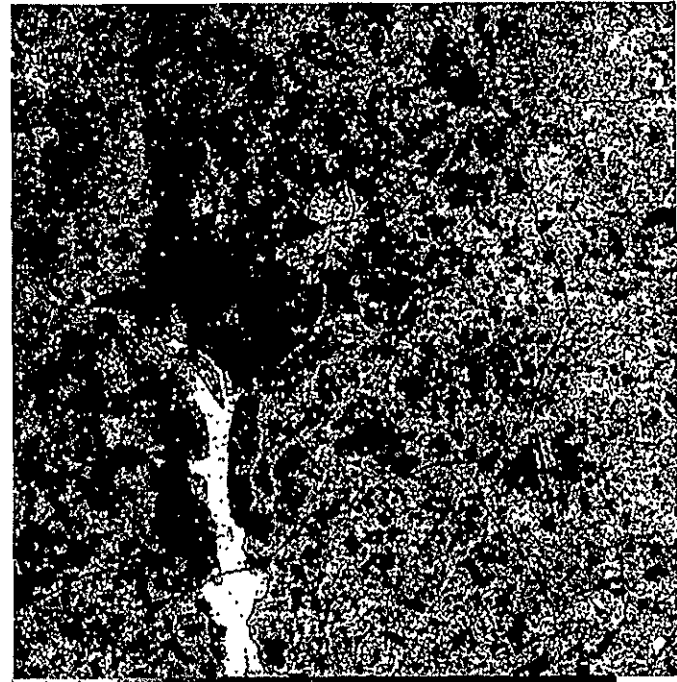
O W   L A   O S   R . S   R M A   L C   L D X .   L D | N U L L   O W   L A   O S   R . S   R M A   L C   L D X   L D   N U L L

FIGURE 4-12. CLASSIFICATION OF THE WASHINGTON URBAN
AREA

TABLE 4-1. TRAINING SET CLASSIFICATION RESULTS

Signature	No. samples	% correct classification 4 band	8 band
LD	150	68.0	80.7
LDX	143	69.2	32.2
LC	405	67.7	76.0
RMA	431	74.9	76.3
RS	692	45.5	65.8
OS	1121	78.7	80.3
LA	504	36.9	49.4
OW	886	99.3	98.5

[a]LT and OUW not considered; RMA = {LR,RM}, OS = {OP,OU}.

TABLE 4-2. URBAN LAND USE SIGNATURES

Type	Abbreviation
Primarily industry	LD
Extractive industry	LDX
Transportation	LT
Commercial and services	LC
Strip & cluster development	LR ⎱ RMA
Multi-family residential	RM ⎰
Single-family residential	RS
Improved open space	OP ⎱ OS
Unimproved open space	OU ⎰
Unimproved, wetland	OUW
Agriculture, with residence	LA
Water	OW

4.5 CONCLUSIONS

4.5.1 Algorithm Evaluation

LANDSAT data has been resampled by means of nearest neighbor interpolation and the TRW Cubic Convolution Process. Visual and numerical evaluation techniques have been employed to compare the two interpolation approaches. Nearest neighbor discontinuities in resampled data and change detection data become noticeable when viewing details of a full scene; such artifacts are, of course, present in the digital data irregardless of scale.

Numerical evaluations of relative and absolute performance of nearest neighbor interpolation and TRW's Cubic Convolution Process indicate the clear superiority of the latter. The impact of interpolation algorithm on classification results, based on initial test data, appears to be small for areas of several hundred pixels in size. For smaller areas, and along boundaries, differences between interpolation methods become more significant. On an individual pixel basis, differences can be quite large.

4.5.2 Implementation Approach

All software implementation of image resampling techniques can be accomplished on minicomputer based systems. In this case, with code optimized in assembly language, the nearest neighbor interpolation will run about three times as fast as TRW's Cubic Convolution process - about 20 minutes for a full MSS scene, all four bands (40MB), versus about 62 minutes for TRW's Cubic Convolution Process.

As pointed out previously (Section 3), operational systems (minimum 30 scenes/day) will achieve the required throughput by two means: introducing as much parallelism as possible into the processing system; and speeding up the interpolation processing time and control point extraction times. The interpolation time can be significantly reduced by implementing the algorithm in special purpose hardware (1 pixel/µs) or by implementing the algorithm in a microprogrammable processor (1 pixel/5µs). Speeding up the control point extraction time will be discussed in the

next task report, Ground Control Point Extraction. System parallelism
was discussed in the previous Section.

5.0 GROUND CONTROL POINT EXTRACTION

5.1 TASK DESCRIPTION

The objective of this task of the contract was to investigate the use of techniques developed by TRW prior to the start of the contract for Ground Control Point (GCP) library buildup, automatic GCP extraction/correlation, percent of successful correlation versus GCP and scene properties, and accuracy. Manual intervention, where necessary, is accounted for and assessed with regard to a production mode of operation.

Scene data for scenes 1062-15190 and 1080-15192 in the Baltimore-Washington area and 1339-17381 and 1411-17391 in Saskatchewan, Canada, were employed. Features were designated in one scene of each pair and stored as 32 x 32 TRW Along-Line Corrected (TALC) reference chips. Corrections for mirror non-linearity, line length and detector commutation offset were implemented by means of the TRW Cubic Convolution Process. TALC search areas (64 x 64) were derived from the other scene of each pair. Chips and their corresponding search areas were selected from all four MSS spectral bands.

A Sequential Similarity Detection Algorithm (SSDA) was employed to automatically search each 64 x 64 uncertainty area for matches with the 32 x 32 reference chip. The search areas (64 x 64) are signficantly larger than the uncertainty region resulting after processing a scene with only one control point (< 50 pixels, including 32 pixels for the chip itself). In the full scene registration mode of operation either manual or automatic techniques can be utilized to locate each chip in its corresponding search area.

After coarse search of an uncertainty region by means of SSDA, a straightforward cross-correlation algorithm is utilized for fractional pixel refinement of the control point location. The use of SSDA with correlation thus combines the advantages of speed and precision.

Location accuracy was evaluated by digitally enlarging the search neighborhood (uncertainty region) 4:1 by Cubic Convolution interpolation at the point the automatic extraction code indicates a feature match.

Manual designation of the actual control point position is then accurate
to $\pm$ 0.25 pixel (line). This position is compared to the algorithm deter-
mined control point position to provide accuracy data.

5.2 TECHNIQUE

Existing techniques for image rectification and registration were developed prior to this contract by TRW. A detailed discussion of the algorithms used in the rectification process was included in a previous contract report (Reference 4) and in Section 3, and so will not be repeated; only a brief summary of the relevant techniques will be included here. Figure 5-1 shows a functional flow diagram for the process. First, bulk NASA scene data on CCT's are reformatted onto a digital disk storage system to permit separating and ordering the individual bands and scan lines of data. The disk storage system must be capable of storing at least one full scene of corrected data. Because nearest neighbor line length correction was applied to the NASA supplied data, a preprocessing operation is required to strip out the replicated pixels in each scan line of data. Deline-length-corrected data can be written back out onto the same disk used to store the reformatted data.

BIAT data for spacecraft ephemeris, heading, altitude and attitude are also input to the rectification processing operation. These parameters are utilized to initialize a 13 state linear sequential estimator (Kalman filter) for the spacecraft attitude time series and altitude bias errors. Each GCP filter update diminishes the size of the uncertainty interval containing each successive GCP sought, and thereby speeds up the GCP location process. (The geodetic coordinates supplied by the USGS or CCRS are converted to line, pixel coordinates for the GCP location search.)

It is necessary to manually identify a control point (RCP or GCP) the first time it is processed. A CRT equipped with an interactive cursor (track ball) is employed for this purpose. The TRW Cubic Convolution Process is employed to digitally enlarge (zoom) 4:1 a 32 x 32 chip centered at each tentative control point location. Designation of the zoomed chip ensures $\leq$ 1/4 pixel designation accuracy. Prior to display, each chip is TRW Along-Line Corrected (TALC) by employing the TRW Cubic Convolution Process in the bulk data scan line direction to correct for line length, detector commutation time, and mirror scan nonlinearity.

Figure 5-1. Functional Flow Diagram for Rectification

The TALC chip centered at the designated position is stored in the Control Point Library (CPL) on disk for subsequent use in the registration process. The same disk which stores bulk sensor data can also be used to store the Control Point Library.

Registration Control Points (RCP's) that have been previously stored in the Control Point Library (CPL) from an earlier scene can be located in the current scene by automatic digital correlation between the RCP in the CPL and a search area in the current scene. This process takes place in two steps: search and precision location. The search step finds the correct alignment within a few pixels via either the Sequential Similarity Detection Algorithm[*] (SSDA) or by approximate manual designation. The search is initialized by the best estimate of the RCP location on the basis of all control points processed up to that time point in the scene, greatly reducing processing time after the first control point. Manual designation is always faster for the first point due to relatively large bias errors $\pm$ 3 or 4 km in apriori spacecraft data on the BIAT's. The precision location process utilized is a straightforward crosscorrelation algorithm with normalization to determine the correlation on integer sample-spacings, with polynomial interpolation to find the precise location to 1/10 of a pixel. In the event that automatic crosscorrelation fails (due to partial cloud cover or poor choice of RCP), the reference and comparison RCP's are zoomed to the CRT for manual crosscorrelation.

The crosscorrelation process in two dimensions results in a matrix of the following form:

$$C(n,m) = \sum_{\delta y, \delta x = -14}^{+14} f(x_i + \delta x + n, y_j + \delta y + m) \ g(x_i + \delta x, y_j + \delta y)$$

where

f, g = respective data values from corresponding registered scenes

x_i, y_j = selected pixel positions (pixels, lines) at which correlation features are located

C = cross correlation matrix

---

[*] See Reference (9) for a detailed description of the algorithm.

A biquadratic polynomial fit to the results for integer values of n,m permits accurate determination of a correlation peak and the corresponding non-integer n,m location of this maximum.

The estimated earth-centered coordinates for each GCP, calculated on the basis of the current estimates from the 13 parameter Kalman filter, are compared to known earth centered coordinates computed from USGS-supplied data to form an error. This error drives the filter and produces a refined estimate of the 13-state error vector. The process repeats until errors are reduced to about 1 pixel average absolute error. No more than 6-9 GCP's are required for this accuracy, in general. Further error reduction is limited only by the accuracy of available GCP's.

There is no real difference between the registration processing operations and those required for rectification. No control points need be designated during registration processing (though more could be designated if features were obscured previously). The computed earth centered coordinates of RCP's, using the last Kalman filter attitude/ altitude refinement obtained during rectification processing, are used as ground truth against which current estimates based upon filter updates during the registration processing are compared. With the exception of locating the first control point, which may require a minute or more depending upon actual BIAT data and image distortion, all succeeding control points in the registration mode are located very quickly and automatically.* In all other respects, registration processing operations are identical to rectification processing operations.

---

*! The extent to which control points lend themselves to automatic
; processing is one of the lines of inquiry being pursued in this task.

5.3 PERFORMANCE RESULTS

Table 5-1 lists the control point chips extracted from scene 1062-15190, their geodetic coordinates and bulk image (line, pixel) coordinates*, and the spectral band from which the data were extracted. All chips were TRW Along-Line Corrected (TALC) for mirror scan nonlinearity, line length and detector commutation time before storage on disk. Figure 5-2 shows the TALC chips from 1062-15190 and the search areas from 1080-15192, before TALC.

Table 5-2 shows the results achieved for band 5 using the SSDA algorithm with a 32 x 32 chip and a 64 x 64 search area. The chip is incremented in units of 2 lines and 2 pixels through an uncertainty evvelope of 64-32 = 32 lines and 32 pixels. That is, the 32 x 32 chip can be shifted $\pm$ 16 lines, $\pm$ 16 pixels relative to the 64 x 64 search area and still overlap completely with search area image data.

Accuracy to $\pm$ 1 line or $\pm$ 1 pixel is the result of ensuring that a minimum number of differences be cumulated (32 x 32 = 1024) and that the difference cumulated be less than some value. Running time is affected by the threshold increment (INCR) and initial threshold (INIT).

For band 5, running times were about 2 seconds. For best performance initial thresholds are about equal to the increments, and both are 1/6 or 1/7 the value of the chip norm.

Table 5-3 summarizes SSDA performance for band 7. Running times and accuracies are commensurate with that for band 5, but for chips 6 and 9. These chips, as indicated in Table 5-3 and Table 5-1, are small spits of land projecting into an otherwise black (water) background. Norms are small and running times are large, due to the cumulation of large numbers of small terms. These particular cases may indicate that there is at least one class of control points not suited to automatic (SSDA) extraction methods.

---

* The coordinates correspond to the center of the feature, as determined in the 4:1 zoomed image detail.

Table 5-1. Control Point List for Scene 1062-15190

CHIP NUMBER	IDENTIFIER	GEODETIC COORDINATES LATITUDE	LONGITUDE	BULK IMAGE COORDINATES Lines	Pixels	SPECTRAL BAND
1	Highway Crossing, I695/I835	39/24/41	-76/39/51	449.7	1562.0	5
2	River Fork, Potomac/Monocacy	39/13/30	-77/27/16	868.6	497.0	7
3	Runway Crossing, Dulles International	38/56/41	-77/27/25	1247.7	625.7	5
4	Runway Crossing, Andrews Air Force Base	38/48/33	-76/52/15	1307.0	1555.6	5
5	Wye Island, East Tip	38/52/59	-76/6/18	1036.7	2645.0	7
6	Fishing Point, West Tip	38/18/31	-76/1/3	1794.0	3060.1	7
7	Blossom Point, West Tip	38/24/31	-77/6/40	1903.0	1397.2	7
8	East Loop of River	38/21/55	-77/46/28	2102.6	435.1	7
9	Point Lookout, South Tip	38/2/9	-76/19/19	2230.0	2753.4	7
10	Capitol Beltway, Interchange 38	39/14/32	-75/54/42			
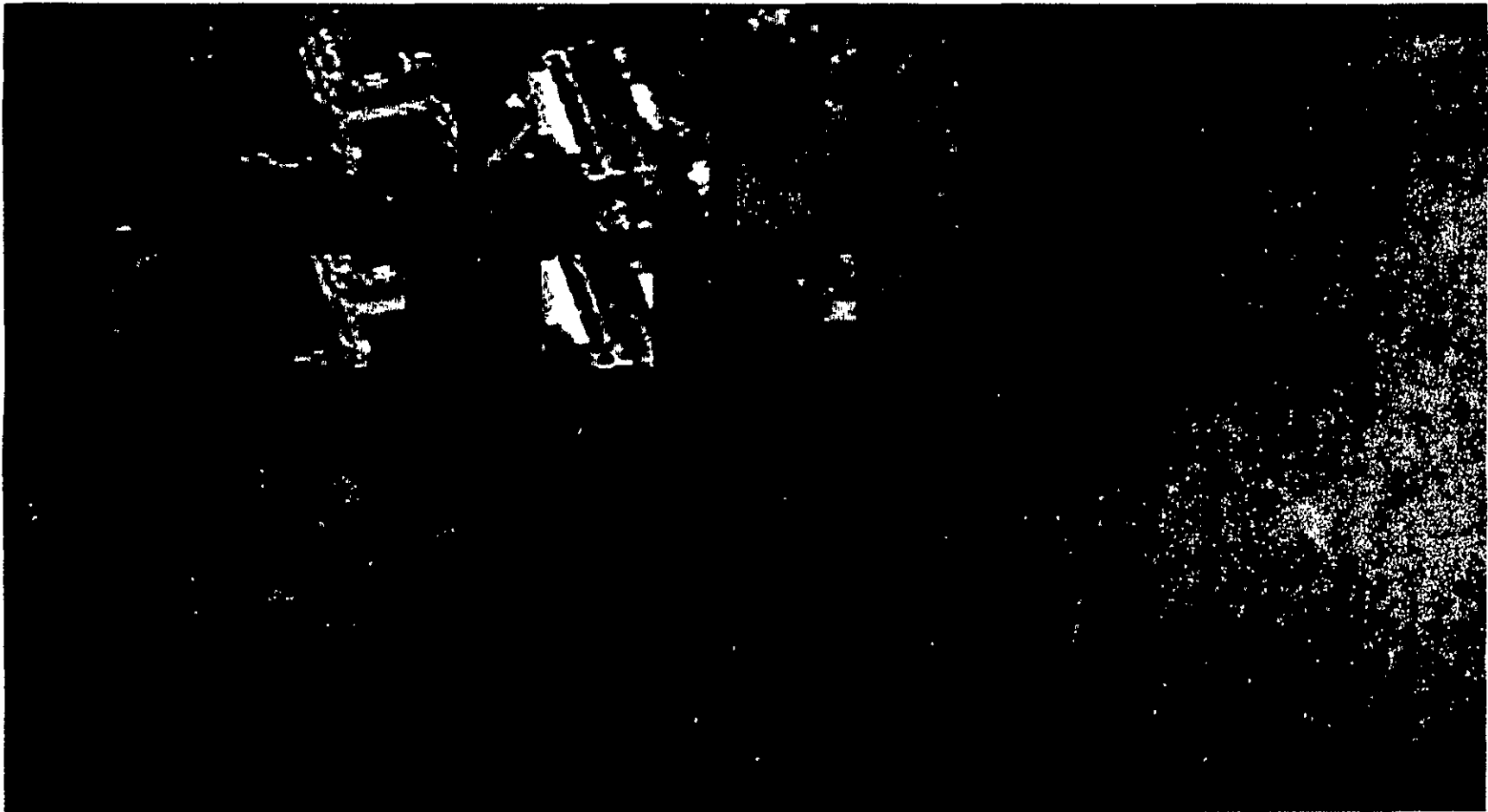
BAND 5 - 1,3,4,10   BAND 7 - all others

Figure 5-2.   Reference Chips and Search Areas for Chesapeake Bay Scenes

32 x 32 TRW Along Line Corrected (TALC) chips are derived from 1062-15190.
64 x 64 bulk search areas are derived from 1080-15192. Bulk data is TALC
processed before feature extraction. Band 5 data is on top two rows; Band 7
data is on bottom two rows.

Table 5-2.   SSDA Performance - Band 5
of Chesapeake Bay Scene

| CHIP NO. | NORM OF CHIP (0-27) | INIT | INCR. | TIME (sec) | ERROR | |
					LINES	PIXELS
1	17	3	4	3.22	-1	.5
		2	4	3.09	-1	.5
		2	3	2.42	0	-.5
3	26	7	6	2.55	1	.5
		7	5	2.87	0	-.5
		6	3	2.38	0	-.5
		5	3	2.35	0	-.5
		4	3	1.95	0	.5
4	31	10	7	2.55	1	.5
		8	7	2.50	1	.5
		7	10	3.54	-1	-.5
		7	8	2.54	0	.5
		6	9	3.02	0	.5
		5	4	2.41	0	.5
		5	5	1.98	0	.5

Table 5-3. SSDA Performance - Band 7
of Chesapeake Bay Scene

CHIP NO.	NORM OF CHIP (0-27)	INIT	INCR	TIME (sec)	ERROR LINES	PIXELS
2	14	5	1	2.38	0	-.25
		4	2	2.41	0	.75
		3	2	2.02	1	-.25
		2	2	1.91	0	-.25
5	14	5	4	2.35	-1	-1
		5	5	2.82	0	0
		4	1	2.25	-1	-1
		3	3	1.90	0	-1
		3	2	1.87	0	-1
6	4	4	3	27.27	0	.75
		3	3	24.63	-.75	1.75
		2	3	25.40	-.75	-.75
		1	3	23.85	.25	.75
7	6	3	3	4.77	-.25	.25
		2	3	2.43	-.25	0
		1	4	4.80	-.25	0
		1	3	1.93	-.25	0
8	21	3	3	13.73	0	-1
		3	2	3.05	0	-1
		2	3	11.83	1	.25
		1	3	10.40	1	-.75
		2	2	2.18	1	.25
9	2	2	2	40.93	-1	-1

With the class of control points exemplied by chips number 6 and 9 aside, it appears that it should be possible to initiate SSDA parameters INIT and INCR on the basis of chip norm. Iteration of these parameters can be performed the first time a registration run is performed, if necessary, to optimize running time for subsequent registrations.

All processing times are based on algorithms implemented in FORTRAN with floating point arithmetic. Conversion of software to assembly language code and integer arithmetic could easily speed up performance by several factors.

Once a coarse search is accomplished by SSDA, the cross correlation algorithm is utilized for location of features to 1/10 of a pixel. Running times for optimized assembly language code is < .5 seconds.

Using data derived from the same Chesapeake Bay site, an effort was made to determine if preprocessing of the chip and search area data would improve SSDA performance. Table 5-4 summarizes running time and preprocessing and SSDA parameters for band 5 and band 7 data. Two cases were considered: Method II, in which the normalization of chip and search area data were referenced to the darker of the two; and Method III, in which data were referenced to the brighter of the two. Both mean (μ) and standard deviation (σ) were adjusted by means of:

$$X_{out} = (X_{in} - \mu_{in}) (\sigma_{out}/\sigma_{in}) + \mu_{out}$$

X = data values

in = input (unadjusted)

out = output (adjusted).

For comparison, performance with unpreprocessed data is shown as Method I.

In all cases accuracy was ± 2 pixels and $\pm.2$ lines, or better. In general, somewhat higher speeds are achieved if data is preprocessed to brighter values, inasmuch as the sum of pixel differences will then more rapidly exceed the incremented threshold and thereby cause a correlation rejection. This is particularly true of band 7 data; band 5 data seems to give about the same running time, with or without preprocessing.

Table 5-4. Running Times for Baltimore-Washington Scene,
Bands 5 and 7, with Preprocessed Data

CHIP NUMBER	BAND NUMBER	METHOD I					METHOD II					METHOD III				
		μ	σ	INIT	INCR	TIME	μ	σ	INIT	INCR	TIME	μ	σ	INIT	INCR	TIME
1	5	16	5	4	4	3.23 3.25	16	5	4	4	3.60 3.20	17	5	4	4	3.50 3.02
3	5	26	9	4	4	2.30	21	9	7	7	3.37 2.82	26	9	7	7	2.59 3.05
4	5	31	14	5	5	2.41	23	12	8	8	2.58 2.58	31	14	8	8	2.53 2.53
10	5	17	7				17	7	7	7	3.34 3.25	22	8	8	8	ERRATIC
2	7	14	5	2	2	2.34	14	5	3	3.	2.70 2.50	15	5	2	2	4.29 3.23
5	7	14	9	3	3	2.33	14	9	4	4	2.33 2.42	15	8	4	4	2.50 2.37
6	7	4	5	3	3	24.63 25.03	2	5	2	2	3.50 3.43	4	5	3	3	3.13 2.85
7	7	6	9	3	3	4.77	5	8	2	2	2.33 2.35	6	9	4	4	3.65 2.43
8	7	21	2	3	3	9.73	16	5	4	4	2.82 3.02	21	2	2	2	2.75 2.66
9	7	2	5	2	2	40.93	1	4	2	2	54.73 51.35	2	5	2	2	2.78 3.22

METHOD I   – No preprocessing of chip and search area data.
METHOD II   – Normalization of mean (μ) and standard deviation (σ) to darker of chip and search area.
METHOD III   – Normalization of mean and standard deviation to brighter of chip and search area.

Table 5-5 identifies control points in Saskatchewan, Canada, which were also evaluated by automatic extraction methods. Figure 5-3 shows the TRW Along Line Corrected (TALC) chips (32 x 32) from scene 1411-17381-6 and bulk search areas (64 x 64) from scene 1339-17391-6. Figure 5-4 shows the TALC chips from 1411-17381-7 and bulk search areas from 1339-17391-7. In all cases the bulk search area data is along line corrected (TALC) before automatic extraction processing.

Results attained with the Canadian control points, corresponding to the Chesapeake Bay results of Table 5-4, are shown in Tables 5-6 and 5-7, respectively, for band 6 and band 7 data. Again, all accuracies are at least ± 2 pixels and ± 2 lines. Also, without affecting accuracy, preprocessing of data for mean and standard deviation adjustment yields improved running times. Note that all timings presented herein are based upon FORTRAN coded programs - significantly improved running times are possible with assembly language coded versions.

An overall compilation of successful extractions is presented in Table 5-8. In general the normalized data permitted 20-40% more successful extractions than was the case with unnormalized data, independent of spectral band.

Additional results were obtained for the Chesapeake Bay site and another site (Monterey Bay). Data at each site spanning large temporal separations (as much as 954 days) were supplied by NASA to permit evaluation of the impact of seasonal factors on the automatic control point location methods outlined in this section. The additional results are presented in Appendix E.

Table 5-5. Control Point List for Canadian Site

CHIP NUMBER	IDENTIFIER	GEODETIC LATITUDE	COORDINATED LONGITUDE
1	Coldspring Lake, E.Pt.	52/20/55	108/35/10
2	North Tip of Lake	52/11/57	107/41/24
3	N.W. Tip of Lake	52/9/51	107/5/17
4	E. Tip of Lake	52/5/44	106/12/36
5	N.E. Pt. Indi Lake	51/43/24	106/29/10
6	So. Tip of Lake	51/38/26	107/21/4
7	Unidentified Feature	51/49/5	107/54/38
8	Crane Lake, S.E. Tip	52/0/49	108/52/14
9	Hook in Bad Lake	51/23/37	108/26/2
10	Hook in Barber Lake	51/23/14	107/39/53
11	Anerley Lakes	51/22/29	107/16/36
12	S.E. Tip Cutbank Lake	51/14/29	106/9/23
13	Pt. in Luck Lake	51/4/17	107/2/45
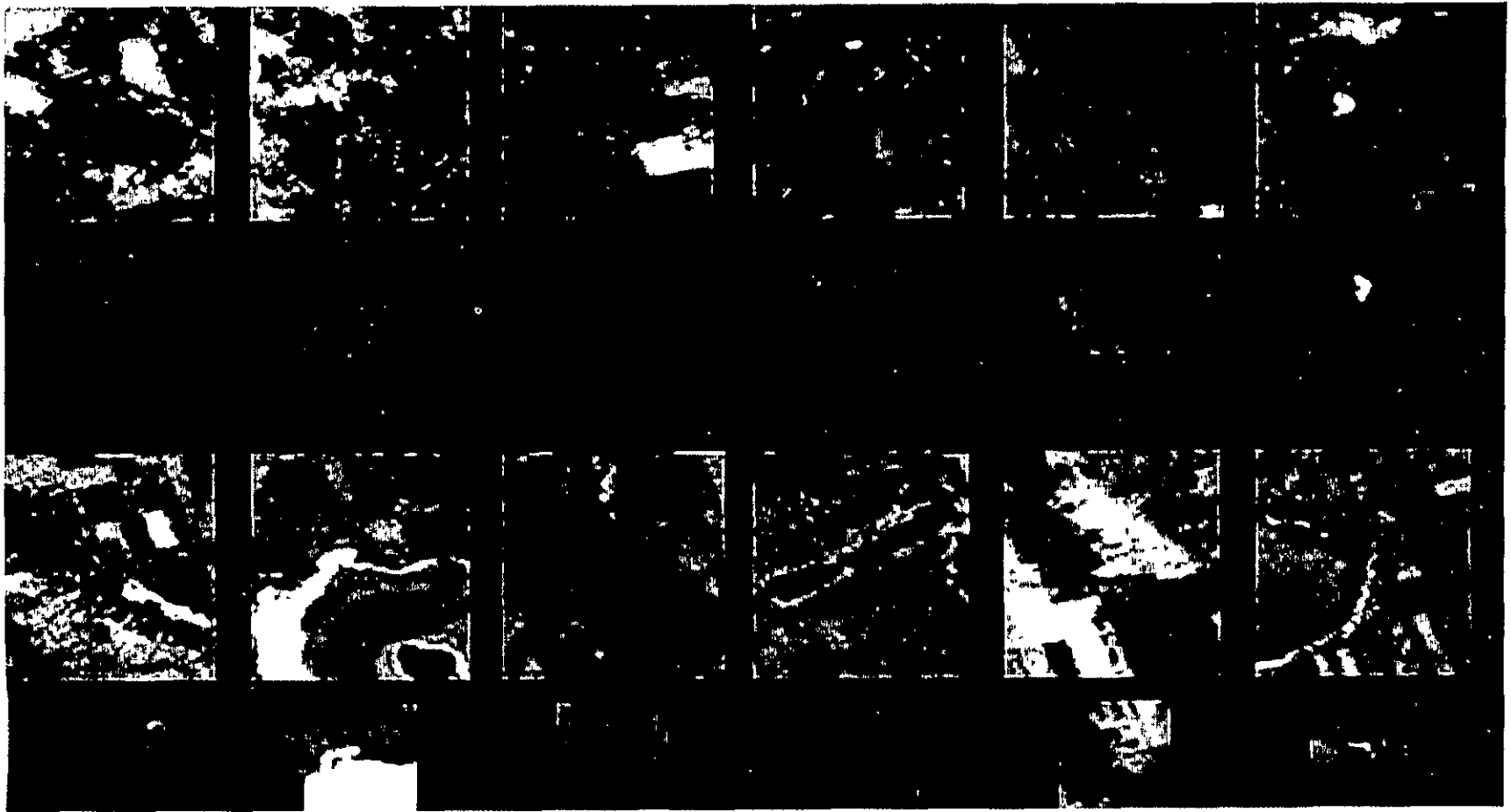
1 2 4 5 6 7

8 9 10 11 12 13

Figure 5-3. Reference Chips and Search Areas for Canadian Scenes - Band 6

32 x 32 TRW Along Line Corrected (TALC) chips are derived from 1411-17381-6;
64 x 64 bulk search areas are derived from 1339-17391-6. Bulk data is TALC
processed before feature extraction.
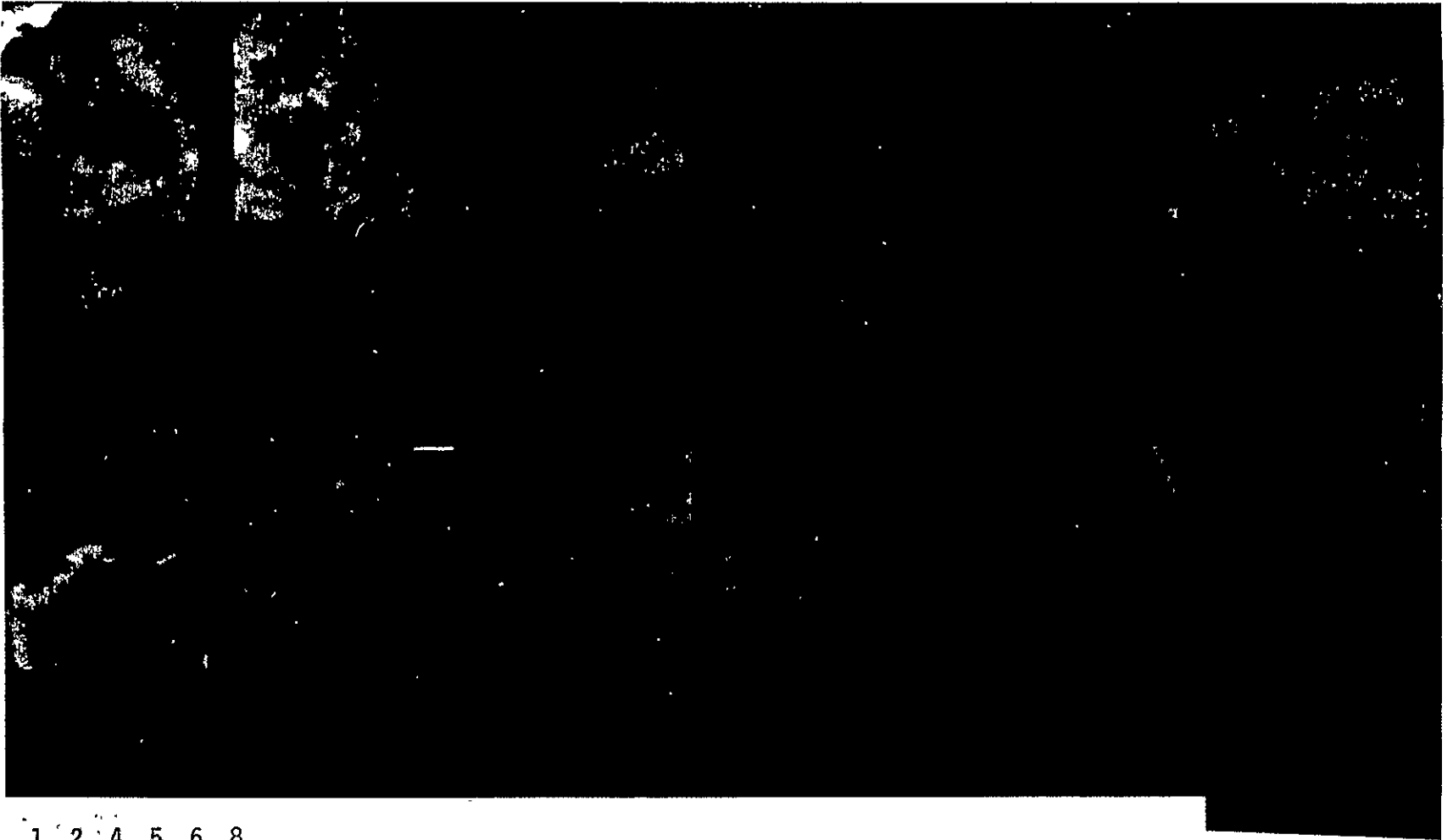
1 2 4 5 6 8
9 10 11 12 13

Figure 5-4.   Reference Chips and Search Areas for Canadian Scenes - Band 7

32 x 32 TRW Along Line Corrected (TALC) chips are derived from 1411-17381-7;
64 x 64 bulk search areas are derived from 1339-17391-7. Bulk data is TALC
processed before feature extraction.

Table 5-6. Running Time for Canadian Data, Band 6

CHIP NUMBER	METHOD I					METHOD II					METHOD III				
	μ	σ	INIT	INCR	TIME (sec)	μ	σ	INIT	INCR	TIME (sec)	μ	σ	INIT	INCR	TIME (sec)
1	26	9	12	12	3.56 3.02	26	9	5	5	2.59 2.58	41	17	10	10	2.61 2.53
2	27	4				27	4	5	5	ERRATIC	43	11	10	10	ERRATIC
3	NOT FOUND					NOT FOUND					NOT FOUND				
4	29	4	5	5	4.17 4.60	29	4	3	3	4.05 3.97	36	13	9	9	3.10 3.05
5	28	8	6	6	3.25 2.81	28	8	5	5	2.69 2.96	35	14	9	9	2.41 2.04
6	33	7	6	6	3.48 3.41	33	7	5	5	2.73 2.87	37	14	8	8	2.70 3.10
7	NOT FOUND					NOT FOUND					NOT FOUND				
8	19	4				19	4				42	14			
9	43	11				43	11				50	12			
10	29	6				29	6	7	7	8.81 13.25	35	10	11	11	3.68 4.13
11	31	6				31	6	5	5	6.43	38	12			ERRATIC
12	40	10	8	8	3.85 3.37	40	10				41	16	9	9	3.07
13	24	8				24	8	7	7	10.63 11.58	41	10			

METHOD I - No preprocessing of data.   METHOD II - Normalization to dark data.   METHOD III - Normalization to bright data.

Table 5-7.   Running Times for Canadian Data, Band 7

CHIP NUMBER	METHOD I					METHOD II					METHOD III				
	μ	σ	INIT	INCR	TIME (sec)	μ	σ	INIT	INCR	TIME (sec)	μ	σ	INIT	INCR	TIME (sec)
1	10	6	7	7	2.82 2.87	10	6	4	4	4.28 4.25	22	13	7	7	2.55 2.93
2	12	3				12	3	3	3	15.72 17.48	23	7	ERRATIC		–
3	NOT FOUND					NOT FOUND					NOT FOUND				
4	14	2	4	4	18.88 19.77	14	2	3	3	57.33 61.85	19	7	7	7	15.63 15.12
5	13	4	4	4	2.73 3.18	13	4	4	4	2.70 3.10	18	8	6	6	3.10 2.70
6	15	3	4	4	5.13 4.75	15	3	3	3	4.42 4.13	21	6	5	5	3.65 3.93
7	NOT FOUND					NOT FOUND					NOT FOUND				
8	7	2			–	7	2			–	22	8	6	6	3.96
9	23	7			–	18	8			–	23	7			–
10	11	4			–	11	4	3	3	5.67	16	8			–
11	14	4			–	14	4			–	20	7			–
12	17	5	5	5	5.75 6.42	17	5	3	3	2.42 2.42	19	9	5	5	2.87 2.90
13	10	3			– –	10	3			– –	19	7			– –

METHOD I - No preprocessing of data.   METHOD II - Normalization to dark data.   METHOD III - Normalization to bright data.

Table 5-8. Accuracy Tables

E = Means Erratic Performance (Dependent on Location of Search Area)

Y = Successfully Located

CHIP NUMBER	CANADA BAND 6 GCP's LOCATED METHOD		
	I	II	III
1	Y	Y	Y
2		E	E
3	CLOUD COVER		
4	Y	Y	Y
5	Y	Y	Y
6	Y	Y	Y
7	CLOUD COVER		
8			
9			
10		Y	Y
11		Y	E
12	Y		Y
13		Y	
TOTAL	5	7	6
BALTIMORE-WASHINGTON, BAND 5			
	Y	Y	Y
3	Y	Y	Y
4	Y	Y	Y
10		Y	
TOTAL	3	4	3

NUMBER	CANADA BAND 7 GCP's LOCATED METHOD		
	I	II	III
1	Y	Y	Y
2		Y	E
3	CLOUD COVER		
4	Y	Y	Y
5	Y	Y	Y
6	Y	Y	Y
7	CLOUD COVER		
8			Y
9			
10		Y	
11			
12	Y	Y	Y
13			
TOTAL	5	7	6
BALTIMORE-WASHINGTON, BAND 7			
2	Y	Y	Y
5	Y	Y	Y
6	Y	Y	Y
7	Y	Y	Y
8	Y	Y	Y
9	Y	Y	Y
TOTAL	6	6	6

5.4 CONCLUSIONS

Automatic control point extraction techniques have been demonstrated which operate with high accuracy and high speed. The combination of SSDA. for rapid search, together with direct cross correlation for refined position determination, offers the prospect of 1/10 pixel accuracy and running time (in optimized assembly language code) of ~1 second per control point.

Homogeneous features with structured borders, most particularly man-made features (roads, airports) derived from band 5, yield the best results in terms of running time, probability of detection and false alarms. Deep bodies of water which have well structured boundaries give comparable performance. Equivalently, the class of features found most suited to automatic extraction methods are those characterized by a bimodal intensity distribution (histogram), with approximately equal proportions in the two modes.

Problem areas for automatic extraction methods of the type utilized in the present study are features containing cloud cover, shallow water bodies (subject to sedimentation changes as well as shape and size variations) and features suffering color inversions over time (including vegetative and agricultural categories). Cloud cover can obscure or otherwise alter the appearance of some features. Many of the water bodies in the Canadian site changed shape and size during a 72 day time period. Sedimentation can also result in a color inversion problem as well. Non complete color inversion, such as in agricultural areas, is a particularly troublesome problem.

Preprocessing the data increases the likelihood of more successful or faster operation of automatic extraction algorithms, with fewer false detections. On the other hand, preprocessing may not be required for some features, such as manmade features, the photometric properties of which do not change significantly with time.

A gain and offset transformation utilized as a preprocessor in this study improved the extraction success rate ~20-40% and also speeded up the search process. With this preprocessing the performance for bands 4 and 5 were quite similar, as was the performance for bands 6 and 7.

Preprocessing the data also has the potential for development of an automatic monitoring capability. With predetermined mean and standard deviation values for the data, absolute bounds can be developed for the sum of absolute differences computed by the SSDA algorithm. Divergence from bound values would indicate an error mode.

Other preprocessing techniques are thresholding, edge detection and inversion. Thresholding would shorten the search times of scenes with areas of only two possible intensities. It would also reduce cloud cover problems; since a low threshold would emphasize water-land contrast, with the clouds fading into the land mass. Inversion of one of the images would apply only to the limited number of scenes with complete inversion. Edge detection would obviate this problem, though skeletal images of large sized features may produce somewhat longer running times, since the bimodal intensity distributions would be highly asymmetric.

6.0 CONCLUSIONS AND RECOMMENDATIONS

6.1 CONCLUSIONS·

6.1.1 Subscene Registration

Precision registration of subscenes (354 pixels x 234 lines) has been demonstrated with fractional pixel accuracy. Three procedures were evaluated: (1) no ancillary data, viz., bulk subarea registration; (2) precision processed reference data; and (3) independently precision processed subscenes. Independently precision processed subscenes did not register as well as subscenes registered to each other and then warped to the precision coordinate system (using one interpolation). High order interpolation (TRW Cubic Convolution Process) was used throughout to achieve sub-pixel accuracy.

If 10 pairs of full scene data are processed, each possessing 15 subscenes each, the image registration of 300 subscenes requires 8 hours, using a single minicomputer with TRW Cubic Convolution implemented in software. If several spacecraft passes (comparison subscenes) are registered to each reference subscene, the processing time is correspondingly reduced due to the faster control point processing. Alternatively, if fewer than 15 subscenes are utilized from each scene, a hardware resampler or a second processor is required to achieve 300 subscenes (4 bands each) per 8 hours. For independent precision correction, the added time required for manual designation of control points necessitates augmentation of software resampling (using either hardware resampling or an array processor).

6.1.2 Full Scene Rectification and Registration

Full scene rectification to accuracies of one instantaneous field of view (79 M) has been demonstrated previously (Reference 4). Extension of the technique to full scene registration of MSS data from different spacecraft overpasses has been demonstrated in this report. For areas possessing good registration control features (road intersections, airports, deep water coastlines, etc.), the measured registration accuracy has been found to be ~0.5 pixel (30 M) rms; worst case error was under 1 pixel. As few as 10 control points are required. For areas in which registration control points are less ideal (shallow lake boundaries) results are similar, but

with somewhat larger registration errors. TRW Cubic Convolution resampling is superior to nearest neighbor with respect to registration accuracy (and thus change detection performance) and image artifacts, such as nearest neighbor produced line and pixel replications and the inability of nearest neighbor to compensate for detection commutation skew.

Utilizing a modest complement of existing off-the-shelf minicomputers and peripherals, processing rates of at least 30 scenes/8 hour day are possible. Either hardware resampling or array processor resampling is required to achieve these rates. Full scene data recorded on 1600 bpi CCT's facilities this high throughput.

6.1.3 Resampling Techniques

Visual and numerical evaluations of nearest neighbor (NN) and TRW's Cubic Convolution (CC) Process have demonstrated the superior quality of the latter. Of the two, only CC can correct sub-pixel distortions, such as exemplified by the commutation time induced offsets. The pixel offset artifacts produced by NN are quite noticeable, in contrast to CC processed data, particularly in change detection imagery derived from registered data. Numerical evaluations of relative and absolute performance of NN and CC indicate the clear superiority of the latter. The impact of interpolation algorithm on classification results appears to be small for areas of several hundred pixels in size. For smaller areas, and along boundaries, differences between interpolation methods become more significant. On an individual pixel basis, such differences can be quite large.

All software implementation of image resampling techniques can be accomplished on minicomputer based systems. Optimized assembly language code for TRW's Cubic Convolution (CC) Process results in running times for a full scene, all four bands (40 MB), of about 62 minutes. (NN resampling in software is three times faster.) Using a microprogrammable processor, full scene CC resampling would require only about 6 minutes. Implementation in special purpose hardware would reduce processing time for a full scene to a little more than one minute, irregardless of interpolation algorithm.

6.1.4 Ground Control Point Extraction

Automatic rapid search of an uncertainty area for matches with control point reference chips is feasible utilizing the sequential similarity detection algorithm (SSDA) and a cross correlation algorithm. After coarse search of an uncertainty region by SSDA, residual errors are <2 pixels. Straightforward cross-correlation refines the control point location to ≲ 1/10 pixel. Assembly language coding results in running times <1 second per control point, for 64 x 64 search areas and 32 x 32 control point chips.

The need for preprocessing control point data so as to normalize average brightness and the dynamic range was established. With such preprocessing, performance of the extraction algorithms is essentially the same with band 4 and band 5 data, and likewise with band 6 and band 7 data. Preprocessing parameters determine running time rather than ultimate accuracy.

Control point properties which lend themselves to automatic extraction techniques were examined. On the basis of data for the sites processed in this contract, desirable control point properties consist of: (a) structured features, with well defined edges which do not change shape, size or color with season; (b) features having homogeneous texture and surround; and (c) features characterized by bimodal intensity distributions (histograms), of roughly equal proportion.

6.2 RECOMMENDATIONS

In view of the results demonstrated herein with full scene registered data, it would be desirable to extend this work and observe changes throughout a full year in one or two selected sites (urban and agricultural) Evaluations on the basis of change detection and multispectral-multitemporal classification would be helpful in demonstrating the utility of a multispectral-multitemporal data base.

Further evaluations of control points derived from a wide range of scene content is desirable. Of particular interest would be evaluations performed on a seasonal and yearly basis.

Inasmuch as control point extraction by manual methods is the slowest part of a production processor, the exploration of new preprocessing techniques (such as negation, edge detection, etc.) would help identify a wider class of features which lend themselves to automatic extraction methods. Of particular interest would be the development of techniques which could automatically search a full scene and determine the location of features having properties useful for registration control.

7.0 REFERENCES AND PAPERS PRESENTED

7.1 REFERENCES

(1) "Experimental Study of Application of Digital Image Processing · Techniques for ERTS Data," TRW Systems Proposal No. 26232.000 (1 March 1974).

(2) ERTS Data User's Handbook, Document No. 71SD4249, NASA Goddard Space Flight Center, September 15, 1971 (Revised November 17, 1972).

(3) S. Portner, "Mirror Velocity Profile," General Electric Company, Space Systems, Beltsville, Maryland (memo dated 5 December 1973).

(4) S. S. Rifman, et.al., "Evaluation of Digital Correction Techniques for ERTS Images - Final Report," TRW Systems Report Number 20634-6003-TU-02 (June 1974).

(5) P. J. Ready and P. A. Wintz, "Information Extraction, SNR Improvement and Data Compression in Multispectral Imagery," IEEE Transactions on Communications, Vo. COM-21, pp. 1123-1131 (October, 1973).

(6) R. H. Caron and K. W. Simon, "Altitude Time-Series Estimator for Rectification of Spaceborne Imagery," Journal of Spacecraft and Rockets 12, 27 (January 1975).

(7) R. H. Caron, "Evaluation of Full-Scene Registered ERTS MSS Imagery Using a Multitemporal/Multispectral Bayes Supervised Classifier," Fourth Annual Remote Sensing of Earth Resources Conference, University of Tennessee Space Institute, Tullahoma, Tenn., dated March, 1975.

(8) J. Wray, "Land Use Maps, 1970, Washington Urban Area, D.C., Md. and Va. (I-858-A), U. S. Geological Survey, Department of Interior.

(9) D. I. Barnea and H. F. Silverman, IEEE Transactions on Computers, Vol. C-21, p. 179 (February, 1972).

7.2 PAPERS PRESENTED

The papers listed in this section were presented at Technical Conferences by TRW personnel utilizing, at least in part, some data furnished by NASA/GSFC in the course of this study. Papers preceded by an asterisk(*) report works which were funded in their entirety by sources other than contract funds.

* (1) R. H. Caron, S. S. Rifman and K. W. Simon, "Application of Advanced Signal Processing Techniques to the Rectification and Registration of Spaceborne Imagery," Technology Transfer Conference, University of Houston, Houston, Texas (24-25 September, 1974).

* (2) R. H. Caron, "Evaluation of Full-Scene Registered ERTS MSS Imagery Using a Multitemporal/Multispectral Bayes Supervised Classifier," Fourth Annual Remote Sensing of Earth Resources Conference, University of Tennessee Space Institute, Tullahoma, Tenn., (24-26 March 1975).

(3) S. S. Rifman, B. Peavy, R. Caron and K. Simon, "Evaluation of All-Digital Registration Methods for LANDSAT MSS Data," Symposium on Machine Processing of Remotely Sensed Data, LARS, West Lafayette, Indiana (3-5 June 1975).

* (4) K. W. Simon, "Digital Image Reconstruction and Resampling for Geometric Manipulation," Symposium on Machine Processing of Remotely Sensed Data, LARS, West Lafayette, Indiana (3-5 June 1975).

(5) S. S. Rifman, K. W. Simon and R. H. Caron, "Second Generation Digital Techniques for Processing LANDSAT MSS Data," Earth Resources Survey Symposium, Shamrock Hilton Hotel, Houston, Texas (8-13 June 1975).

(6) K. W. Simon, S. S. Rifman and R. H. Caron, "Precision Digital Processing of LANDSAT MSS Data," Eleventh International Symposium on Space Technology and Science, Tokyo, Japan (30 June - 4 July 1975).

APPENDIX A
ALTERNATIVE SUBSCENE PRECISION REGISTRATION PROCESS

An alternative approach to registration of a bulk image to a precision corrected image was reported in the rough draft version of this report and is repeated here for reference. The process described in Section III is preferable, especially if several subareas are to be processed for each scene or several subareas are to be registered to one subarea.

The alternative approach is outlined in Figure A-1. First, the reference image must be processed so as to determine the warp from a TRW along-line corrected (TALC) bulk image to the precision image. Then, the specific warp for an arbitrarily selected subarea in the precision image is evaluated. Addition of this warp from comparison TALC subarea to TALC reference subarea yields the total warp from comparison TALC subarea to reference precision subarea.

Mathematically, if the TALC reference subarea is defined in coordinate system u,v and the reference precision subarea is defined in coordinate system x,y, the reference image processing operation produces a warp of the form:

$$\delta x = u - x = a_0 + a_1 x + a_2 y + a_3 xy$$
$$\delta y = v - y = b_0 + b_1 x + b_2 y + b_3 xy \qquad \text{(A-1)}$$

Likewise, if the comparison TALC subarea is defined in coordinate system w,t, the warp from comparison TALC subarea to the reference TALC subarea is of the form:

$$\delta u = t - u = c_0 + c_1 u + c_2 v + c_3 uv$$
$$\delta v = w - v = d_0 + d_1 u + d_2 v + d_3 uv \qquad \text{(A-2)}$$

wherein the c's and d's are computed as in Section II. The a's, b's, c's and d's are known and the x,y coordinates for the reference subarea are input; thus, $\delta x(x,y)$ and $\delta y(x,y)$ are readily calculated, and hence, u,v

are known from Equations (A-1). Using Equations (A-2), δu and δv can be calculated, and thus, the total warp:

$$
\begin{aligned}
\Delta x &= (u-x) + (t-u) = t-x \\
&= \delta x + \delta u \\
&= A_0 + A_1 x + A_2 y + A_3 y \\
\Delta y &= \delta y + \delta v \\
&= B_0 + B_1 x + B_2 y + B_3 xy
\end{aligned}
\tag{A-3}
$$

can be calculated. Fitting the warp to the four points (x,y) in the selected precision subarea determines A_0, A_1, ..., B_3 by means of two independent systems of four linear equations in four unknowns (just as in Section 2). The warp process is also accomplished as described in Section 2.

APPENDIX B

PRECISION CORRECTED CCT TAPE FORMAT

The format of the TRW precision corrected CCT's is identical to
that of the NASA bulk CCT's. Since output precision grid scan lines
do not correspond to single detector outputs after the geometric cor-
rection process, calibration bytes are no longer applicable and thus are
entered as zero. The precision corrected line length is always 3240
picels corresponding to exactly 185 km in the output projection.

The output projection is Universal Transverse Mercator (UTM) using
the Clarke spheroid of 1866 in N. America with a semi-major axis of
6378206.4m and flattening of $(294.978698)^{-1}$. The central scale factor is
.9996 and the false easting is 500 000m. The UTM zones are 6° wide,
starting with zone 1 from 180°W and increasing eastward to zone 60 from
174°E to 180°E. The UTM zone is calculated from the spacecraft nadir
longitude at format center. Orientation of the vertical axis of the
map projection relative to grid north is calculated to be $\theta_{AZ} - \Delta\lambda \sin\phi$
where θ_{AZ} is the nominal orbit azimuth with respect to north, $\Delta\lambda$ is the
longitudinal separation from the central meridian, and ϕ is the latitude
of the format center.

Tha annotation and identification records are copied directly from
the input bulk data tapes. Insufficient space is available for the in-
creased precision of the annotation data and this record format is cur-
rently being revised. UTM zone, format center, and grid azimuth are
currently provided with each set of tapes in written form.

APPENDIX C. EXAMPLE OF INTERPOLATION PROCESS

As described previously, geometric correction of bulk image data takes places in two stages: an along-scan one-dimensional interpolation followed by an across-scan one-dimensional interpolation. In this section an along-scan interpolation example will be described in detail.

Figure C-1 shows an array of 18 bulk image grid points in the u-v coordinate system having pixel values f_1, f_2, ..., f_{18}. It will be assumed for the purposes of this Appendix that it is desired than an along-scan interpolated pixel value F be computed at the point indicated on the figure. Let it further be assumed that for this point that the geometric distortion to be corrected is:

$$\delta x \; = \; u-x \; = \; a_0 + a_1 x + a_2 v + a_3 xv$$

$$= \; A_0(v) + A_1(v)x$$

$$= \; -0.3,$$

for some bulk image scan line v and pixel u, and for some along-scan-interpolated pixel at x (same scan line v). The geometric distortion determination modeling and coefficient calculation steps must of course preceed interpolation.

The one-dimensional 4-point interpolation of a pixel value for F is then given by the equation on the top of Page 70, which reduces to:

$$F(\delta x = -0.3) = f_8 h_1 + f_9 h_2 + f_{10} g_3 + f_{11} h_4 \qquad (C-1)$$

where
$$h_1 = h(1.3)$$
$$h_2 = h(0.3)$$
$$h_3 = h(-0.7)$$
$$h_4 = h(-1.7).$$

The weight function h can be, for example, either of the two functions shown in Figure 4-1, or for that matter, any other interpolation kernel.[*]

---

[*] Note that for 6-point interpolation there will be six terms summed in an equation similar to Equation (C-1).

A graphical representation of the four h values used for TRW's Cubic Convolution Process is given in Figure C-2. A graphical representation of the summation in Equation (C-1) is shown in Figure C-3.

Across-scan line interpolation proceeds in identically the same manner as just described, but interpolation is along columns of along-scan-interpolated data (in the x-v coordinate system). Final output is interpolated along- and across-scan and is represented in the x-y coordinate system as a regular grid of x,y pixels.
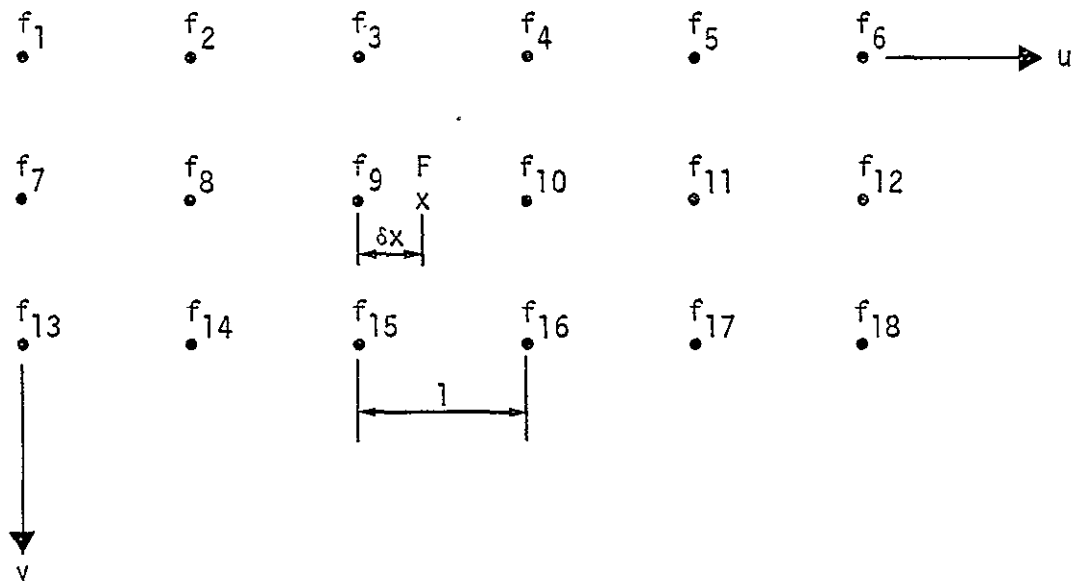
FIGURE C-1. ALONG-SCAN INTERPOLATION OF PIXEL F
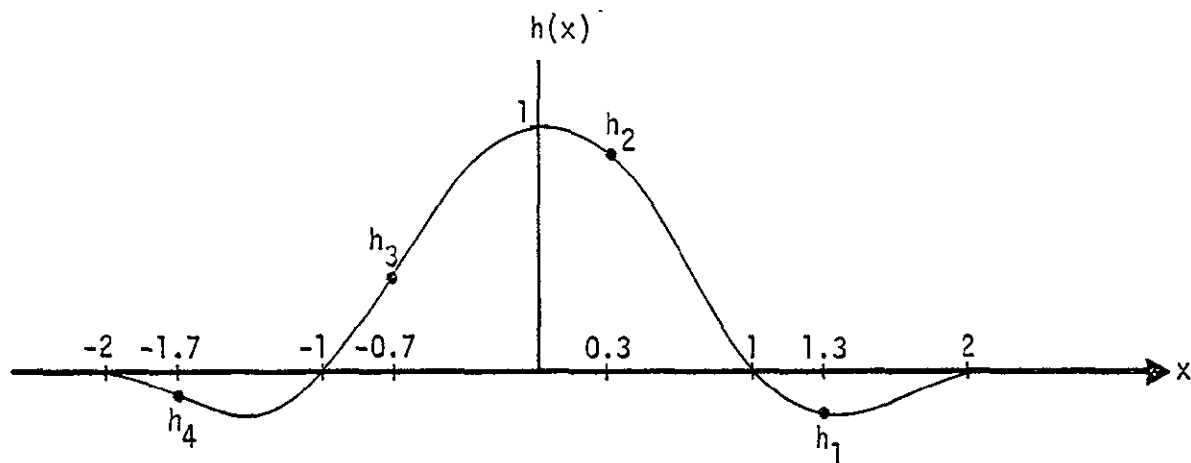
FIGURE C-2. WEIGHT VALUES FOR FOUR-POINT INTERPOLATION
A value of δx = -0.3 is assumed.
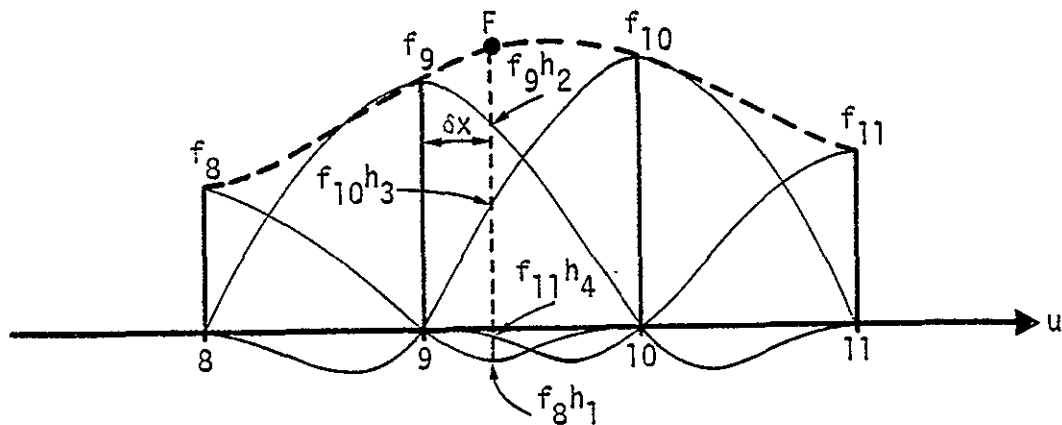
FIGURE C-3. SYNTHESIS OF INTERPOLATED VALUE F

This example illustrates four-point interpolation, given bulk data values f_8, f_9, f_{10}, and f_{11}. The value F is the sum of four values $f_8 h_1$, $f_9 h_2$, $f_{10} h_3$ and $f_{11} h_4$. Only the interval between points 8 and 11 is illustrated.

APPENDIX D. EVALUATION OF RESAMPLED MIRROR REFLECTION DATA

Artificial features, comprising solar reflections from an array of 3 mirrors, were contained in scene 1800-15081 CCT data furnished by NASA. Figure D-1 shows printouts of the bulk MSS data from bands 4, 5, 6, and 7, after removal of replicated pixels NASA introduced for line length correction. No geometric or radiometric* corrections whatsoever have been applied to the data recorded in these printouts. Note that one feature produces a two pixel wide saturation of the detectors in all 4 spectral bands (127 for bands 4,5, and 6; and 63 for band 7). Another feature appears to be 1 or 1 1/2 pixels wide and while bright, does not saturate the detectors in any spectral band. A third feature, five lines above the saturation signal, is the dimmest of the reflection signals. It is still twice as bright as the background pixel values in bands 4 and 5, 50% brighter than background in band 6, and is barely distinguishable from the background pixels in band 7.

Following geometric correction of the data and resampling using TRW's Cubic Convolution Process, the printouts in Figure D-2 were obtained. Note that none of the data for any of the spectral bands reaches the saturation levels of the bulk data (Figure 1). Note also that the medium_intensity mirror reflection data in all 4 spectral bands is also decreased in magnitude. In the case of the least intense reflection signal, the bulk and resampled peak values are very close. There are two reasons for this result: (1) the very small size of the bright mirror reflection features against a relatively dark background, coupled with the process of resampling data on a grid different from the original, in the course of geometrical correction (that is, distortion) of the bulk data; and (2) there is a small effect due to the particular resampling implementation of the Cubic Convolution Process utilized in this study.

---

* The data has been radiometrically calibrated and decompressed by NASA. This may not have been the case with the data reported by Evans (Reference D-1), accounting for small differences between the values printed out in Figure D-1 and those in Reference D-1.

Appendix C illustrates in detail the resampling calculation in one dimension. Figure D-3 illustrates the situation applicable to the results reported herein, using data values for band 4, derived from Figure D-1-a. The along-scan interpolated pixel locations in the bulk image u-v coordinate system are shown by x's. The along-scan interpolated value at position A will in value lie between 28 and 21, the precise value being determined by the along-scan distortion δx (see Appendix C). For example, if point A lies precisely in the middle between the 28 and 21 values, it would have a value of:

$$F(A) = 34f_{cc}(1.5) + 28f_{cc}(0.5) + 21f_{cc}(-.5) + 21f_{cc}(-1.5)$$

$$= 34 \times (-.125) + 28 \times (.625) + 21(.625) + 21(-.125)$$

$$= 23.75$$

assuming the Cubic Convolution interpolation kernel. Likewise, point B would have a value somewhere between 29 and 25. Point C would actually have a value in excess of 127, because it lies between two large values surrounded by relatively small values. However, in the particular software implementation employed for this activity, the data values are limited to the range 0-127; i.e., no negative values or values exceeding 127 are permitted as a result of the interpolation summation.

Figure D-4 shows an example of along-scan interpolation of band 7 data (all bulk values for which are 63 or less). Note that the along-scan interpolated data has a peak of 68, which is greater than the detector saturation value of 63 (Figure D-1-d). The software did not truncate the data since its magnitude did not exceed 127.

Following across-scan interpolation of data at A and C, the final resampled data, represented in the bulk image u-v coordinate system of Figure D-3 by •'s, is located at position D. As explained above, the data value at D will typically lie between the values at A and B. Likewise, the value at E will lie between the values at G and C. In this case (see Figure D-2a), the actual value at E was 109. The value at F was actually 99.

In summary, the particular geometric distortion in this scene resulted in the need to resample data at a fractional pixel location removed from the peak saturation level. The resampling process effectively constructed a smooth curve between a very bright pixel value and an adjacent small pixel value, and thus computed a value somewhere between the two extremes. With the exception of nearest neighbor interpolation (which, depending on the actual distortion values δx and δy, might result in either the bright or a dark value at an interstitial location) any other interpolation process will result in a new computed value which will in general be different from the two extrema. The order of the algorithm (2 point, 4 point, 6 point, etc.), and the particular interpolation kernel will determine the actual interstial value, which will, in general, lie between the two extrema for any interpolation process having any reasonable smoothness properties. Between two adjacent extrema values, the particular kernel and order of the interpolation process will determine the degree (if any) of overshoot or undershoot.

Finally, it is worth pointing out that a slightly modified version of the resampler implementation utilized for this work might yield slightly different performance in the situation of high contrast single pixel sized features. Namely, if data is not truncated to the range 0-127 following along-scan interpolation, but is truncated following across-scan interpolation only, slightly less attenuation of bright values would result. This effect can be seen in the saturation signal data for band 7 reproduced in Figure D-2. Note that the two dimensionally resampled data for band 7 differs from saturation by 4 levels, whereas for bands 4,5, and 6, this difference is as much as 21 levels.

It should be reiterated that it is not possible to determine herein if the resampled data for band 7 is more "accurate" than the resampled data for the other bands, since the only way to evaluate this question would be if precise dimensions and location data (to 0.1 pixel accuracy) is available for the mirror/IFOV[*] geometry. The very process

---

[*] Instantaneous Field-of-View of a single detector.

of saturation of a detector of finite resolution precludes precise determination of actual source location, and in effect has resulted in a virtual object of one or two pixels in dimension. Analyses previously performed, such as contained in Reference (4) of Section 7.2 in this report, give a more complete evaluation of optional and suboptional interpolation processes. The optional interpolation method described in the aforementioned paper could be adapted to features similar to the mirror reflection data considered herein, at the possible cost of reduced performance with features of different properties generally considered in this overall study.

It is concluded that the 4-point Cubic Convolution kernel adopted for work during this contract offers the best overall solution to inter-polation of current LANDSAT data, barring utilization of a higher order interpolator or one optimized for a particular type of image data.

Data resampled by TRW's Cubic Convolution Process for the second swath of scene 1800-15081 (containing the mirror reflections) was recorded on a CCT in the standard NASA word interleaved format, at 800 bpi. This tape was furnished to NASA/GSFC along with a black and white transparency containing the mirror reflection subscene (bulk and re-sampled), all spectral bands. The positive transparency was generated at a scale of 1:1, 141, 975.3 using a 50µ square spot.

REFERENCE

D-1. W.E. Evans, "Marking LANDSAT Images with Small Mirror Reflections," Proceedings of the NASA Earth Resources Survey Symposium, pp. 1185-1196, NASA TM X-58168, Houston, Texas (June 1975).

```
DIVA(A=0),BAND=(2I1)? 05

FLIN,FPIX,NLIN,NPIX=(4I4)? 1605 870  15   20

 20  22  22  22  22  23  22  20  20  23  26  27  26  23  20  22  22  22  22  20
 23  23  23  25  29 [48] 29  20  22  22  22  22  23  25  25  27  22  22  22  22
 21  21  23  27  31  33  37  33  31  27  23  23  23  22  23  23  26  24  24  24
 22  20  22  23  26  29  35  37  35  27  22  22  22  20  20  20  20  20  20  22
 26  25  24 [110  83] 25  34  30  34  34  28  21  21  21  21  21  21  21  21  24
 24  24  25  30  32  29  30  29  30  30  29  25  24  24  20  22  22  22  22  22
 26  27  23  26  23  26  27  27  29  29  44 [127 127  22] 29  23  22  22  23  27
 28  25  25  25  29  31  29  29  29  28  29  31  29  23  22  22  25  25  28  29
 24  29  27  26  26  24  27  31  31  29  27  26  26  26  26  26  27  26  27  25
 26  29  27  23  29  29  26  23  26  26  27  27  29  27  27  27  26  27  26  30
 26  28  26  28  45  48  25  25  28  26  28  28  30  26  26  30  28  28  28  25
 26  29  30  32  33  30  26  25  26  29  26  29  29  26  29  30  29  26  33  32
 26  27  29  33  35  37  37  33  26  23  26  27  30  26  26  26  26  26  29  29
 29  31  25  23  28  28  23  37  29  25  29  29  29  29  29  25  22  23  22  22
 35  29  26  29  33  33  29  26  31  27  26  29  29  29  26  21  23  23  26  27
TASK?  (RS,SP,RU,EX  (CR)=RS)  RS
```

D-1-a. Bulk Data, Band 4

```
DIVA(A=0),BAND=(2I1)? 06

FLIN,FPIX,NLIN,NPIX=(4I4)? 1605 870  15   20

 13  14  13  14  14  14  14  13  14  15  20  21  20  16  13  13  14  14  14  13
 15  15  16  16  25 [45] 23  14  14  12  12  14  16  19  18  15  14  14  14  14
 14  13  14  20  24  27  31  26  24  21  13  12  13  13  13  15  18  18  16  14
 14  14  14  15  20  23  29  35  29  21  14  14  14  12  14  12  12  14  14  17
 21  17  19 [112  71] 23  28  28  30  30  21  15  13  13  13  12  12  13  13  15
 15  15  18  29  29  24  24  24  25  28  22  15  12  12  14  14  14  12  12  15
 19  19  19  19  16  20  21  21  25  25  45 [127 127  98] 25  15  14  15  15  22
 23  19  19  23  25  28  25  24  24  24  25  28  24  16  14  15  19  18  21  25
 16  26  22  16  18  16  24  27  24  24  20  21  18  18  20  20  23  20  21  21
 17  27  21  17  27  23  16  17  23  21  24  27  28  23  24  21  21  23  20  28
 28  25  21  25  51  47  16  21  24  24  25  25  25  21  23  25  24  23  21  21
 23  25  28  31  31  25  19  19  23  23  23  24  24  22  24  25  23  24  29  26
 20  25  27  29  35  40  40  29  21  20  20  25  25  20  21  20  20  22  26  22
 29  29  18  16  21  23  40  42  25  21  24  25  28  25  23  21  16  15  14  16
 37  24  18  26  31  34  24  20  26  23  20  24  26  23  20  14  13  15  20  20
TASK?  (RS,SP,RU,EX  (CR)=RS)  RS
```

D-1-b. Bulk Data, Band 5

Figure D-1. Bulk Data Printouts for Scene 1800-15081.

DIVA(A=0),BAND=(2I1)? 07

FLIN,FPIX,NLIN,NPIX=(4I4)? 1605 870   15   20

```
36  38  38  34  34  38  34  36  34  31  32  34  41  43  36  38  38  41  41  36
40  40  38  34  40 [49] 36  38  38  34  36  34  34  34  34  40  38  36  38  40
34  34  32  34  31  29  32  39  34  34  34  27  39  34  32  31  32  37  39
34  36  38  36  31  31  32  34  34  29  29  36  36  32  36  38  34  34  33  33
36  36  41 [99  57] 24  29  34  34  34  36  36  36  32  34  36  36  34  36  36
33  35  37  45  33  27  31  37  29  33  29  35  39  39  27  39  37  39  41  37
34  32  32  34  31  29  26  26  29  26  50 [127 127 62] 45  36  34  39  36  32
40  36  36  36  34  36  40  38  36  32  30  42  42  40  42  42  36  30  34  32
37  34  29  37  32  32  37  34  32  32  31  32  39  41  37  34  27  29  32  31
34  34  27  33  38  38  34  36  33  29  31  33  33  33  31  32  31  31  33  32
34  32. 31  34  55  48  32  36  27  27  29  32  34  32  31  32  31  34  32  31
32  37  35  33  37  37  37  31  33  33  31  35  31  33  35  33  33  35  35  37
34  34  34  36  43  45  45  39  32  29  34  32  31  27  31  36  34  32  31  32
40  36  30  36  34  34  43  45  38  36  34  34  32  30  29  39  32  36  38  40
39  37  34  34  41  37  34  37  32  29  31  32  31  29  39  39  32  41  41  37
```
TASK? (RS,SP,RU,EX <CR>=RS) RS

D-1-c. Bulk Data, Band 6

DIVA(A=0),BAND=(2I1)? 05

FLIN,FPIX,NLIN,NPIX=(4I4)? 1605 870   15   20

```
20  22  21  18  18  21  20  19  17  16  16  17  21  22  20  21  22  23  22  22
23  24  24  19  22 [21] 20  23  21  21  23  20  19  18  20  23  24  27  27  24
20  20  19  17  15  13  16  20  17  19  22  22  22  22  21  18  16  18  21  22
20  20  22  19  15  15  13  13  14  14  15  20  22  20  22  23  20  19  17  16
19  19  21 [32  15] 11  12  16  15  15  19  21  20  22  21  22  20  19  21  21
18  17  20  22  14  12  12  11  12  15  14  19  23  24  20  22  22  21  22  20
17  16  17  18  14  12  11  12  12  10  17 [62  62  15] 22  21  22  20  19  16
21  20  20  17  17  19  19  20  18  15  14  22  21  25  24  25  19  15  18  14
18  17  15  20  18  17  17  15  16  15  16  18  22  24  20  15  14  15  16  16
18  16  13  17  19  19  19  18  16  14  14  15  15  14  15  14  14  17  15  15
16  14  15  16  21  21  18  18  11  12  13  15  16  14  15  14  14  17  16  15
16  17  16  15  15  17  20  15  15  14  14  16  14  15  16  14  16  16  16  16
17  16  16  16  17  18  18  17  14  14  16  14  13  12  14  18  19  15  17  16
19  17  16  19  18  17  20  19  18  20  16  16  16  13  15  15  17  21  22  22
17  18  19  17  19  16  16  19  16  14  16  16  15  13  13  15  19  26  24  19
```
TASK? (RS,SP,RU,EX <CR>=RS) EX

D-1-d. Bulk Data, Band 7

Figure D-1 (Cont.). Bulk Data Printouts for Scene 1800-15081.

```
OIVA(R=0),BAND (2I1)? 14

FLIN,FPIX,NLIN,NPIX=(4I4)? 2224 840  20  20

11  21  23  20  -9  20  21  24  23  22  21  21  13  21  13  13  11  21  12  2
24  24  19  19  19  21  21  23  23  22  20  20  20  24  23  22  21  21  2  3
21  22  19  18  23  21  21  13  20  21  23  15  21  21  27  23  23  24  23  21  23
21  24  24  21  22  22  22  22  42  23  13  47  43  21  21  21  21  23  23  21
22  21  22  23  22  21  24  27  44  32  23  24  25  22  23  23  21  25  21  21
21  22  22  20  19  20  24  23  21  23  35  32  23  21  21  22  22  22  21  21
21  20  20  19  20  16  12  23  22  36  37  24  23  21  21  21  19  20  23  21
23  21  22  22  16  47  80  44  24  35  23  33  27  21  19  20  19  23  20  22
26  24  25  25  15  52  107  54  20  31  29  33  32  23  15  17  22  13  21  21
25  25  25  22  22  29  36  37  27  29  29  30  29  27  24  23  23  13  22  21
26  24  23  25  25  20  19  22  26  27  27  28  29  53  103  97  13  27  22  21
27  25  24  27  25  22  24  24  27  27  27  27  28  47  99  89  14  26  21  22
28  29  28  26  24  24  24  29  29  28  29  28  28  26  21  20  24  21  22  24
29  30  25  24  28  26  24  25  24  27  31  31  29  26  25  25  25  25  24  25
27  28  25  26  28  23  24  23  23  24  27  27  27  25  26  26  26  26  25  26
25  25  25  29  26  22  32  35  27  22  24  24  25  26  28  27  25  27  27  26
24  24  25  27  25  25  48  49  29  22  27  26  27  27  29  27  25  29  29  27
25  25  25  27  28  29  35  37  15  22  25  28  26  27  29  23  26  20  29  26
22  24  24  26  28  32  32  30  21  28  25  23  24  26  29  25  25  28  28  25
21  20  23  26  26  30  23  35  37  26  29  22  24  26  29  23  25  25  25  24
```
                D-2-a.   Resampled Data, Band 4

```
IVA(R=0),BAND=(2I1)? 15

FLIN,FPIX,NLIN,NPIX=(4I4)? 2224 840   20   20

12  13  12  12  12  12  15  17  14  14  14  15  12  12  12  12  13  12  11  12
14  14  12  10  13  13  12  15  12  14  15  15  14  14  16  15  14  11  10  12
14  14  12  11  12  12  13  13  12  13  12  13  14  13  21  20  17  13  12  12
14  12  12  13  13  14  13  16  25  26  12  11  11  12  15  16  18  18  15  12
13  12  12  14  13  14  15  20  40  33  19  17  16  12  10  12  16  16  15  15
13  14  13  13  12  11  16  22  24  30  30  25  22  15  11  11  12  11  12  15
14  13  12  13  13  6   5   18  25  32  33  24  16  12  12  12  11  12  11  12
19  16  17  17  9   43  74  35  20  31  31  28  21  14  13  12  12  12  10  11
22  21  21  18  7   62  105  45  17  26  26  29  28  16  7   6   7   12  11  12
21  21  16  14  14  24  36  28  22  23  24  26  27  13  13  11  12  14  14  12
20  17  14  16  18  16  14  16  20  20  21  24  26  53  105  101  73  19  14  12
21  18  18  21  18  18  18  19  23  21  20  22  24  43  93  95  65  17  14  15
23  25  23  21  18  19  22  24  26  24  23  24  23  21  16  13  9   14  15  19
26  26  22  16  25  21  15  19  18  25  25  24  24  19  19  16  15  18  18  21
24  23  17  21  24  19  17  15  14  19  24  21  23  22  24  20  20  20  19  22
19  19  18  20  20  16  23  32  17  15  21  21  21  25  28  23  23  22  21  22
17  19  20  25  20  20  45  51  20  17  23  24  24  25  25  21  21  14  24  23
21  22  25  24  24  27  36  25  17  15  21  24  23  23  23  21  21  25  24  22
18  19  19  22  27  31  30  29  28  23  20  21  20  22  24  21  20  22  21  21
13  13  18  23  25  26  31  36  42  37  24  18  18  22  25  22  20  19  18  18
```
                D-2-b.   Resampled Data, Band 5

        Figure D-2.   Resampled Data Printouts for Scene 1800-15081.

DIVA(A=0),BAND=(2I1)? 16

FLIN,FPIX,NLIN,NPIX=(4I4)? 2224 846   20   20

```
I2  35  37  36  34  24  35  30  30  24  34  31  37  48  33  33  34  35  27  35
35  36  36  34  34  36  37  29  33  33  30  31  35  37  39  48  27  38  15  35
33  35  36  34  36  37  34  32  35  33  34  34  31  31  32  36  43  38  36  37
33  35  35  38  40  39  33  36  47  39  35  37  32  33  32  34  36  35  37  35
36  35  23  37  37  36  33  35  42  36  36  27  24  35  33  31  35  34  34  35
37  32  31  32  33  31  32  31  28  28  36  34  31  33  37  37  38  37  32  32
35  34  32  33  36  31  35  29  31  32  34  31  27  38  35  34  33  37  35  32
29  32  34  35  33  59  68  34  24  32  34  33  32  34  36  32  29  34  35  35
27  32  35  34  34  63  88  36  28  30  33  32  34  33  31  31  33  34  35  37
30  33  35  32  34  43  45  29  25  38  35  38  33  33  36  35  31  37  35  37
33  29  35  31  33  32  31  38  26  24  25  27  27  55 111 105  58  41  34  34
30  33  38  35  32  32  32  31  31  30  38  38  27  31 101  95  49  43  25  35
31  40  41  39  35  35  35  34  35  41  37  35  34  27  33  31  35  41  41  32
31  34  33  28  33  30  36  39  32  38  35  33  32  38  31  37  41  38  31  27
32  28  31  35  28  29  35  32  32  35  33  32  31  34  33  34  35  33  35  37
32  29  34  33  26  32  41  43  34  35  31  27  29  31  33  32  29  29  32  31
32  33  34  31  29  31  52  52  33  35  29  26  28  31  33  33  31  31  33  31
33  33  32  34  33  31  40  41  34  31  29  31  33  32  35  31  34  33  32  33
32  30  31  35  35  32  34  38  41  34  31  31  30  33  31  29  31  35  34  33
33  31  33  34  32  34  39  43  45  42  33  29  33  31  32  27  26  31  34  31
```
<div align="center">D-2-c. Resampled Data, Band 6</div>

DIVA(A=0),BAND=(2I1)? 17

FLIN,FPIX,NLIN,NPIX=(4I4)? 2224 843   20   20

```
18  20  20  29  18  20  19  15  16  17  13  19  23  22  21  21  31  21  21  20
20  20  20  19  19  21  16  14  15  16  15  17  19  23  21  22  11  22  22  20
18  19  19  18  20  20  17  16  15  19  18  16  16  15  15  19  22  20  25  21
20  20  20  21  22  23  13  20  22  20  21  20  18  19  15  18  17  18  27  24
22  21  20  21  22  22  18  19  18  17  21  20  19  22  23  33  13  19  14  23
20  19  18  18  19  18  16  14  12  13  17  17  16  19  21  22  22  31  19  15
18  19  19  19  21  19  14  14  14  12  13  14  13  16  21  24  31  22  21  18
14  18  19  18  19  25  24  11  13  12  14  13  14  18  23  19  23  21  21  17
12  16  18  17  17  27  26   9   9  12  14  13  15  18  17  19  22  20  21  19
13  16  19  17  17  22  26  11  10  11  10  13  14  14  28  27  21  13  27  21
14  14  17  15  15  18  17  11   9   9   3  10   9  21  59  51  12  20  20  21
15  16  15  17  17  17  15  13  14  14  15  17  18  20  55  45  15  23  23  20
15  19  21  20  19  18  16  17  19  19  19  17  14  13  17  17  26  23  22  17
14  16  16  18  17  15  19  16  16  15  15  15  15  15  17  21  25  21  17  14
13  14  15  17  13  15  19  17  17  16  15  15  14  15  15  17  18  16  14  11
14  15  18  15  11  15  18  23  19  18  15  12  12  13  15  12  12  13  13  12
15  15  16  14  13  15  20  21  17  18  12  11  12  14  15  14  14  14  13  15
15  15  14  15  15  14  15  17  19  16  12  13  12  14  14  14  16  13  13  15
16  15  15  16  15  14  13  15  19  15  14  13  12  15  12  12  14  14  16  15
18  18  17  16  14  15  16  16  17  17  15  12  15  14  12  12  11  15  18  17
```
<div align="center">D-2-d. Resampled Data, Band 7</div>

<div align="center">Figure D-2 (Cont.). Resampled Data Printouts for Scene 1800-15081.</div>
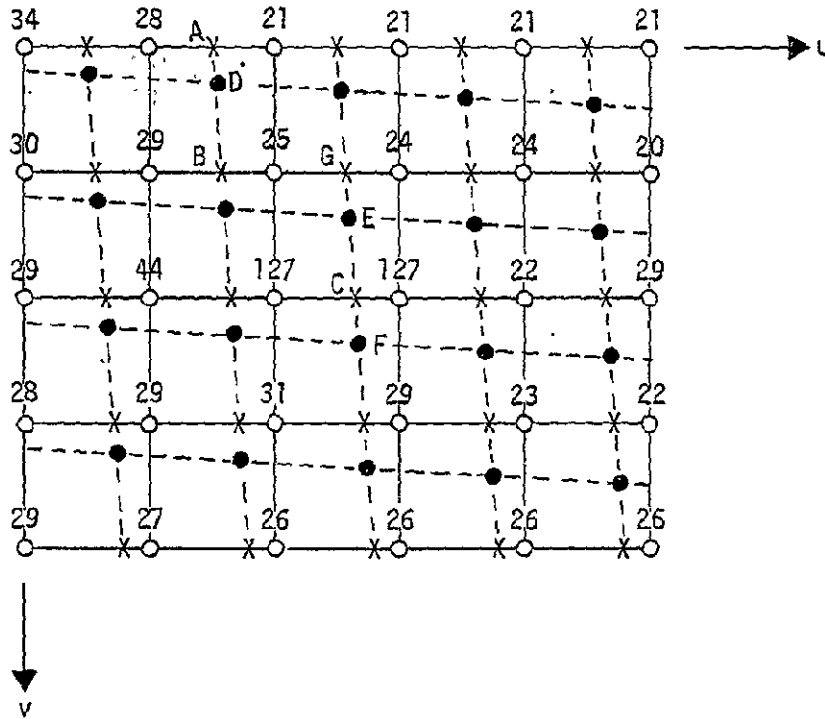
Figure D-3. Detail of Band 4 Data.

Mirror Reflection Data. The o points
and the corresponding numbers are de-
rived from actual bulk NASA data. The x
points represent typical locations of along-
scan resampled data. The • points show the
location of two-dimensional (along- and
across-scan) resampled data, plotted in the
bulk image coordinate system u-v. In the output
system x-y, the • points lie on a regular
(square) grid.

```
24  13  21  21  13  22  21  20  22  21  13  17  17  21  24  21  21  22  21  24
13  17  15  17  14  13  18  17  26  23  23  22  21  13  15  15  19  22  22  22
24  15  14  14  12  11  14  11  15  21  21  20  22  21  15  18  16  15  15  17
23  27  19  13  13  15  11  15  20  13  25  21  21  21  19  19  21  20  17  14
23  23  13  11  11  13  12  14  14  18  25  23  19  22  21  21  11  19  17  11
17  17  12  11  11  12  11   9  21  68  56  11  22  21  21  13  15  15  17  11
19  15  17  19  19  13  17  14  14  22  21  25  24  25  13  17  13  14  11  12
45  20  17  16  16  15  16  15  15  17  21  24  20  15  14  14  15  16  15  14
17  13  19  19  18  15  14  13  14  15  14  14  11  14  17  13  15  11  11  15
13  22  21  13  18  12  11  11  14  15  14  14  14  11  16  16  15  15  11  11
13  14  16  17  16  14  14  13  15  14  14  16  14  14  16  16  16  13  15  17
15  16  17  13  17  15  13  13  15  11  18  12  16  13  17  11  11  15  11  11
```

Figure D-4. Printout for Along-Scan Resampled Scene 1800-15081-7.

APPENDIX E. CONTROL POINT EXTRACTION EXPERIMENT

E.1 TASK DESCRIPTION

LANDSAT MSS bulk CCT data were furnished by NASA to permit evaluation of automated control point location techniques under conditions of wide seasonal variations. Data were evaluated for two sites: Monterey Bay (scenes 1039-18172, 1813-18063, 1921-18022, and 1993-17590) and the Chesapeake Bay (1080-15192, 1350-15192, 1800-15081, and 1872-15061). Note that the data spanned a period of time of 954 days at the Monterey Bay site, and a period of 792 days at the Chesapeake Bay site.

Control points were selected arbitrarily from one scene at each site. Table E-1 lists the control points selected from the Monterey Bay site (1039-18172) and Table E-2 lists those from the Chesapeake Bay site (1800-15081). As may be seen from these two tables, a wide variety of control point types were defined for evaluation, encompassing airports, road intersections, land/water boundaries and agricultural features. Data representative of all four MSS bands were also utilized. Control points were selected in the course of visual examination of transparencies of a representative scene or two from each site; no maps or other information were available or utilized.

Bulk digital data were formatted onto digital disk storage so as to separate the spectral bands and order the pixels. Replicated pixels introduced by NASA for line length adjustment were removed. Next the control point chips (32 lines x 32 pixels) were manually designated using a CRT display with a trackball-controlled cursor. Control point chip data were TRW Along-Line Corrected (TALC)* prior to storage in a disk file. The chip data so stored were read from the formatted bulk data stored on the large disk (after removal of replicated pixels), and not from the refresh disk of the CRT display, so as to minimize noise and other distortions possible with the non-parity disk of the CRT display. Search area files (each 64 lines x 64 pixels) were created in the same manner as control point chip files.

---

* TALC correction includes line length, mirror scan nonlinearity, and detector commutation offset. TRW's Cubic Convolution Process is used for along scan resampling.

The control point chip and search area extraction codes utilized are identical (with one exception) to that of TRW's precision correction/registration software utilized for full scene production processing. For the purposes of this study, however, the operator typed in from the keyboard the approximate control point locations in lines/pixels. In the production processing code BIAT data (spacecraft ephemeris and attitude) are used to estimate the control point positions, given data files for geodetic location of the control points. Due to the late arrival of most of the tapes furnished for this task, it was not possible to employ the production version and, in any event, no maps were available to build up the geodetic location files required.

Two algorithms were employed for automatic control point location: Sequential Simularity Detection Algorithm (SSDA) for rapid location of a small ($\pm$ 5 pixel, $\pm$ 5 line) uncertainty region; and precision cross-correlation location of control points to $\sim$ 1/10 pixel.[*] The latter fits two paraboloids to the correlation values (one in the scan direction, and one orthogonal to it), and the locations of the paraboloid extrema then correspond to the control point position.

The two automatic location algorithms possess self-monitoring features. In the event performance deviates from predetermined values, an indication is signalled to the operator by means of keyboard print-outs of E.C.'s (possible error conditions). The control point chip and "best guess" search area position, found through either SSDA alone or SSDA/correlation, are then displayed on the CRT. The operator can then manually register the two areas if the search area appears to contain the control point. If the control point is not evident or is greatly altered in the search area, the operator can move on to the next control point or designate and store the new feature (update the control point library). The latter option was not employed for this study, since the objective was to evaluate the effects of even large

---

[*] See Section 5.0 of this report for further details of the algorithms employed.

seasonal variations on features used as control points; such an option would naturally be employed during production processing.

Manual evaluation of control point location accuracy, when one or the other automatic algorithm indicated an abnormality ("E.C.", or possible error condition), was accomplished to 1/4 pixel accuracy. This accuracy was achieved by digital enlargement (a factor of 4:1) of the TALC chip and corresponding search area features using TRW's Cubic Convolution Process. Two-dimensional enlargement, supplemented by a capability for displaying either enlarged detail (flicker) by keyboard control, permits an operator to easily determine maximum overlap as one feature is moved relative to the other. Such displacements are in steps of 1 pixel (or line) in the enlarged details, and hence correspond to steps of 1/4 pixel (or line) in the original data. The software cumulates the total of line and pixel movements (if any) and prints the results at the keyboard.

In summary, the "nominal" situation evaluated in this study comprised SSDA with correlation for final accuracy (1/10 pixel). If SSDA or correlation indicated a possible error condition (E.C.), manual registration evaluation was employed to determine the SSDA/correlation accuracy (1/4 pixel error due to manual measurement). Manual registration per se resulted in 1/4 pixel net location error. Processing times for SSDA were also determined.[*] Particular attention was also given to the question of whether or not the self-monitoring features would respond correctly to abnormal situations with an E.C. flag, and to the use of some preprocessing of chip and search area data as a means to speed up and/or compensate for abnormal conditions.

---

[*] Processing time for correlation (± 5 pixels, ± 5 lines) is < 0.5 seconds in all cases. Manual times varied, but typically were < 30 seconds.

E.2 RESULTS

Tables E-3, E-4, and E-5 summarize SSDA results for the Monterey Bay site for search areas derived, respectively, from scenes 1813-18063, 1921-18022, and 1993-17590. Chip numbers for this site are listed in Table E-1. The default mode column contains running time and SSDA error results for a given predetermined set of SSDA and chip/search area preprocessing (gain/offset) parameters. The mean and standard deviation of chip and search area data were adjusted to a mean and standard deviation value which was the same for both sets of data.

If a condition is labeled "Nominal" under the Comment column, the correlation and SSDA algorithms gave no E.C. return and ultimate control point location accuracy, determined automatically by correlation, was $\sim$ 1/10 pixel (the errors in the Default Mode column correspond only to SSDA performance, per se). A non-nominal situation is identified under the Comment column as either an "SSDA E.C." or a "correl (ation) E.C." Further, the search area appearance (contrast, shape, etc.), observed during manual operation is given. The errors listed under the Default Mode column are thus SSDA errors measured by manual (flicker) means, rather than by means of correlation, for a non-nominal case.

The chips subject to an E.C. flag were subject to further study to determine if any adjustment of the default parameter values for SSDA and the preprocessor (gain/offset adjustment) would permit automatic correlation (Nominal performance under Additional Comments column), or at least speed up SSDA running time and improve SSDA accuracy. If the control point feature was unrecognizable (due to changes over long periods of time in the size, shape, or other characteristics of the features), no such optimization effort was undertaken. In some cases, due to orbital changes and/or changes in framing, control points lay outside the area of framed data. These conditions would, of course, be immediately known in the production mode without operator intervention.

The search area data for Table E-3 was 774 days removed in time from the chip data. Nonetheless, for 6 of the 11 features utilized (one or more spectral bands), nominal performance was achieved in

either the default mode or after optimum adjustment of gain (standard deviation) of preprocessed chip and search area data. For 3 of the 5 remaining features, the control point was not recongizable at all in the search area. In the remaining two cases, the background was altered to such an extent that only manual techniques would permit location of the nominal control point position. SSDA processing time in the 6 nominal cases ranged from 1.10 sec - 2.58 sec. No SSDA processing time (optimal) exceeded 6.75 seconds. No SSDA processing time (nominal or otherwise) exceeded 7.59 seconds. For all cases in which an E.C. flag was indicated there were shape, size, or background variations which were valid - in no case was an E.C. flag unwarranted. For the 3 cases (out of 6) in which gain adjustment during preprocessing produced a nominal condition from an E.C. condition, it would be a simple matter to automate the adjustment without need for manual adjustment.

For the data listed in Table E-4 (882 days removed from the date of the chip data) only two of the eleven features produced nominal results. Three were unrecognizable, two were outside the framed image area, and the remaining 4 were subject to significant changes in background appearance, contrast inversion, or change in the size and/or shape of the control point feature. Maximum SSDA processing time (nominal conditions) was 3.13 sec; maximum SSDA processing time overall was 6.90 sec (optimized).

The data in Table E-5. (954 days removed from the chip data) indicate 4 of the 11 features correspond to nominal results, 2 were outside the framed image area, 2 were completely unrecognizable, and 3 were subject to significant changes in background appearance and contrast inversion. Maximum nominal SSDA time was 2.42 sec, and maximum SSDA time overall was 7.73 sec (optimized).

SSDA results for the Chesapeake Bay site are included in Tables E-6, E-7, and E-8, respectively, for scenes 1080-15192, 1350-15192, and 1872-15061. A summary of both the Monterey Bay and Chesapeake Bay results is given in Table E-9. Note that for both sites, the best performance in terms of percentage detection of recognizable (and

unobscured) control point features is not necessarily achieved for
scenes closest together in time, nor is the poorest performance achieved
with scenes farthest apart in time. Note also that there is a mix of
types of features used as control points used for each site, but that 7
of the 11 features at the Monterey Bay site were agricultural, whereas
only 4 of the 11 at the Chesapeake site were agricultural. The rest
were road intersections, airports, and bends in lakes or other land/water
boundaries. Problems of contrast inversion or alteration in background
appearance and similar changes are more likely to be observed with
agricultural features, and hence, the somewhat poorer performance of
automatic algorithms with these types of features is not surprising.
The number of unrecognizable features in the Monterey Bay site is also
greater than that in the Chesapeake Bay site, for similar reasons.

With respect to which spectral band(s) gives best overall per-
formance results, in most cases for a given feature there was a tend-
ency for one spectral band to out-perform the others. For agricultural
features, the optimal band does not appear to establish a clear trend.
Apparently the time during the crop calendar as well as the particular
crop can have a significant impact. Infrared bands appear best for
land/water interfaces and the visible bands appear best for roads and
airports. The determination of optimal band combinations clearly re-
quires analysis of a larger data base than was available in the course
of this study.

E.3 CONCLUSIONS AND RECOMMENDATIONS

Automatic control point location performance has been evaluated
for two sites, encompassing a broad range of seasonal variation. Per-
formance was generally better in an urban environment having well-de-
fined land/water boundaries (Chesapeake Bay site) than in a rural/agri-
cultural environment (Monterey Bay site). The percentage of detection
of recongizable control points using only automatic techniques ranged
from 33% to 75% in the rural environment for data separated in time by
774 days- 954 days. Were it possible to update control points within a
crop calendar, or at least every year or so, it should be possible to
improve significantly on this performance.

In the urban environment,.also rich with well-defined land/water
bounaaries, performance with automatic algorithms ranged from 67% to 90%
(percentage of recognizable control points found automatically). This
data base was separated in time by 72 days to 720 days. Unrecognizable
features, which changed drastically over such long time spans, ranged
from under 10% (of all control point features within the framed area)
in the Chesapeake Bay site to 33% in the Monterey Bay site.

In all cases where the automatic location methods achieved rela-
tively poor results, an.E.C. message was automatically printed.at the
keyboard alerting the operator. The code automatically displayed data
on a CRT for manual registration (if required). The percentage of the
time this occurred, including both recognizable and unrecognizable fea-
tures within the framea image area, ranged from 50-80% at the Monterey
Bay site, and from 20-40% at the Chesapeake Bay site.

Running times in the automatic mode averaged 2-4 seconds through-
out the study, not including correlation (< .5 seconds per feature).
The longest running time of all was < 8 seconds. When successful., auto-
matic location methods yielded $\sim$ 1/10 pixel location accuracy. When un-
successful, and manual methods were resorted to, accuracy was $\sim$ 1/4 pixel.

Since control points were selected in a random manner, and due to
the relatively small sampling of data evaluated in this study (3 passes
at each of 2 sites), it is quite likely these results may not be truly
typical of that which might be expected in a production processor. If
anything, these evaluations are rather more rigorous than might be ex-
pected in practice, for the reasons just given, and because no updating
of control points was attempted, even though temporal separations ap-
proached 3 years in one case.

A more comprehensive attempt at control point location performance
evaluation is certainly warranted. Such an effort should utilize a vastly
larger data base than that considered herein, and also should attempt to
correlate results with ground truth (maps, county records, etc.), and the
crop calendar. In the absence of such an activity, this-study clearly
indicates that more emphasis be placed on preprocessing control point

reference and search data. Greater care in selection of control point features (such as roads, airports, certain agricultural features and certain land/water boundaries) should also enhance the success rate of automatic location methods. Those agricultural or similar features and their surrounding areas which suffer contrast inversions preferably should be avoided if it is desired to minimize manual interactions.

TABLE E-1. CONTROL POINT CHIPS FROM 1039-18172 (Monterey Bay Site)

ID NUMBER	BAND	CENTER LINE	PIXEL	DESCRIPTION
1	5⎫	1092	1204	Agricultural
2	6⎪	1092	1203	Agricultural
3	* 7⎪	1093	1204	Agricultural
4	* 4⎫	1247	1372	Agricultural
5	5⎬	1248	1371	Agricultural
6	6⎭	1247	1372	Agricultural
7	5	0693	2131	Agricultural
8	5	0731	2207	Road Intersection
9	* 4⎫	1049	2698	Airport
10	5⎭	1049	2696	Airport
11	4	1110	2817	Agricultural
12	* 6⎫	1480	2984	Bend in Lake
13	7⎭	1479	2984	Bend in Lake
14	5	1435	2979	Agricultural
15	5	1824	2559	Agricultural?
16	6	1738	1481	Agricultural
17	* 6⎫	1573	2886	Bend in Lake
18	7⎭	1574	2886	Bend in Lake

NOTE: Brackets denote different spectral bands of the same feature.

*   Denotes the spectral band for a given feature giving best performance overall (See Tables E-3, E-4, and E-5)

TABLE E-2. CONTROL POINT CHIPS FROM 1800-15081 (CHESAPEAKE BAY SITE)

ID NUMBER	BAND		CENTER LINE	PIXEL	DESCRIPTION
1		5	0827	1676	Road Intersection
2		5 ⎫	1477	0841	Agricultural
3	*	4 ⎬	1478	0842	Agricultural
4	(* Equal)	6 ⎫	1252	0625	River Fork
5		7 ⎬	1253	0624	River Fork
6		5	1696	1668	Airport
7		6	2167	2587	Spit of Land in Bay
8		7	2266	2561	Spit of Land in Bay
9	(* Equal)	6 ⎫	1323	0667	Agricultural
10		5 ⎬	1323	0668	Agricultural
11		7	1471	3085	River Fork
12	*	5 ⎫	1977	1036	Agricultural
13		4 ⎬	1977	1036	Agricultural
14		4	1024	1374	Road Intersection
15	*	5 ⎫	0925	1398	Agricultural
16		4 ⎬	0925	1398	Agricultural

NOTE: Brackets denote different spectral bands of the same feature

* Denotes the spectral band for a given feature giving best performance overall (See Tables E-6, E-7, and E-8)

TABLE E-3. SSDA RESULTS FOR SCENE 1813-18063 (MONTEREY BAY SITE)

SEARCH AREA FOR CHIP NO.	DEFAULT MODE T(sec)	ΔY(lines)	ΔX(pixels)	COMMENTS	OPTIMAL PERFORMANCE T	ΔY	ΔX	ADDITIONAL COMMENTS
1	9.37	-1.00	-3.00	Shape altered- SSDA E.C.	7.59	-0.75	-3.00	Preprocessing Gain Adjust-SSDA E.C.
* 2	2.10	1.00	1.50	" " Correl E.C.	1.10	0.38	0.94	Preprocessing Gain Adj. - Nominal
3	1.50	1.62	-0.81	Nominal				
* 4	2.20	-3.00	2.50	Background Altered SSDA E.C.	2.58	-1.02	2.26	Preprocessing Gain Adjust - Nominal
5	6.08	16.00	8.00	" " SSDA E.C.	2.23	0.01	-0.80	Preprocessing Gain Adj. Correl. E.C.
6	2.03	-3.25	2.25	" "				Default is Optimum
7	6.03	0.25	12.75	" "				Default is Optimum
8	7.77	6.98	15.67	Contract Inversion SSDA E.C.	6.75	0.50	-13.50	Gain Adjustment SSDA E.C.
* 9	6.63	-3.00	-12.00	Change in Back- ground-SSDA E.C.	2.57	-0.76	0.04	Gain Adjustment - Nominal
10	7.50	1.25	-9.75	" "				Default is Nominal
11	2.13	----	----	CP Not Recogniz- able - Correl E.C.				
* 12	1.78	-0.88	-0.17	Nominal				
13	1.73	-1.86	1.89	Nominal				
14	2.15	----	----	CP Not Recogniz- able - Correl E.C.				
15	3.08	----	----	" "				
16	----	----	----	Background Altered Correl E.C.	1.15	0.27	0.37	Gain Adjustment - Nominal
* 17	2.23	0.28	0.52	Nominal				
18	2.38	1.30	-1.69	Nominal				

* Denotes spectral band for a given feature giving best performance overall

TABLE E-4. SSDA RESULTS FOR SCENE 1921-18022 (MONTEREY BAY SITE)

SEARCH AREA FOR CHIP NO.	T(sec)	DEFAULT MODE ΔY(lines)	ΔX(pixels)	COMMENTS	OPTIMAL PERFORMANCE T	ΔY	ΔX	ADDITIONAL COMMENTS
1	2.13	----	----	CP Unrecognizable - Correl E.C.				
2	1.20	----	----	" "				
* 3	2.38	1.51	0.34	" "				
* 4	3.13	-2.26	1.16	Nominal				
5	6.98	-1.50	0.75	Background Different - SSDA E.C.				Default is Optimal
6	8.08	-2.25	-10.75	" "	6.71	-0.25	3.25	Gain Adjustment-SSDA E.C.
7	6.32	5.70	7.99	Background Altered- SSDA E.C.	5.72	0	0	" "
8	7.50	1.75	15.50	Contrast Inversion-SSDA	6.90	0.75	14.50	" "
* 9	2.45	-3.50	-8.75	Shape & Size Altered-SSDA	2.48	-2.25	2.75	" "
10	6.38	-1.75	-11.25	" " " "	7.38	-2.25	-7.50	" "
11	2.58	----	----	CP Unrecognizable-Correl E.C.				
12	----	----	----	Skipped-Off Edge of Scene				
13	----	----	----	" " " " "				
14	----	----	----	" " " " "				
15	5.66	----	----	CP Unrecognizable-SSDA E.C.				
16	2.15	0.72	1.28	Nominal				
* 17	2.02	3.00	-3.75	Change in Size & Shape Correl E.C.	1.70	0.75	-3.50	Gain Adjust. Correl E.C.
18	2.12	4.00	-3.75	" " " "	1.62	1.75	-3.50	" "

* Denotes spectral band for a given feature giving best performance overall

TABLE E-5. SSDA RESULTS FOR SCENE 1993-17590 (MONTEREY BAY SITE)

SEARCH AREA FOR CHIP NO.	DEFAULT MODE			COMMENTS	OPTIMAL PERFORMANCE			ADDITIONAL COMMENTS
	T(sec)	ΔY(lines)	ΔX(pixels)		T	ΔY	ΔX	
1 ⎫	2.12	----	----	CP Not Recognizable-Correl E.C.				
2 ⎬	1.16	15.75	-4.40	Contrast Inverted-Correl E.C.				Default Optimal
* 3 ⎭	2.20	-8.50	2.75	" . ." " "				" "
* 4 ⎫	2.18	-1.96	0.57	Nominal				
5 ⎬	7.07	3.00	-2.00	Shape Changed-SSDA E.C.	2.02	3.25	-2.00	Correl E.C.
6 ⎭	12.70	-6.00	-13.00	" " " "	2.18	-2.94	-0.10	Correl E.C.
7	6.27	0.37	0.97	Contrast Inversion-SSDA E.C.				Default Optimal
8	7.70	-8.25	15.00	Contrast Inversion-SSDA E.C.	7.37	-6.12	10.63	Correl E.C.
9 ⎫	1.25	-2.41	1.90	Nominal				
* 10 ⎭	1.17	-0.60	-0.25	Nominal				
11	6.95	----	----	CP Not Recognizable-SSDA E.C.				
12 ⎫	----	----	----	Skipped - CP Off Edge of Scene				
13 ⎭	----	----	----	" " " " "				
14	----	----	----	" " " " "				
15	7.50	----	----	CP Not Recognizable-SSDA E.C.				
16	1.13	0.93	0.10	Nominal				
* 17 ⎫	2.42	0.95	-0.30	Nominal				
18 ⎭	2.48	1.97	-2.44	Nominal				

---

* Denotes spectral band for a given feature giving best performance overall

SEARCH AREA FOR CHIP NO.	DEFAULT MODE T(sec)	ΔY(lines)	ΔX(pixels)	COMMENTS	OPTIMAL PERFORMANCE T	ΔY	ΔX	ADDITIONAL COMMENTS
1	1.12	0.32	0.36	Nominal				
* 2 }	1.28	-0.65	-0.07	Nominal				
3 }	1.15	-1.56	1.14	Nominal				
4 }	12.85	----	----	CP Has Small Contrast - SSDA E.C.	2.94	-2.15	2.22	Preprocessing Gain Adj. - Nominal
* 5 }	13.02	----	----	" "	2.62	0.81	0.25	
6	1.18	-0.80	-0.82	Nominal				
7	3.50	0.03	0.69	Nominal				
8	4.90	1.15	0.80	Nominal				
9 }	12.50	----	----	CP Has Small Contrast - SSDA E.C.	5.92	----	----	CP Not Recognizable- SSDA E.C.
* 10 }	13.00	----	----	" " "	2.22	2.12	0.36	CP Difficult to Recognize -Nominal
11	----	----	----	CP Shape Altered-SSDA E.C.	1.35	-3.00	3.00	Preprocessing Gain Adj. - Nominal
* 12 {	1.84	0.09	-0.60	Nominal				
13 {	2.15	0.06	-0.64	Nominal				
14	1.10	5.25	-3.75	CP Has Small Contrast - Correl E.C.	2.13	3.25	-4.25	Preprocessing Gain Adj. Correl E.C.
* 15 {	1.43	1.64	-1.10	Nominal				
16 {	1.60	1.65	-1.16	Nominal				

---

* Denotes the spectral band for a given feature giving best performance overall.

TABLE E-7. SSDA RESULTS FOR SCENE 1350-15192 (CHESAPEAKE BAY SITE)

SEARCH AREA FOR CHIP NO.	DEFAULT MODE			COMMENTS	OPTIMAL PERFORMANCE			ADDITIONAL COMMENTS
	T	ΔY	ΔX		T	ΔY	ΔX	
1	1.15	-0.63	-0.06	Nominal				
2	1.28	0.84	2.23	Nominal				
* 3	1.17	-2.20	1.26	Nominal				
* 4	13.30	----	----	Contrast Inversion-Correl E.C.	1.91	0.27	0.34	Preprocessing Gain Adjustment - Nominal
5	13.30	----	----	Contrast Inversion-Correl E.C.	2.33	1.66	-3.19	Preprocessing Gain Adj.-Nominal
6	1.16	-2.50	1.25	Shape & Size Altered-Correl E.C.				Default is Optimal
7	4.00	1.27	-0.56	Nominal				
8	4.72	-2.50	1.25	Shape Altered-Correl E.C.				Default is Optimal
9	7.12	----	----	CP Not Recognizable-SSDA E.C.				
10	2.98	----	----	CP Not Recognizable-SSDA E.C.				
11	----	----	----	CP Outside Scene-SSDA E.C.				
* 12	2.27	-1.03	-0.15	Nominal				
13	2.55	-0.91	-0.07	Nominal				
14	3.00	5.00	-3.25	Contrast Low-Correl E.C.	2.13	3.00	-0.50	Preprocessing Gain Adj.-Correl E.C.
* 15	1.41	1.05	-0.89	Nominal				
16	1.41	-0.97	1.09	Nominal				

* Denotes the spectral band for a given feature giving best performance overall.

TABLE E-8.   SSDA RESULTS FOR SCENE 1872-15061 (CHESAPEAKE BAY SITE)

SEARCH AREA FOR CHIP NO.	DEFAULT MODE T(sec) ΔY(L) ΔX(P)			COMMENTS	OPTIMAL PERFORMANCE T(sec) ΔY ΔX			ADDITIONAL COMMENTS
1	2.12	-0.81	2.35	Contrast Inverted-SSDA E.C.				Default Optimal
* 2	8.97	3.00	-6.25	Background Altered-Correl E.C.	2.80	1.05	1.82	Preprocessing Gain-Correl E.C.
3	2.22	-0.03	0.96	Nominal				
* 4	3.05	-0.14	-0.91	Nominal				
5	2.57	2.50	-2.50	River Channel Altered-Correl E.C.	1.13	2.50	-2.75	Preprocessing Gain-Correl E.C.
6	1.09	-0.78	0.71	Nominal				
7	3.52	2.28	-0.93	Nominal				
8	4.54	1.54	-1.79	Search Area Obscured by Clouds-Correl E.C.				
* 9	2.35	----	----	CP Unrecognizable-SSDA E.C.				
10	6.46	----	----	CP Unrecognizable-SSDA E.C.				
11	----	----	----	CP Outside Image-Skipped				
* 12	1.95	1.11	-2.26	Nominal				
13	2.08	1.21	-2.13	Nominal				
14	3.05	6.50	-3.50	Background Altered-Correl E.C.	2.10	6.50	-3.25	Preprocessing Gain-Correl E.C.
* 15	1.22	1.62	-1.47	Nominal				
16	----	----	----	Contrast Poor-SSDA E.C.	1.20	1.72	-1.49	Preprocessing Gain Adjustment-Nominal

* Denotes the spectral band for a given feature giving best performance overall.

TABLE E-9. SUMMARY OF SSDA RESULTS

SITE	SEPARATION (DAYS) FROM REFERENCE SCENE	NUMBER FOUND (NOMINAL)	NUMBER INSIDE FRAME	NUMBER UNRECOGNIZABLE FEATURES	MAXIMUM SSDA TIME (OPTIMIZED) ALL FEATURES	AVERAGE SSDA TIME (OPTIMIZED) ALL FEATURES	% DETECTION OF RECOGNIZABLE FEATURES (NOMINAL)
MONTEREY BAY							
1813-18063	+774	6	11	3	6.75 sec.	2.86 sec.	75%
1921-18022	+882	2	9	3	6.90	3.23	33%
1993-17590	+954	4	9	2	7.73	4.06	57%
CHESAPEAKE BAY							
1080-15192	-720	9	11	1	4.90	2.14	90%
1350-15192	-450	6	10	1	4.72	2.21	67%
1872-15061	+ 72	6	10	2	4.54	2.42	75%